Robust Modelling of the Glucose-Insulin System for Tight Glycemic Control of Critical Care Patients

Jessica Lin

A thesis submitted in partial fulfilment
of the requirements for the Degree of
Doctor of Philosophy
in
Mechanical Engineering
at the
University of Canterbury,
Christchurch, New Zealand.

20 July 2007

Acknowledgements

This research gave me a lot more than fulfilling the requirements for a PhD.

My supervisors, Professor J. Geoffrey Chase and Dr. Geoffrey M. Shaw, have been great mentors and friends to me. Professor Geoff Chase has always challenged me to think and to question, and motivated me with his chocolate-related briberies and "appropriate suffering". Dr. Geoff Shaw gave me the opportunity to first-handedly experience the real-life side of biomedical engineering research, and always believed in me. Most important of all, Professor Chase and Dr. Shaw were always passionately involved in the research, and supported me with their approachable presence.

My sincere thanks also go to Dr. Dominic Lee and Dr. Chris Hann for their inputs. I greatly appreciate their ability to communicate mathematical and statistical concepts in a "suitable for engineers" way. They were also very enthusiastic and approachable. This research simply would not be possible without them.

This research has been a great joint effort between many parties to bring it to its current stage. My thanks extend back to all the people ever involved in the ICU glycemic control project from teams AIC1 to AIC6. I also want to say thank you to Professor Graeme Wake and Mr. Bob Broughton who brought their expertise into our early stage of glycemic system model research.

I also thank all my loving friends and family who supported me and make my life fulfilling. The deepest thanks go to my parents for their unconditional support and inspiration. They are the people who planted the seed in me that drives me to seek knowledge and solutions. Special thanks go to my aunt Guei-May and uncle Feng-Gi for their never-changing believe and overwhelming support. Thanks

to my grandparents for always pushing me to seek goodness, and simply being loving and believing. Also thanks to my special someone for his unimaginable great patience and his “stress management” during my write-up. My thanks further go to his caring family for their support.

My time through my PhD research has been very enjoyable, and great credits need to go to the Centre for Bioengineering at the University of Canterbury and all the students who were there with me. The centre has been a friendly and comfortable environment to work in, and the people in the centre have been the best friends a person could wish for. Thanks for all the good times and inspiration. You let me learn so much more than what my research encompassed. Finally, thanks to the Foundation of Research, Science and Technology for the Top Achiever Doctoral Scholarship through my PhD study. In particular, the conferences I attended through the foundation’s funding really extended my vision in the research field.

Contents

List of Figures

List of Tables

Nomenclature

α_G	Michaelis-Menten constant for insulin-stimulated glucose removal saturation
α_I	Michaelis-Menten constant for plasma insulin disappearance saturation
ACCP	American College of Chest Physicians
APACHE	Acute Physiology and Chronic Health Evaluation
BG	blood glucose
cdf	cumulative distribution function
CGM	continuous glucose measurement
CGMS	continuous glucose measurement system (Medtronic Inc.)
EGP	endogenous glucose production
G	blood glucose concentration above G_E
G_E	equilibrium blood glucose level
HGI	Hyperglycemic Index
I	blood plasma insulin concentration
I_B	endogenous insulin production
ICU	intensive care unit
IQR	inter-quartile range
IVGTT	Intravenous Glucose Tolerance Tests
k	rate of insulin transport and utilisation in the interstitium
k_{pr}	rise rate of exogenous plasma glucose appearance
k_{pd}	decay rate of exogenous plasma glucose appearance
MPC	model predictive control
n	plasma insulin decay rate
NRLS	non-linear recursive least square

P	external nutrition infusion rate
p/pdf	probability density (function)
PD	proportional-derivative
p_G	rate of endogenous glucose removal
PI	probability interval
PID	proportional-integral-derivative
POCT	Point of Care Tests
Q	interstitium insulin concentration
RCT	randomised controlled trial
S_I	insulin sensitivity index
SPRINT	Specialized Relative Insulin and Nutrition Tables
std	standard deviation
u_{ex}	exogenous insulin input
V_G	glucose distribution volume
V_I	insulin distribution volume

Abstract

Hyperglycemia is prevalent in critical care, as patients experience stress-induced hyperglycemia, even with no history of diabetes. Hyperglycemia has a significant impact on patient mortality, outcome and health care cost. Tight regulation can significantly reduce these negative outcomes, but achieving it remains clinically elusive, particularly with regard to what constitutes tight control and what protocols are optimal in terms of results and clinical effort.

Hyperglycemia in critical care is not largely benign, as once thought, and has a deleterious effect on outcome. Recent studies have shown that tight glucose regulation to average levels from 6.1–7.75 mmol/L can reduce mortality 17–45%, while also significantly reducing other negative clinical outcomes. However, clinical results are highly variable and there is little agreement on what levels of performance can be achieved and how to achieve them.

A typical clinical solution is to use ad-hoc protocols based primarily on experience, where large amounts of insulin, up to 50 U/hr, are titrated against glucose measurements variably taken every 1–4 hours. When combined with the unpredictable and sudden metabolic changes that characterise this aspect of critical illness and/or clinical changes in nutritional support, this approach results in highly variable blood glucose levels. The overall result is sustained periods of hyper- or hypo- glycemia, characterised by oscillations between these states, which can adversely affect clinical outcomes and mortality. The situation is exacerbated by exogenous nutritional support regimes with high dextrose content.

Model-based predictive control can deliver patient specific and adaptive control, ideal for such a highly dynamic problem. A simple, effective physiological model is presented in this thesis, focusing strongly on clinical control feasibility. This model has three compartments for glucose utilisation, interstitial insulin

and its transport, and insulin kinetics in blood plasma. There are two patient specific parameters, the endogenous glucose removal and insulin sensitivity. A novel integral-based parameter identification enables fast and accurate real-time model adaptation to individual patients and patient condition.

Three stages of control algorithm developments were trialed clinically in the Christchurch Hospital Department of Intensive Care Medicine. These control protocols are adaptive and patient specific. It is found that glycemic control utilising both insulin and nutrition interventions is most effective. The third stage of protocol development, SPRINT, achieved 61% of patient blood glucose measurements within the 4–6.1 mmol/L desirable glycemic control range in 165 patients. In addition, 89% were within the 4–7.75 mmol/L clinical acceptable range. These values are percentages of the total number of measurements, of which 47% are two-hourly, and the rest are hourly. These results showed unprecedented tight glycemic control in the critical care, but still struggle with patient variability and dynamics.

Two stochastic models of insulin sensitivity for the critically ill population are derived and presented in this thesis. These models reveal the highly dynamic variation in insulin sensitivity under critical illness. The stochastic models can deliver probability intervals to support clinical control interventions. Hypoglycemia can thus be further avoided with the probability interval guided intervention assessments. This stochastic approach brings glycemic control to a more knowledge and intelligible level.

In "virtual patient" simulation studies, 72% of glycemic levels were within the 4–6.1 mmol/L desirable glycemic control range. The incidence level of hypoglycemia was reduced to practically zero. These results suggest the clinical advances the stochastic model can bring. In addition, the stochastic models reflect the critical patients' insulin sensitivity driven dynamics. Consequently, the models can create virtual patients to simulated clinical conditions. Thus, protocol developments can be optimised with guaranteed patient safety.

Finally, the work presented in this thesis can act as a starting point for many other glycemic control problems in other environments. These areas include the cardiac critical care and neonatal critical care that share the most similarities to the environment studied in this thesis, to general diabetes where the population

is growing exponentially world wide. Furthermore, the same pharmacodynamic modelling and control concept can be applied to other human pharmacodynamic control problems. In particular, stochastic modelling can bring added knowledge to these control systems. Eventually, this added knowledge can lead clinical developments from protocol simulations to better clinical decision making.

Chapter 1

Introduction

Automated blood glucose control has been a major pursuit of many researchers for at least three decades due to the toll taken by diabetes and its complications. The incidence of both Type 1, Type 2 and insulin dependent Type 2 diabetes is growing and predicted to reach epidemic incidence level in western populations [Alberti and Zimmet, 1998; King, 1999; ADA (American Diabetes Association), 2002; Nyomba et al., 2003; IDF (International Diabetes Federation), 2003; Wild et al., 2004; Williams, 2005; CDC (Centers for Disease Control and Prevention), 2005, 2006; Koster et al., 2006; Lee et al., 2006; Li et al., 2006; Mainous et al., 2006; Milton et al., 2006; Narayan et al., 2003, 2006; Hossain et al., 2007]. In 2001, over 120 million people were affected by diabetes worldwide, and this number is expected to rise to 300 million by the year 2025, with annual costs growing exponentially with the number of cases [Thomson et al., 2001; ADA (American Diabetes Association), 2002; Nyomba et al., 2003; IDF (International Diabetes Federation), 2003; Wild et al., 2004; Williams, 2005; CDC (Centers for Disease Control and Prevention), 2005, 2006; Koster et al., 2006; Lee et al., 2006; Li et al., 2006; Mainous et al., 2006; Milton et al., 2006; Narayan et al., 2003, 2006; Hossain et al., 2007]. In addition, the cost of diabetes and its complications are predicted to reach up to 10% of health care costs by 2020 [ADA (American Diabetes Association), 1998; PWC (PriceWaterhouseCoopers), 2001]. In New Zealand, the New Zealand Ministry of Health [2002] conservatively estimates that in 1996 almost 5000 adults were newly diagnosed with diabetes, approximately 81,000 were known to have diabetes, and almost 1500 deaths were attributable to diabetes. In addition, the number of new diagnoses of diabetes in 2011 is forecast to exceed 11,000, the number of people known to be living with diabetes may exceed 145,000, and the number of deaths attributable to diabetes may exceed 2,100.

Elevated blood glucose levels, or hyperglycemia are a result of dysfunctional glucose regulatory mechanisms, which implies some degree of impaired insulin secretion and/or insulin resistance. Untreated hyperglycemia, over time, can lead to costly complications such as retinopathy, cataracts, ulcers, skin infections, heart disease, peripheral vascular disease, cerebrovascular disease (stroke) and neuropathy (nervous system disease), to name a few of the more serious and costly long-term outcomes of this chronic disease [Barrett-Connor and Khaw, 1988; Alberti and Zimmet, 1998; Capes et al., 2000; Bistrian, 2001; Van den Berghe et al., 2001; Livingstone and Ferns, 2003; Ben-Mahmud et al., 2006]. The immune system also fails to function optimally in the presence of high blood glucose levels [Marik and Raghavan, 2004; Jeandidier and Boullu-Sanchis, 2006; Turina et al., 2005]. At 8 mmol/L, the immune response is only 50% or less effective, and at 10 mmol/L, the immune response is essentially completely ineffective [Weekers et al., 2003]. An ineffective immune response can have obvious significant consequences in terms of fighting off bacterial or viral infections, in addition to the other complications noted. The overall outcome is a chronic disease state with costly long-term complications that impose significant health and economic burden on the patient, their families, and the broader society.

The prevalence of hyperglycemia in critical care has grabbed its own research focus in recent years due to several landmark studies by Van den Berghe et al. [2001, 2003] and Krinsley [2003b, 2004]. These studies led to several additional clinical and model-based studies [Van den Berghe et al., 2006; Van den Berghe, 2004a; Krinsley, 2003a; Chase et al., 2005c; Doran et al., 2004b; Wong et al., 2006b; Laver et al., 2004; Goldberg et al., 2004b]. As a result, it has become a significant research area in its own right, and has been recently reviewed by Chase et al. [2006b, 2007].

Critically ill patients often experience stress-induced hyperglycemia, even with no history of diabetes [Bloomgarden, 2003; Capes et al., 2000; Christensen, 2001; Coursin and Murray, 2003; Esposito et al., 2003; Finney et al., 2003; Krinsley, 2003a; McCowen et al., 2001; Mizock, 2001; Ousman, 2002; Peck, 2004; Umpierrez et al., 2002; Van den Berghe et al., 2001, 2003]. The increased counter-regulatory hormone and cytokine response stimulates endogenous glucose production and increases effective insulin resistance. Absolute and relative insulin deficiency is also a contributing factor. In addition, some steroid-based therapies antagonise insulin action and production, further exacerbating the problem.

Studies also indicate that high glucose content nutritional support regimes result in excess blood glucose levels [Patino et al., 1999; Weissman, 1999; Woolfson, 1980; Elia et al., 2005]. More recently, reductions in enteral nutrition [Elia et al., 2005; Ahrens et al., 2005; Kim et al., 2003] or its carbohydrate content [Patino et al., 1999] led to reductions in glycemic levels. In addition, the reduced use of dextrose as a diluent in intravenous medication resulted in reductions in glycemia [Krajicek et al., 2005]. Similarly, analysis of carbohydrate feeding levels with respect to the American College of Chest Physicians (ACCP) guidelines indicated that 33–66% reductions in carbohydrate content reduced the risk of mortality compared to feeding at the current ACCP guideline levels [Krishnan et al., 2003]. Finally, reducing either feed or glucose diluent has also been shown to alleviate the impact of the hyperglycemic counter-regulatory response that drives this problem [Mizock, 2001; McCowen et al., 2001; Thorburn et al., 1995; Larsen et al., 2002].

Clinically, hyperglycemia can be a marker of severity of illness and is directly associated with mortality. In addition, it is also associated with increases in other negative clinical outcomes, including severe infection [Bistrian, 2001], sepsis and septic shock [Das, 2003; Branco et al., 2005; Oddo et al., 2004; Marik and Raghavan, 2004], myocardial infarction [Capes et al., 2000], and polyneuropathy and multiple-organ failure [Van den Berghe et al., 2001; Langouche et al., 2005]. In each of these cases or patient subgroups, lower blood glucose levels were associated with reduced mortality and/or complications. Similar studies have associated early hyperglycemia (in a patient stay) with mortality in trauma patients [Laird et al., 2004; Jeremitsky et al., 2005; Holm et al., 2004]. Finally, there is also evidence of significant reductions in the need for dialysis, bacteremia testing and the number of blood transfusions with aggressive blood glucose control using intensive insulin therapy [Van den Berghe et al., 2001, 2003; Krinsley, 2003b]. All of these results point towards the conclusion that the control of blood glucose levels in critical care have a significant clinical impact.

1.1 Significance of Glycemic Control in Critical Care

There are two initial landmark studies that have observed and defined the glycemic control problem in the intensive care units (ICU) and the impact of tight control

on mortality and other clinical outcomes. First, Van den Berghe et al. [2001, 2003] showed that tight blood glucose control to less than 6.1 mmol/L reduced cardiac surgical ICU patient mortality by up to 45% in a randomised controlled trial. Krinsley [2003b, 2004] reported a 17–29% total reduction in mortality over a wider, more critically ill, ICU population with a higher glucose limit of 7.75 mmol/L. This mortality reduction was observed by comparing the controlled groups to a matched cohort of retrospective data with enough patients to show statistical power for the intervention.

An interesting point arises from comparing the retrospective study of Krinsley [2003b, 2004] with the randomised trial of Van den Berghe et al. [2001, 2003] for any such study. Van den Berghe et al. [2001, 2003] made a comparison to an essentially equally treated and matched cohort whose average blood glucose was allowed, or more specifically, controlled, to be relatively high (9–10 mmol/L). However, as recent evidence has shown, the higher glucose levels in the control group may have skewed the differences in clinical outcome between groups [Chase et al., 2006b]. Thus, comparing two cohorts of similar given hyperglycemia and condition subjected to different glycemic treatments may provide a more objective comparison rather than having a group deliberately controlled to a less desirable level of care.

In particular, given that the benefit of tight control appears to be continuous or analog with increasingly tight and lower glucose levels, a comparison of a high level to a lower level may well predetermine the clinical study's outcome or skew it. In contrast, comparing two matched cohorts who received the best care approach available for glycemic levels and similar care otherwise (e.g. a retrospective recent past cohort) more directly shows the difference of introducing a new tight glycemic control approach.

Hence, the retrospective before-after study design of Krinsley [2003b, 2004] may be more appropriate for investigating the effects of introducing tighter glycemic control into the ICU. More specifically, a randomised controlled trial (RCT) in a single hospital risks contamination in care across groups as well as requiring a no-change in care or specifically controlled group. In the latter choice, as in Van den Berghe et al. [2001], it is difficult to pick a controlled glycemic level indicative of otherwise unaltered care. Thus, the control group is either contaminated or essentially undefined in a RCT unless different hospitals with

matched cohorts are used. However, this last choice is effectively equivalent to the retrospective cohort used in before-after trials. Nevertheless, in either study, the outcome shows that tight control does have a significant impact despite any criticisms of either study format [Chase et al., 2007].

Currently, the exact reasons for the reductions in mortality and other clinical outcomes are not fully known, but have been extensively analysed in these original and other works [Bellomo and Egi, 2005; Diringer, 2005; Finney et al., 2003; Krinsley, 2003a; Langouche et al., 2005; Mesotten et al., 2004; Van den Berghe, 2004b,a; Van den Berghe et al., 2005]. However, recent studies by Weekers et al. [2003] on a rabbit model do indicate some major causes. Specifically, tight control reduces glucotoxicity due to high blood glucose, or hyperglycemia, which in turn:

1. Reduces oxidative stress and superoxides.
2. Reduces stress hormone responses.
3. Reduces damage to the endothelium and vascular walls [Langouche et al., 2005].
4. Increases immune response and bacteriocidal activity.

These results have been supported by a variety of recent, closely related studies [Soop et al., 2002; Hansen et al., 2003; Jeschke and Herndon, 2004; Butler et al., 2005; Dandona et al., 2006; Gubern et al., 2006]. All of these studies examine aspects of systemic inflammation that is common in critical illness, immune response, and the resulting impact or damage at a cellular level.

Both Van den Berghe et al. [2001, 2003] and Krinsley [2003b, 2004] used ad-hoc glycemic control protocols that did not employ models or control theory, and relied only on exogenous (intravenous) insulin intervention to reduce blood glucose levels. In particular, they were both rules-based protocols based on clinical experience and titration-based sliding scale. They were also both altered as needed by clinical staff and thus not necessarily general to any or all patients.

The main clinical differentiators of these two landmark studies are the glycemic limits used and the levels of critical illness of the cohorts, as measured by Acute Physiology and Chronic Health Evaluation II (APACHE II) score. In particular,

Krinsley [2003b, 2004] studied a broader, more representative critical care cohort with a much greater level of critical illness, reporting an average APACHE II score of 16.9 (IQR: 13–24). Due perhaps to the severity of illness of their cohort, a higher titration limit and goal was established. In contrast, Van den Berghe et al. [2001, 2003] reported a much lower median APACHE II score of 9 (IQR: 6–13), in combination with their much lower glycemic target limit.

Two important results can be drawn from these two initial clinical studies. First, tighter control with lower glycemic limits appears to offer increased benefit in terms of reduced mortality and reductions in other measurable negative clinical outcomes. Second, the level of critical illness is generally proportional to observed hyperglycemia and insulin resistance [Van den Berghe et al., 2003; Krinsley, 2003a; Lind and Lithell, 1994; Christiansen et al., 2004; Mentula et al., 2005; Basi et al., 2005], which will result in a decreased ability to reduce blood glucose with insulin alone for more critically ill cohorts. However, neither study addressed issues such as blood glucose variability, time within a desired glycemic band, nor other typical control system oriented performance metrics that would help further clarify the requirements for tight glycemic control. For example, how tight must the controlled glycemic range be around an average value, and what target level or range is most optimal.

These two conclusions, together with other unaddressed issues, form the basis of the overall glycemic control problem definition in the critically ill population. In addition, the potential for applying dynamic systems modelling and control methods to achieve significant clinical improvements is clear. More specifically, while other studies are being undertaken to further validate many of the results already available across broader populations and cohorts, the clinical evidence for tight control is greater than for the oftentimes current practice of tolerating a level of hyperglycemia [Angus and Abraham, 2005].

1.2 Glycemic Control Problem Outline

There are typically three main elements in any control problem:

1. Sensors and signal processing — measurement of controlled parameters
2. Dynamic modelling and parameter identification — placing measurements into a dynamic systems framework to better identify trends and future response to intervention
3. Control method or protocol — application of steps 1 and 2 to optimise intervention and response.

Sensors and signal processing determine the quality and frequency of data for the controller. The dynamic model and parameter identification methods relate to the (predictive) accuracy of any controller, and thus its ability to safely and accurately lower glucose levels in this case. Finally, the control algorithm employs both these elements to determine the appropriate intervention to achieve a set performance goal. Generically, these three elements are all inter-related and lower complexity or quality from one is typically offset by requiring greater quality or complexity from the others. Figure 1.1 shows a schematic of the basic control schemes employed to outline the general control problem and its major elements in the context of glycemic control.

While evidence for, and a desire to provide, quality glycemic management in the critical care are growing, intensive care units also present a highly controlled environment where the general glycemic control problem can be stripped down to its most basic form. In particular, the inputs and outputs of the control system are more easily measured, monitored, and modelled in critical care, given the typical use of intravenous insulin, and intravenous or enteral nutrition delivery. Thus, starting from the intensive care unit, the glycemic control system that arises from this platform can be extended to other glycemic control problems, and eventually benefit general diabetic patients in everyday life. Figure 1.2 shows this pathway starting from intensive care working its way down the pyramid, where the number of variables, non-linearities and uncertainties that increases the difficulty of the control design problem increases at each level. Very importantly, although each layer of the pyramid poses different conditions and

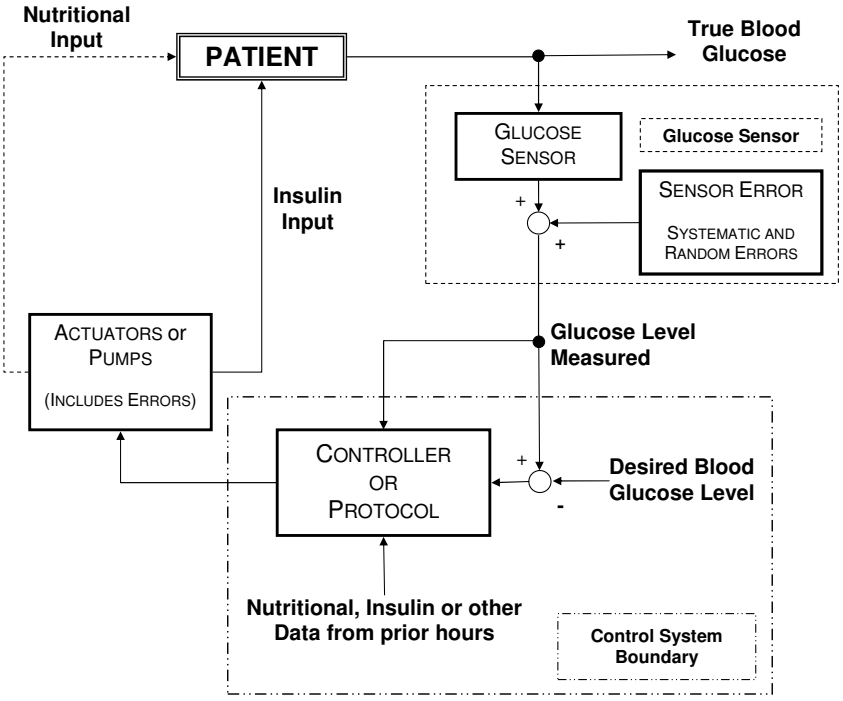

Figure 1.1 Basic model-based glycemic control system schematic showing the primary blocks encompassing sensing, actuation and control implementation. The control system boundary is shown by dash-dot lines, and the nutritional input line is dashed to indicate that this quantity may be controlled as part of glycemic control or set based on other clinical requirements. Sensor errors are shown as a separate block due to their potential size and impact on control. There may be some error in the actuators or pumps depending on their design specifications such as dosing limits and precision. This schematic diagram shows all possible set up of glycemic control systems. Arrows are suggestive and may not all exist in one setting.

problems that may be encountered, they share the same fundamental metabolic system models for the pharmacokinetics of insulin and the pharmacodynamic interaction of glucose and insulin. Therefore, glycemic control research in the ICU holds an important role as the central portion or key to future, broader diabetes solutions.

1.3 Sensors and Signal Processing

In glycemic control, the primary measurement available is plasma glucose level. Current glucose sensing methods can be broken into four broad areas for control applications. These areas represent distinctions in quality, time, software storage and links, and data density, all of which impact the resulting control problem.

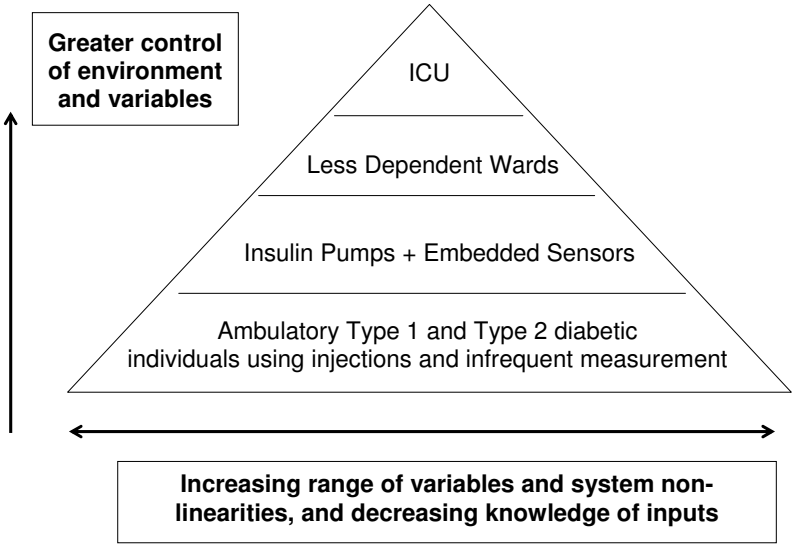

Figure 1.2 Pyramid description of glycemic control problems in terms of ability to control variables based on knowledge of their value or input (vertical axis), and the range of variables to be considered and resulting level of uncertainty (horizontal axis).

Lab or Gold Standard Measures consist of laboratory reference measurements using standard techniques. They offer the lowest error ($< 3\%$) and best repeatability [Peet et al., 2002]. Turnaround time for results can be quite long due to the logistics of sending samples to a lab. However, modern blood gas analysers can now be installed in specific units offering similar results to clinical staff within 1–3 min [Peet et al., 2002; Beneteau-Burnat et al., 2004; Papadea et al., 2002].

Point of Care Tests (POCT) can be linked directly to patient databases and records and are becoming standard in many ICUs. They range from blood gas analysers to specialised POCT pin-prick test strip devices. Accuracy ranges from blood gas analysers ($< 3\%$) [Peet et al., 2002; Beneteau-Burnat et al., 2004; Godje et al., 1997; Solnica et al., 2001] to pin-stick results (typically 7–12%) [Louie et al., 2000; Buhling et al., 2003]. Data density is typically no greater than hourly due to discomfort and the effort required around other clinical duties.

Pin-Stick Bedside Test Kits are the current standard in many ICUs and most ambulatory diabetic individuals. They offer rapid results in less than 30

seconds and require only 1–2 min of total clinical effort, but have errors of 7–12% over common glycemic ranges [Chen et al., 2003; Solnica et al., 2003; Weitgasser et al., 1999; Johnson and Baker, 1998, 1999; DirectNet, The Diabetes Research in Children Network Study Group, 2005; Demers et al., 2003]. They are rarely used more than hourly. In critical care, pin-stick measures can be used to extract subcutaneous blood or sampled from an arterial line. The latter approach eliminates the 5–20 min lag in plasma glucose levels that can exist between plasma and interstitial fluid [Rebrin et al., 1999; Wilinska et al., 2004; Boyne et al., 2003].

Semi-Invasive "Continuous" Sensors are emerging sensors offering automated or semi-automated measurements of blood glucose concentration. The most commonly reported types, at this writing, are the continuous glucose measurement system (CGMS) from Minimed/Medtronic Inc. and the GlucoWatch^{TM} Biographer [DirectNet, The Diabetes Research in Children Network Study Group, 2004; Goldberg et al., 2004a; Weinzimer et al., 2003]. They offer very frequent measurements every 5–15 min, but with errors up to 40% reported over a wide variety of studies [DirectNet, The Diabetes Research in Children Network Study Group, 2004; Goldberg et al., 2004a; Weinzimer et al., 2003; Garg et al., 1999; Dunn et al., 2004; Pitzer et al., 2001; Tierney et al., 2000, 2001; Tsalikian et al., 2004; Javid et al., 2005; Kovatchev et al., 2004; Gilligan et al., 2004; Klonoff, 2002].

Portable blood gas analysers offer the best quality results for fitting models to determine control inputs due to their lower error. At the other end of the spectrum, emerging sensors, such as the CGMS from Medtronic Inc., offer very high data density, but with much greater error. The standard pin-stick bedside testing kit is still the most commonly used measure in all situations. It offers greater ease of use than a portable or local blood gas analyser with slightly greater error, but much lower data density than emerging continuous sensors. Finally, note that plasma insulin measurement would offer added information for modelling and control. However, the lab turnaround time for this measurement is generally too long to be of direct use in real-time clinical control.

Hence, there is a significant tradeoff involved in selecting the type of measurement or accounting for the type available in a specific clinical setting. Less frequent measurement requires greater prediction capability from the model.

More frequent measurement allows potentially much simpler models. In contrast, greater errors will require more intensive signal processing, as well as models more robust to those errors in patient specific parameter fitting and prediction.

Perhaps the most common clinical measurement issue in glycemic control is frequency. More frequent measurement than most typical clinical practice has been a hallmark of both initial landmark glycemic control studies [Van den Berghe et al., 2001, 2003; Krinsley, 2003b, 2004], varying between 1 and 4 hours. However, specialised additional staff were required to manage the extra workload reported. Other pilot studies and surveys have reported the extra clinical burden of intensive insulin therapy for glycemic control as "burdensome" or "taxing" [Mackenzie et al., 2005; Bland et al., 2005; Waeschle et al., 2005; Di Nardo et al., 2004; Scholtz et al., 2005]. Hence, the ability to limit or automate measurement via implanted continuous sensors could be seen as critical. Thus, emerging sensors offer significant promise for automating glycemic control in this regard.

Frequent measurement and its impact on glycemic control have also been studied both in simulation [Wong et al., 2005; Chase et al., 2005a; Lonergan et al., 2006b] and clinically [Chase et al., 2005a; Wong et al., 2006a,b], including the analysis of long-term retrospective data [Hann et al., 2005]. Results show that fewer, less frequent measurements often result in greater glycemic variation in critical care and poorer outcome [Doran, 2004; Shaw et al., 2005; Lonergan et al., 2006b], as might be expected from a strictly control system perspective. Similar results have been seen in treating ambulatory diabetic individuals [Hirsch and Brownlee, 2005; McDonnell et al., 2005].

Overall, the different types of measurement offer a series of fundamental tradeoffs. Typically, a given unit will have a standard set of measures and practices, which the control engineer will have to work with, removing choice in the types of sensors. It might be expected that if current semi-invasive sensors continue to improve, they will come to replace many of the other types. However, significant hurdles related to error, ease of use, and reliability remain [Klonoff, 2005a,b]. Hence, while there may currently be little choice in many practical cases, this area is rapidly developing.

Currently, pin-stick bedside test kits are most commonly found in ICUs, with typical error of 7–12% and offer results in 30 seconds or less. The tradeoff between

its fast turnover time and comparatively small error, and its labour requirement and associated discomfort will need to be investigated to achieved specific control performance goals.

1.4 Model-Based Glycemic Control

Currently, most typical ICU practice in glycemic management is comprised of ad-hoc protocols based primarily on experience, where relatively large amounts of intravenous insulin, up to 50 U/h, are titrated against glucose measurements variably taken every 1–4 hours. When combined with the unpredictable and sudden metabolic changes that characterise this aspect of critical illness and/or clinical changes in nutritional support, this approach results in highly variable blood glucose levels. The overall result is sustained periods of hyper- or hypoglycemia, characterised by oscillations between these states, which can adversely affect clinical outcomes and mortality. The situation is exacerbated by exogenous nutritional support regimes with high dextrose content. Hence, there is an emerging, strong need for the more rigorous analysis and methods that model-based control methods bring to this type of problem.

A physiological model that captures the glucose-insulin system dynamics is thus the basis for more optimally addressing the glycemic control problem. Metabolic modelling of the glucose-insulin system has a very deep history in the published literature. The vast majority of these models have their roots in basic compartment modelling with differential equations [Carson and Cobelli, 2001]. To date, the primary use of metabolic models has been the development of model-based measures to assess metabolic parameters, with a particular focus on measuring insulin sensitivity [e.g. Bergman et al., 1979, 1981, 1985; Pacini and Bergman, 1986; Yang et al., 1987; Mari, 1998; Mari et al., 2001, 2003; Lotz et al., 2006b; Toffolo et al., 1999, 2006].

However, a model for glycemic control in the ICU needs to be applicable for real-time clinical control, addressing the needs and limitations typical of most ICUs. Metabolic models that are complex in physiological details, although accurate given rigorous laboratory data, are not often practical for real-time glycemic control utilising less frequent and noisier blood glucose measurements. Therefore,

a model suitable for glycemic control in the ICU needs to satisfy the following basic criteria:

- Accurately capture insulin and glucose pharmacokinetics, and glucose-insulin pharmacodynamics typical of critically ill patients.
- Feature a simple structure preferably requiring only blood glucose levels as physiological feedback.
- Address inter- and intra-patient variability over time.
- Have rapidly identifiable patient specific model parameters.

Given an accurate model satisfying these criteria, model-based glycemic control can offer individualised control adaptable to the critically ill patients' highly dynamic physiological condition. Furthermore, such a physiological model may also be used as a patient simulator for protocol development given realistic patient specific parameters [Hann et al., 2005; Wong et al., 2006a; Lonergan et al., 2006b,a]. Additional knowledge of critically ill population's variable dynamics can further enhance model-based control with more accurate predictive performance.

1.5 Control Performance Measures

Understanding the difficulties and defining desired controller performance is the first step to controller design. A variety of performance metrics have been used in different critical care glycemic studies, with their differences often confounding direct comparisons between studies. These metrics can be summarised as four basic goals:

Average Blood Glucose Level: calculated over all measurements [Krinsley, 2003b, 2004] or over limited measurements, such as first morning measurement [Van den Berghe et al., 2001, 2003]. The average is the simplest performance measure and the one used in both landmark clinical studies. However, it provides no further information on glucose excursions or tightness of control. An important consideration is the use of a trapezoidal mean

to obtain the proper mean value if the sampling period is irregular [Doran, 2004; Shaw et al., 2005]. In addition, an average value should utilise all blood glucose measurements and not just a morning average, as in Van den Berghe et al. [2001, 2006], which can hide variability and poor control.

Time in a Glycemic Band: calculated as the time or percentage of measurements in a specific band, such as 4–6.1 mmol/L [Lonergan et al., 2006b; Wong et al., 2006a,b] or 4.5–6.1 mmol/L [Plank et al., 2006]. Maximising this metric is essentially equivalent to minimising the Hyperglycemic Index (HGI) or area under the blood glucose level curve [Van den Berghe, 2004b; Vogelzang et al., 2004]. This metric provides a surrogate measure of the average value, as well as an indication of the tightness of the glycemic control result. Using multiple overlapping or contiguous bands provides a good definition of the total glucose distribution under control.

Glucose Variability: measured as the standard deviation or 90% interval over the data. This metric has only been employed recently [Chase et al., 2005a; McDonnell et al., 2005] and measures the tightness of blood glucose control around the average or target value. It is also increasingly important in managing Type 1 diabetes [Kovatchev et al., 2004, 2005; Hirsch and Brownlee, 2005]. However, it provides no indication of the absolute glycemic levels obtained and some methods assume normal or other statistical distributions that may not match the data. Hence, confidence intervals determined from the data may prove more useful. Note that recent studies indicate the variability in control may be a critical determinant of outcome [Chase et al., 2007].

Hypoglycemic Episodes: measured as the number or percentage of measurements that are below a defined hypoglycemic threshold. The typical definition is 2.2 mmol/L, although some studies use higher thresholds [Lonergan et al., 2006b; Plank et al., 2006]. Variability also captures some of this information when associated with the average or median glucose values. More importantly, this measure is a critical indicator of the safety of the control methods used.

To date, only the first metric, the average glucose value, has been correlated with the clinical mortality outcome for different cohorts of patients. More specifically, it is currently assumed, based on limited results to date, that tight control

and mortality are linked by average glucose value obtained. However, recent results also linked range and/or peak glucose values to critical care mortality [Christiansen et al., 2004; Doran, 2004; Holm et al., 2004; Krinsley, 2003a; Shaw et al., 2005], providing impetus to using other metrics as well. Finally, variability indicating the tightness of control may also play a significant role in determining outcome [Chase et al., 2007], as well as reducing exposure to hyperglycemic levels.

In addition, as discussed in Section 1.1, studies by Van den Berghe et al. [2001, 2003] and Krinsley [2003b, 2004] showed potential correlation between the level of critical illness and achievable glycemic regulation, rather than achieving mortality reduction more evenly across the cohort. Thus, using the same protocol with a different cohort may not obtain substantially the same results, and similarly for a different protocol on substantially the same cohort. Therefore, protocols that produce similar results in one metric, but different outcomes in others, may have different overall clinical outcomes.

Hence, a controller designed with a "well-balanced" goal that is adaptable to different levels of illness would be considered ideal. Nevertheless, the consequent protocol should fit inside the limitations of a given ICU's clinical practice and work flow. In particular, with the ICU being a very intense environment, minimal labour requirements and good ergonomics are critical factors in control protocol design, particularly for ensuring compliance and uptake of the resulting protocol by clinical staff.

1.6 Critical Care Glycemic Control Summary

The significance of glycemic management in critical care is undeniable by the 17–45% reduction in mortality when average blood glucose levels are regulated to between 6.1–7.75 mmol/L. This level of change or impact for a single clinical protocol is rarely seen in intensive care research and represents a chance to create an atypical disruptive step change in care. In addition, intensive care units present a highly controlled environment ideal for model-based glycemic control development and validation. Sharing similar insulin-glucose metabolic dysfunctions, solutions to the critical care hyperglycemia problem may eventually extend

to wider populations suffering from diabetes.

With current sensor technology allowing real-time control loops to be closed, model-based glycemic control offers significant advantages over traditional ad-hoc protocols where vicious cycles of hyper- and/or hypo- glycemia are not uncommon. Hence, there are significant opportunities to improve safety and quality of care. Model-based glycemic control thus offers the following advantages:

- It is accurate and adaptable to different patients
- It is adaptable to evolving critical illness
- It provides systematic glycemic reduction or regulation
- It will perform to specifically designed performance criteria
- It can deliver predictions of intervention outcomes
- It ensures better patient safety, particularly against hypoglycemia

The last two points are what drives the glycemic control development towards model predictive control (MPC). These two qualities of MPC promise more intelligible glycemic control solution over other methods. Finally, during model and controller design, ICU environment requirements and limitations must be carefully considered, and the desired controller performance goals be carefully chosen.

In the rest of this thesis, Chapter 2 presents a physiological model for model-based glycemic control in the ICU, addressing the model requirements raised in Section 1.4. Chapter 3 then presents the parameter identification method for fast identification of model parameters. Control protocols are explored in Chapter 4, where some clinical trial results are presented and controller performance matrices discussed. Finally, the highly dynamic glucose-insulin metabolism of the critically ill is studied and modelled in Chapters 5 and 6, creating a stochastic metabolic control model to improve results. The consequent critical care patient simulator is presented in Chapter 7. The thesis concludes in Chapters 8 and 9 with conclusions and future avenues of suggested research effort.

Chapter 2

Glucose-Insulin Regulatory Model

The basis of many control problems is a dynamic system model. An accurate biomedical control system model can capture, as well as predict, patient behaviour. Such a model offers a safe and fast means for protocol development without the limitation of clinical data scarcity [Stokes, 2000].

For decades, the human glucose-insulin system dynamics have been extensively studied, and models were created with different levels of detail and complexity to suit different applications. The vast majority of existing models have their roots in basic compartmental modelling with differential equations [Carson and Cobelli, 2001], and their complexity range from second [Lehmann and Deutsch, 1992; Ackerman et al., 1965] to 19^{th} [Parker et al., 1999] order. To date, the primary use of metabolic models has been the development of model-based measures to assess metabolic parameters, with a particular focus on measuring insulin sensitivity [e.g. Bergman et al., 1979, 1981, 1985; Pacini and Bergman, 1986; Yang et al., 1987; Toffolo et al., 1999, 2006; Mari, 1998; Mari et al., 2001, 2003]. The main feature in the development of many metabolic models has been increasing levels of physiological accuracy and/or resolution with a concomitant increase in the number of patient specific parameters to be identified and the overall model complexity.

In recent years, control-relevance has been getting more attention in metabolic system modelling as the demand and potential for automated glycemic control grows. Ideally, the most detailed physiological model can offer the most accurate predictive control. Yet, with increasing model complexity and the concomitantly increasing number of variables to be identified, clinically available data density and control computation time caps the complexity of clinically feasible control

models. Hence, control-relevant models need to be simple, yet accurately capture and predict clinical observations. In addition, critical care situations typically have a lesser amount of data available for fitting patient specific parameters compared to the frequent sampling typical of clinical physiology studies. Consequently, most clinical model-based control applications look for the simplest model to be effective.

This chapter presents the essence of the glucose-insulin physiology, and examines several forms of existing metabolic control-relevant models. Finally, a system model is presented with a suitable depth of dynamics for glycemic control application in the intensive care environment.

2.1 Physiological Basis of the Glucose-Insulin System

Given the extensive history of metabolic modelling of the glucose-insulin system, this thesis will not go into great length in this regard. In particular, a number of very good reviews exist that offer a broader overview [e.g. Carson and Cobelli, 2001; Parker and Doyle, 2001; Ferrannini and Mari, 2004; Lehmann and Deutsch, 1996]. A briefer overview of the basic model types used for clinical glycemic control is presented to illustrate the basic approaches employed in the field thus far. For reference, the fundamental physiological basis of the glucose-insulin system dynamics are illustrated in Figure 2.1.

Metabolic control systems and models start with titration models and controllers, such as the bio-stator [Albisser et al., 1974]. However, perhaps the best known model is the Minimal Model of Bergman et al. [1979, 1981]. This simple compartment model has two equations for glucose disappearance, and one for insulin kinetics:

Glucose disappearance:

$$\dot{G} = (X - P_1)G(t) + P_1 G_b + P(t) \tag{2.1}$$

$$\dot{X} = -P_2 X(t) + P_3(I(t) - I_b) \tag{2.2}$$

Insulin Kinetics:

$$\dot{I} = -nI(t) + \frac{u(t)}{V} \tag{2.3}$$

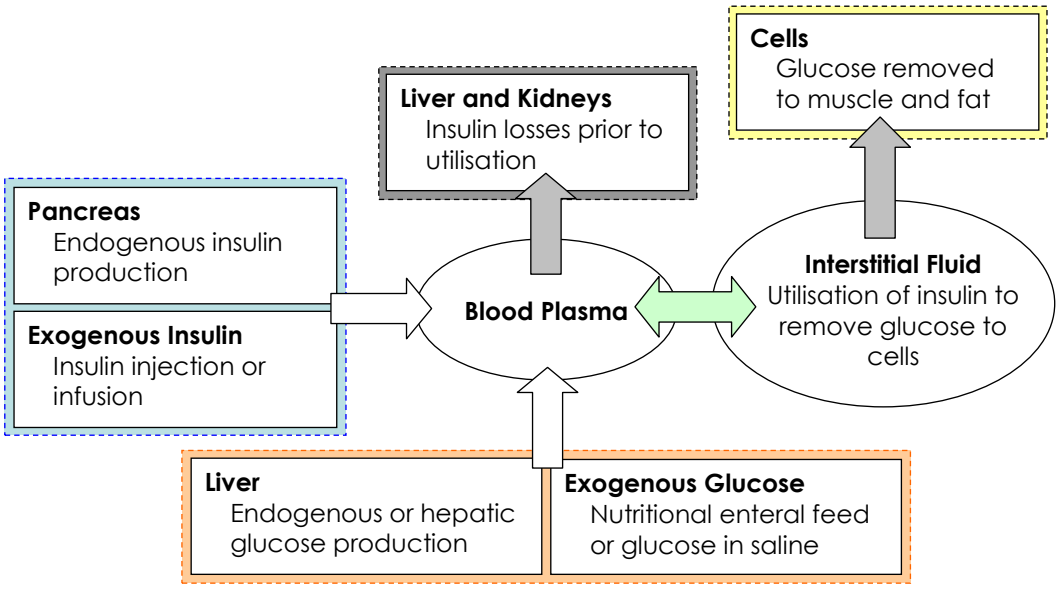

Figure 2.1 Basic outline of the fundamental physiology of glucose sources, insulin sources and their utilisation to remove glucose. Bi-directional arrows indicate potential for flow in both directions of glucose and/or insulin. Exogenous insulin is assumed intravenously administered in this case, and exogenous glucose appears via absorption from the gut or intravenous nutrition.

where t is the time, $G(t)$ is the total plasma glucose concentration at time t, $X(t)$ is proportional to insulin action in a remote compartment, and $I(t)$ is the plasma insulin concentration. Inputs to the system include $P(t)$, glucose appearance from external glucose sources, and $u(t)$, exogenous insulin. There are two terms that define the steady state or basal plasma glucose and insulin levels under no external influences, G_b and I_b. Three patient specific parameters, P_1, P_2 and P_3, arise from this model, with the ratio P_3/P_2 being the insulin sensitivity index. Signs of P_1 and P_2 are changed from the original publication in Equations (2.1) and (2.2) to have these parameters numerically positive valued per accepted sign conventions. A graphical representation of this Minimal Model definition is shown in Figure 2.2.

This model has since evolved into several forms, which are reported across a wide range of the literature. Most of the existing compartment models used for physiological studies or control have some origin in the Minimal Model. More importantly, this model clearly illustrates the three basic dynamic terms that must be captured for any glycemic control problem:

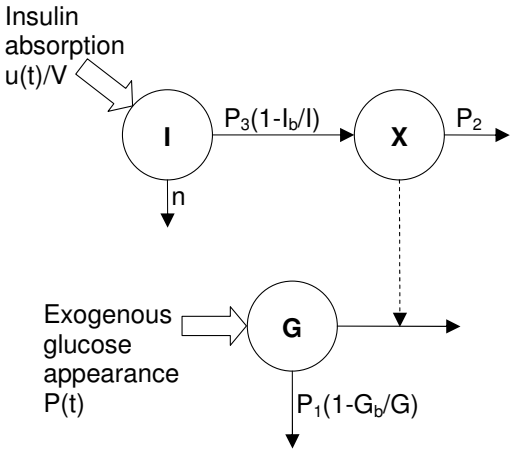

Figure 2.2 Minimal Model of Bergman et al. [1979, 1981]

1. Insulin pharmacokinetics and distribution — from exogenous input to action in the periphery

2. Glucose pharmacokinetics and/or appearance, where meal models for $P(t)$ in Equation (2.1) would add compartments

3. Glucose-insulin pharmacodynamics accounting for the insulin-mediated removal of glucose

For each point, more or less compartments or terms may be used, as compared to Equations (2.1)–(2.3). Additionally, nonlinearities for specific observed, or hypothesized, physiological dynamics may be added as necessary. Finally, terms or parameters may be re-defined such that they look similar in these equations, but have somewhat different physiological meanings. Thus, this model is a basis for most compartment models that followed, although significant evolution has occurred since its introduction.

However, the Minimal Model has some significant limitations, particularly with regard to use in clinical glycemic control [Doran et al., 2004a,b]. More specifically, it does not account for saturation of glucose removal by insulin [Prigeon et al., 1996; Natali et al., 2000; Rizza et al., 1981], saturation of insulin transport [Thorsteinsson, 1990; Frost et al., 1973; Ellemann et al., 1987; Prigeon et al., 1996], measurable and unmeasurable glucose compartments [Cobelli et al.,

1992, 1999; Vicini et al., 1997; Caumo et al., 1999], or the dynamics of insulin receptors and their mass [Hovorka et al., 2004], to name a few. All of these issues have been raised in the extensive physiological modelling literature, and several modified versions of this model developed as a result.

Another low-order model developed for glycemic management was created by Salzsieder et al. [1990a], and focused on Type I diabetes. This model has been verified in dogs [Salzsieder et al., 1985; Fischer et al., 1987], as well as humans [Salzsieder et al., 1990a,b; Fischer et al., 1990]. The third order differential equation system contains glucose (G) and insulin (I) effects, as well as overall net endogenous glucose balance (EGB):

$$\dot{G} = EGB(t) + CHO(t) \tag{2.4}$$

$$\dot{EGB} = -(b_1 + b_2)EGB(t) - b_3(I(t) + I^*(t)) + b_1(b_0 - CHO(t)) \tag{2.5}$$

$$\dot{I} = -kI(t) + I_{exg}(t) + I_G(t) \tag{2.6}$$

where $G(t)$, the blood glucose concentration, and $I(t)$, the plasma insulin, are both measurable state variables. The net overall endogenous glucose balance, $EGB(t)$ is not directly measurable. Five patient specific model parameters k and b_i $(i = 0, \ldots, 3)$ are to be identified. Absorption patterns of meals are described by $CHO(t)$, and I_{exg} is the exogenous insulin. $I_G(t)$ is the artificial beta cell algorithm developed by Salzsieder et al. [1990a] for feedback control. I^* is the insulin equivalent of muscular exercise. The symbols in Equations (2.4)–(2.6) are modified from the original paper for easy readability and consistency in this thesis. This model can be presented graphically, as shown in Figure 2.3

This model is successful at capturing steady state behaviour and slow dynamics for Type I diabetics. However, the model has incomplete representation of kinetics in glucose utilisation after interruption of insulin therapy, and overestimates glucosuria in the presence of insulin [Fischer et al., 1990]. These shortcomings are a result of under-modelling the insulin compartment, which is also a major identified weakness of the Minimal Model [Doran et al., 2004a,b].

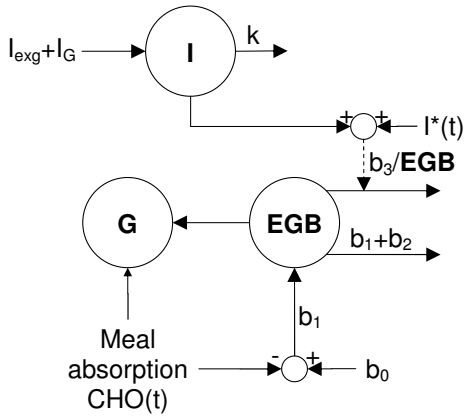

Figure 2.3 Glucose-insulin model of Salzsieder et al. [1990a,b]

At the other end of the spectrum of model complexity, the most detailed control-relevant physiological model to date is the 19^{th} order compartmental model of Parker et al. [1999]. This model was also developed for glycemic management of Type I diabetic patients. A schematic of the model is shown in Figure 2.4 with several compartments or other terms defined for each box shown in the figure.

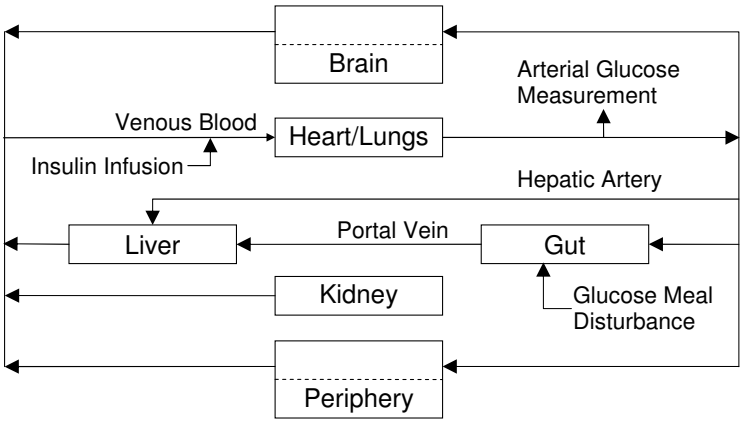

Figure 2.4 Schematic of the glucose-insulin system model of Parker et al. [1999]

Individual compartment models within the boxes shown are obtained by mass balance, and the brain and periphery represents slow or delayed effects. With measurements from a continuous glucose measuring (CGM) system, this model was designed for model predictive control (MPC). However, as current CGM sensors lack the desired clinical accuracy, studies by Parker et al. [1999, 2001]

showed successful simulation results that are yet to be fully realised in clinical testing. Nevertheless, the model is physiologically faithful to all known dynamics.

Another major issue with such a detailed and complex model is computational time involved in patient parameter identification. The use of a "nominal patient" with parameters based on mean values reported in the literature can reduce computational intensity, making MPC possible with such a model [Parker and Doyle, 2001]. However, careful sensitivity studies must be carried out to identify critical parameters, which should be patient specific, such as insulin sensitivity, and thus ensure crucial dynamics are not lost through over-simplifying the parameter identification process and/or over over-reliance on population parameters.

Finally, another model was designed for MPC by Hovorka et al. [2004], and was originally intended for Type I diabetic patients. However, it has recently been taken in similar form into an intensive care unit control setting [Plank et al., 2006]. A graphical representation of this model is shown in Figure 2.5.

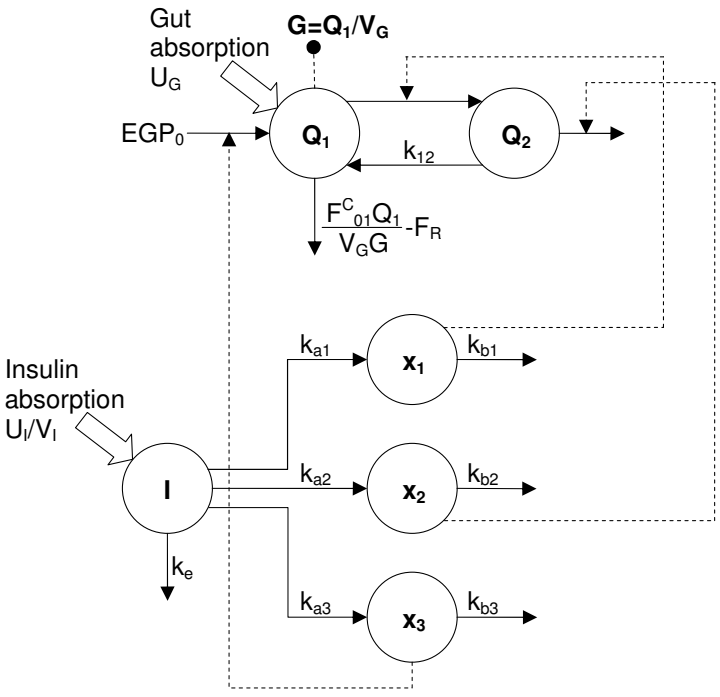

Figure 2.5 Glucose-insulin compartmental model of Hovorka et al. [2004]. Q_1 and Q_2 are glucose masses in the accessible and inaccessible compartments, I is plasma insulin, x_i represent insulin action of glucose transport, disposal and endogenous glucose production.

This model features many different transfer rates k_i between compartments and losses. EGP_0 represents endogenous glucose production (EGP) extrapolated to zero insulin concentration. F_{01}^c is the total non-insulin-dependent glucose flux, and is dependent on F_{01} to be identified for individual patients:

$$F_{01}^c = \begin{cases} F_{01} & \text{if } G \geq 4.5 \text{ mmol/L} \\ \dfrac{F_{01}G}{4.5} & \text{otherwise} \end{cases} \tag{2.7}$$

F_R is the renal glucose clearance defined:

$$F_R = \begin{cases} 0.003(G-9)V_G & \text{if } G \geq 9 \text{ mmol/L} \\ 0 & \text{otherwise} \end{cases} \tag{2.8}$$

Overall, the model uses 9 population values or generic constants, and requires a further 6 patient specific parameters to be identified. Nonlinearity comes from insulin action on parameters of glucose production, glucose distribution/transport and glucose disposal, and difference in the activation/deactivation profile of the three insulin actions.

All these models were developed with control-relevance in mind. They all share some fundamental similarity in the way that they each address the basic glucose-insulin interaction. Greater degrees of detail are added according to the different focus of each group. In particular, Salzsieder et al. [1990a], Parker et al. [1999] and Hovorka et al. [2004] all considered non-linearities in their models to better match clinically observed dynamics. Nevertheless, the Minimal Model, being "minimal", still captures the essential glucose-insulin dynamics, and has thus served as a starting point for countless studies.

In the next section, a Glucose-Insulin Regulatory model is developed from the Minimal Model. This model proposes a balance between simplicity and accuracy to best address control-relevance in the intensive care units. In particular, model parameters must be identifiable without intensive data collection to suit an ICU environment. The Minimal Model is used as a starting point because it describes the fundamental dynamics in the simplest form. Model non-linearities are added to improve necessary control accuracy while maintaining the generalisability of

the model, particularly with respect to data acquisition limitation in the critical care environment.

2.2 Glucose-Insulin Regulatory Dynamic System Model for Critically Ill Patients

Intensive care units represent a highly controlled environment where most glucose-insulin system inputs and outputs can be accounted for and modelled. The Minimal Model by Bergman et al. [1981] is a simple model that effectively captures the fundamental dynamics of the glucose-insulin system. Thus it serves as a starting point in this thesis for developing a control-relevant dynamic system model. However, several significant changes required to create a more physiologically relevant and more clinically accurate model are discussed in detail in this section.

As identified by various groups over the years, the first required addition to this model is one that accounts for un-utilised insulin in the blood plasma or insulin that has bound and then unbound to cell walls, tissues or insulin receptors. This addition has a similar effect to splitting the insulin compartment into a slow path and a fast path, which indicates the existence of fast and slow absorption channels and the presence of local insulin degradation [e.g. Cobelli et al., 1999; Turnheim and Waldhausl, 1988; Hovorka et al., 2003]. Hence, it defines a more accurate pharmacokinetic model for insulin distribution.

More specifically, Turnheim and Waldhausl [1988] studied the pharmacokinetic modelling of intravenous insulin injection, and concluded that the concentration of plasma insulin following a bolus injection declines with at least two exponentials or two different rates. The first is a rapidly disappearing component of insulin representing elimination from the intravascular space, and the second is a more slowly disappearing component that reflects elimination from the interstitial fluid and the tissues that utilise insulin. These two components have mean half-lives of 2.4 and 50–130 min, respectively.

Next, during the 1970s and 1980s, several papers were published regarding the plasma insulin disappearance kinetics in humans. Many found flaws in the first order (linear) assumptions of insulin disappearance that had been predominantly

used in previous models [e.g. Cobelli et al., 1999; McGuire et al., 1979]. These flaws were assumed to be based on the narrow range of insulin levels studied, with the first reported non-proportionality between plasma concentration and plasma disappearance rate published by Sonksen et al. [1973]. Other experimental studies were undertaken considering the concentrations resulting from a series of intravenous insulin infusions at different rates in both normal and diabetic subjects, as reviewed in Thorsteinsson [1990]. These studies concluded that insulin disappearance is often governed by Michaelis-Menten saturation dynamics.

In addition, insulin mediated glucose clearance is controlled primarily by insulin sensitivity, which links insulin concentration and glucose levels. As the dose of exogenous insulin is increased in controlled hyperglycemic clamp studies, insulin sensitivity decreased [Prigeon et al., 1996]. This result occurs because the effect of insulin saturates at the receptor and/or in transport, limiting utilisation [Natali et al., 2000]. Hence, there is a need for a saturable mechanism on insulin action. Natali et al. [2000] added Michaelis-Menten saturation of insulin action on fractional glucose extraction in a circulatory model, and obtained good fits to clinical data with limitations only occurring in the first 60 min, which were attributed to an irregular onset of insulin action during this initial phase.

Finally, to reduce model complexity and better match known physiological responses, a term must be included to suppress endogenous insulin secretion during periods of high exogenous insulin infusion [DeFronzo et al., 1979]. This situation is often encountered in critical care where relatively high insulin infusion rates are not uncommon [e.g. Van den Berghe et al., 2001; Doran et al., 2004a]. These large doses occur primarily due to the high levels of insulin resistance encountered in these patients when they are hyperglycemic.

The glucose-insulin regulatory system model developed by adding all these terms and modifications is significantly different from the Minimal Model. It is presented in Equations (2.9)–(2.13), which also includes a simple two compartment model for glucose appearance under enteral infusion feeding. A schematic of the model is shown in Figure 2.6.

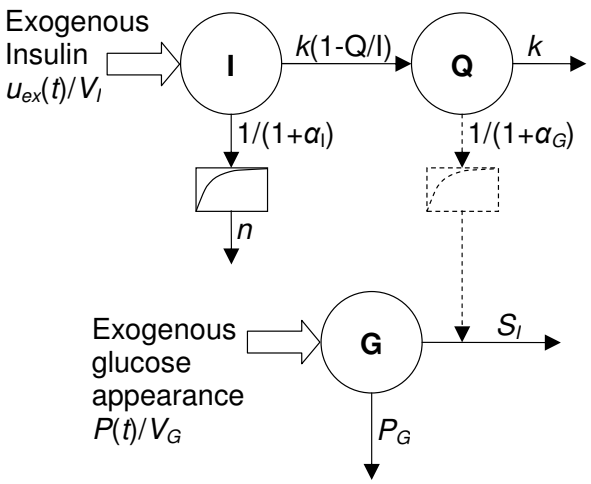

Figure 2.6 Glucose-insulin regulatory model for critically ill patients

$$\dot{G} = -p_G G - S_I(G + G_E)\left(\frac{Q}{1 + \alpha_G Q}\right) + \frac{P(t)}{V_G} \tag{2.9}$$

$$\dot{Q} = -kQ + kI \tag{2.10}$$

$$\dot{I} = \frac{-nI}{1 + \alpha_I I} + \frac{u_{ex}(t)}{V_I} + \frac{I_B e^{-Cu_{ex}(t)}}{V_I} \tag{2.11}$$

$$P(t_i < t < t_{i+1}) = \bar{P}_{i+1} + (P(t_i) - \bar{P}_{i+1})e^{-k_{pd}(t-t_i)} \quad \text{where } \bar{P}_{i+1} < P(t_i) \tag{2.12}$$

$$P(t_i < t < t_{i+1}) = \bar{P}_{i+1} + (P(t_i) - \bar{P}_{i+1})e^{-k_{pr}(t-t_i)} \quad \text{where } \bar{P}_{i+1} > P(t_i) \tag{2.13}$$

The symbols G [mmol/L] denotes the glucose above an equilibrium level, G_E [mmol/L], and I [mU/L] is the plasma insulin resulted from exogenous insulin input. The effect of previously infused insulin being utilized over time in the interstitium is represented by Q [mU/L], with k [1/min] accounting for the effective life of insulin in the system. Patient endogenous glucose removal and insulin sensitivity are p_G [1/min] and S_I [L/mU/min] respectively. The parameter V_I [L] is the insulin distribution volume and n [1/min] is the constant first order decay

rate for insulin from plasma. External nutrition and insulin input are expressed in $P(t)$ [mmol/min] and $u_{ex}(t)$ [mU/min] respectively. In Equations(2.12)–(2.13), k_{pr} [1/min] and k_{pd} [1/min] are the rise and decay rates of exogenous (enteral) plasma glucose appearance, and $\bar{P}_i$ and $\bar{P}_{i+1}$ are the stepwise consecutive enteral glucose feed rates used to model dextrose control. The glucose distribution volume is V_G [L]. Michaelis-Menten functions are used to portray saturations, with parameter α_I [L/mU] used for saturation of plasma insulin disappearance, and α_G [L/mU] for saturation of insulin-stimulated glucose removal. Endogenous insulin production is I_B [mU/min] under no presence of exogenous insulin. The constant C defines the suppression of endogenous insulin production in the presence of exogenous insulin.

This model has two patient specific parameters, p_G and S_I. These two parameters are the critical parameters that distinctively describe the dynamics between different patients and the dynamics within a single patient. By identifying these parameters, which are time-varying, for each individual, the model is thus adaptive to different patients under different metabolic conditions. Both parameters exist in the $\dot{G}$ equation in Equation (2.9). Therefore, the identification of these parameters only requires measurements in blood glucose levels, G. This specifically addresses the glycemic control requirements/limitations in an ICU environment where measurement in Q is not available and the lab turnaround time for plasma insulin concentration I measurements is too long to be real-time control applicable.

2.2.1 "Effective" Insulin and Losses

The convolution integral solution to Equation (2.10), Q, represents the "effective" insulin. This term accounts for un-utilised insulin in the interstitium [Guyton and Hall, 1996] or insulin that had bound and then unbound to cell walls, tissues or insulin receptors [Duckworth and Kitabchi, 1981]. Other models typically use multiple compartments to capture a similar effect, such as the multiple glucose compartments and paths used in Hovorka et al. [2002, 2003]. This glucose partitioning approach is quite common in various forms [e.g. Carson and Cobelli, 2001; Callegari et al., 2002; Ollerton, 1989]. In addition, the use of long and short acting insulin compartments [Hovorka et al., 2002, 2003] provides a similar spreading of insulin-glucose utilisation over time, as represented by the convolution integral,

Q. Hence, Q represents the insulin ready in the interstitium for action that has appeared from the plasma compartment and not yet been utilised.

Existing reported interstitially bonded, or effective, insulin half-life values associated with intravenous administration range from 25 to 130 minutes [e.g. Natali et al., 2000; Mari and Valerio, 1997; Turnheim and Waldhausl, 1988]. When the effective insulin half-life parameter, k, approaches infinity, the term approaches the instantaneous blood insulin concentration, which is analogous to the Minimal Model of Bergman et al. [1981]. A summary of the definition and reported clinical values of k, which defines the spreading of insulin action by transport to the interstitium and its action there, is found in Doran [2004].

The value of k is less than n in Equation (2.11). Therefore, $n-k$ is effectively the irreversible loss of insulin going from blood plasma to the interstitium. This loss occurs in the kidneys and liver, and/or as a result of saturation effects that limit immediate utilisation. More detailed analysis and validation can be found in [Lotz et al., 2006b].

2.2.2 Saturation Dynamics

The model has been developed to account for a non-linear saturation of exogenous insulin disappearance rate from plasma in Equation (2.11) and its saturable utilisation to reduce blood glucose levels in Equation (2.9). The addition of transient insulin kinetics via a convolution integral accounts for the accumulation dynamic seen in prior clinical trials [Doran et al., 2004a], and better matches physiological knowledge. This model therefore effectively splits the glucose compartment into fast and slow (or available and unavailable) compartments over a continuum rather than discrete states [e.g. Vicini et al., 1997].

Many studies have investigated insulin saturation in vivo. Prigeon et al. [1996] demonstrated that as peak plasma insulin concentration increases in vivo, insulin sensitivity, as derived from the Minimal Model drops, which provides evidence for insulin saturation in the underestimation of S_I using the Minimal Model. Prigeon et al. [1996] proposed two saturable sites; one for insulin transport from plasma to interstitial sites, the other for insulin action. Many other studies have also supported one or both of these two saturation mechanisms [e.g. Natali et al.,

2000; Thorsteinsson, 1990]. Both saturation mechanisms are included in this model using Michaelis-Menten functions in Equations (2.9) and (2.11).

In Equation (2.11), the disappearance rate of insulin from plasma is directly proportional to the plasma insulin concentration at low plasma insulin level, but becomes independent of the plasma insulin level when plasma insulin concentration exceeds a certain threshold. Thorsteinsson [1990] suggested that insulin removal rate from plasma obeys saturation kinetics that can be expressed as a Michaelis-Menten function. In Chase et al. [2003], clinical results also suggested the presence of insulin pooling in plasma, where the effect of insulin on glucose removal appeared significantly belated. To account for insulin pooling in plasma, particularly at high doses, the parameter, α_I, in Equation (2.11) bounds the plasma insulin disappearance rate, as shown in Figure 2.7.

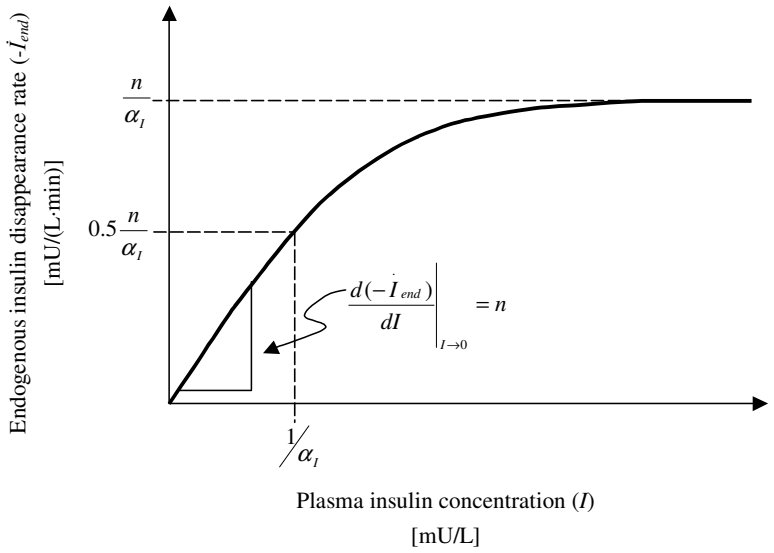

Figure 2.7 Saturation in plasma insulin removal rate

Saturation in insulin-stimulated glucose removal has been evidenced in several clinical investigations. Prigeon et al. [1996] reported that insulin sensitivity decreases as peak plasma insulin concentration increases. Caumo et al. [1999] also reported decreased insulin sensitivity with increased plasma insulin level, and that insulin sensitivity becomes independent of plasma insulin level as insulin level increases beyond ∼40 [mU/L]. The Michaelis-Menten parameter, α_G, in Equation (2.9) defines the saturation mechanism on insulin-stimulated glucose removal. The inverse of α_G represents the level of insulin integral, Q, or

delayed insulin, at which the insulin-stimulated glucose removal rate reaches half maximum.

2.2.3 Equilibrium Blood Glucose

In Equation (2.9), G_E is the equilibrium blood glucose level, whereas Bergman et al. [1981] used the basal blood glucose level. This parameter represents the patient specific equilibrium state under constant feed and insulin infusion. Due to ongoing exogenous insulin infusion and carbohydrate nutrition, basal blood glucose level is difficult to determine for ICU patients. In general, G_E can be obtained for a patient under steady conditions or as a long term moving average [Hann et al., 2005]. The presence of insulin and/or dextrose infusion does not affect the physiological meaning of this term.

2.2.4 Endogenous Insulin Production

Equation (2.11) includes the term $I_B \exp^{-Cu_{ex}(t)}$ as the endogenous insulin production rate. Under presence of significant exogenous insulin, $u_{ex}(t)$, the endogenous insulin production may be suppressed and effectively removed from the model. This dynamic reduces model complexity and matches accepted assumptions for the suppression of endogenous insulin production by exogenous infusion [Insel et al., 1975; DeFronzo et al., 1979; Ellemann et al., 1987; Transberg et al., 1981].

In this model, knowing the possibly variable level of I_B between patients is not critical. As this model is developed for use in intensive care glucose control applications, exogenous insulin is almost always present and often at higher levels. Therefore, the inclusion of this term is more for physiological completeness, rather than metabolic control accuracy. Although it may be ignored when studying most critical care intensive insulin therapies, removing this term completely from Equation (2.11) can sometimes result in the steady state plasma insulin concentration of zero, which is physiologically inaccurate.

In reality, the endogenous insulin production rate is highly variable and difficult to obtain quickly or accurately as it requires basal insulin and/or C-peptide measurements not typically or quickly available in the ICU [e.g. Ferrannini and Cobelli, 1987a; Ferrannini et al., 2005; Sherwin et al., 1974; Van Cauter et al., 1992; Ellemann et al., 1987]. In addition, many hyperglycemic critically ill patients have been found to be also severely hyperinsulinaemic due to large insulin doses and/or excess endogenous insulin. This is a result of high insulin resistance and impaired glucose-insulin regulation. Overestimating a patient's endogenous insulin production rate can therefore lead to a controller seeing the patient as more insensitive to insulin, and thus administering a large amount of insulin that can result in a hypoglycemic episode. Hence, from a control and physiological standpoint, it is safest to under estimate its value.

In conclusion, the effect of endogenous insulin is thus primarily included in the time-varying parameter, p_G, that represents the body's ability to regulate blood glucose without exogenous insulin during insulin therapies. This approach essentially presents each patient as a clean slate, which is captured in a patient specific p_G, without making assumptions for clinically unavailable data, I_B. This approach, given the relatively smaller contribution of the $-p_G G$ term ensures any endogenous insulin action is captured without relying on potentially poor estimates of endogenous insulin. Note that I_B may be used directly, as in other models, if it is regularly measured, which does not occur in critical care. The consequent result is overall safer insulin administration.

2.2.5 Dextrose Modelling and Control

In this model, non-steady stepwise enteral glucose rate fluxes may also be employed for control in Equations (2.12)–(2.13). Postprandial glucose kinetics for an oral glucose load and continuous feeding are characterized by suppression of net hepatic glucose output [Abumrad et al., 1982; Kiwanuka et al., 2001; Ludvik et al., 1997; Radziuk et al., 1978]. Time periods for complete absorption of an oral glucose load range from 120 to 270 min [Radziuk et al., 1978; Abumrad et al., 1982; Cummins, 1952; Consoli, 1992; Ludvik et al., 1995] with a peak ingested glucose appearance in plasma after 15–40 min [Radziuk et al., 1978; Ferrannini et al., 1988]. Slower absorption was evidenced in a mixed-meal formulation [Kiwanuka et al., 2001; Pehling et al., 1984]. A high percentage of oral

glucose appears systemically due to a small first-pass splanchnic uptake [Radziuk et al., 1978]. Whether such dynamics are applicable to non-steady-state enteral glucose infusions, where variations in glucose load are much smaller, is unknown. However, Radziuk et al. [1978] showed no discernible difference in systemic oral glucose appearances with a half-sized oral glucose load.

The exponential rates for the rise and decay of exogenous glucose appearance, k_{pr} and k_{pd}, are used to simply model the effect of transient net hepatic glucose output and glucose disposal. Impaired splanchnic and peripheral glucose uptake in diabetes and stress induced hyperglycemia imply a slow decay in glucose appearance following nutritional feed reduction [Kiwanuka et al., 2001; Ludvik et al., 1997; Nielsen et al., 1998; Basu et al., 2004, 2001; Firth et al., 1985]. The rate of peripheral appearance of oral glucose is approximately equal to the intestinal absorption rate, which implies a rapid rise in glucose appearance following a nutritional feed increase [Radziuk et al., 1978].

2.2.6 Endogenous Glucose Removal, p_G, and Insulin Sensitivity, S_I

The most critical model parameters for fitting and prediction accuracy are the time-varying parameters p_G and S_I [Hann et al., 2005]. In earlier work by Chase et al. [2003], the Minimal Model was simplified into a two-compartment model. This simplified model has two patient specific parameters p_1 and p_4, which are essentially P_1 and the ratio P_3/P_2 from the Minimal Model of Equations (2.1)–(2.3). However, in the model of Equations (2.9)–(2.13), p_G and S_I have very different physiological meanings from p_1 and p_4 in Chase et al. [2003] and the similar parameters in the Minimal Model [Bergman et al., 1981]. Hence, these parameters and their time-varying definitions are a primary difference in this model from its origins.

The model also does not include a specific endogenous glucose production term, as it is suggested to be at least partly suppressed with significant insulin administration in both normal and stressed states [Thorell et al., 2004]. In clinical settings and particularly critical care, endogenous glucose production is not readily measurable, which would make it difficult to accurately include in a model.

In addition, no literature has yet reported satisfactory estimates or models for this dynamic, especially in critical care. The effect of endogenous glucose production in this model is therefore mitigated into p_G, simplifying the model and providing a reference inter- and intra-patient. Increased endogenous production rates will thus be absorbed and reflected as lower values of p_G, whether consistently or varying over time. Overall, p_G thus represents the balance between endogenous insulin action, non-insulin mediated glucose removal and endogenous glucose production, all in a single patient specific term.

The definition and methods of determining insulin sensitivity have been extensively studied, primarily in clinical diabetes research settings. Many studies suggest insulin sensitivity is highly dependent on experimental protocol and the dynamic model adopted [e.g. Bettini et al., 1995; Caumo et al., 1999]. Hyperinsulinaemic euglycemic clamp tests with different levels of plasma insulin concentration also give very different insulin sensitivity levels, including intra-individual variation and saturation effects [Natali et al., 2000; Prigeon et al., 1996; Katz et al., 1993; Beard et al., 1986; Saad et al., 1994]. In Equations (2.91) to (2.11), the added saturation mechanism on the effect of insulin thus creates a unique index of insulin sensitivity, S_I, in contrast to other model-based measures. This approach allows S_I to (potentially) more closely approximate the true tissue sensitivity to insulin. Overall, the S_I term represents the effective insulin sensitivity, in inverse proportion to insulin resistance, of the specific patient. It is uniquely independent of insulin transport and saturation dynamics in this model formulation.

2.3 Control Model Comparison and Summary

The Minimal Model has been studied widely because of its simplicity and effective portrayal of the basic dynamic of the glucose-insulin regulatory system. The model developed for glycemic control in critical care in this chapter kept a simple structure, while addressing the Minimal Model's observed clinical inadequacies for critical care glycemic control. As a result, while structurally similar, the model presented is significantly different in dynamics and physiological relevance or accuracy. Table 2.1 compares the model developed in this chapter with the four models studied in Section 2.1.

Table 2.1 Glucose-Insulin Regulatory System Model Summary

		Real-time clinical control applications	
Model	Intended Model Use	Advantages	Disadvantages
Minimal Model [Bergman et al., 1979, 1981]	Insulin sensitivity/ metabolic study	• Is simple • Captures fundamental dynamics	• Lacks higher order/ saturation dynamics
Salzsieder et al. [1990a,b]	Developing an artificial pancreas for Type 1 diabetic individuals	• Produces accurate steady state solutions and steady dynamics for Type 1 diabetes	• Requires real-time plasma insulin data which is unobtainable in an ICU • Requires intensive computation to identify 5 patient specific parameters • Has incomplete representation of glucose utilisation due to under-modelling of insulin kinetics
Parker et al. [1999]	MPC of Type 1 diabetes using CGM systems	• Models detailed whole body dynamics	• Requires excessive computational efforts for real-time control • Uses CGM systems which currently lack required measurement accuracy • Lacks control robustness
Hovorka et al. [2004]	MPC of Type 1 diabetes and ICU patients	• Includes detailed non-linearities	• Requires intensive computation to identify 6 patient specific parameters

Compared with the Minimal Model of Figure 2.2, the critical care control model of Figure 2.6 has a more physiologically identified form. The Minimal Model's final form in Equations (2.1)–(2.3) lumped many metabolic effects together, such as interstitial transport rates and different losses in the system. The model of Equations (2.9)–(2.11), in contrast, is more representative of non-abstract compartments by definition.

First, the concept of a "remote" insulin action compartment X in the Minimal Model is harder to grasp, compared to the interstitial compartment Q in Equation (2.10). This latter interstitial compartment has been widely studied, with transport rates experimentally identified [e.g. Nestler et al., 1988; Natali et al., 2000; Prigeon et al., 1996; Turnheim and Waldhausl, 1988; Kraegen and Chisholm, 1984]. Second, the different transport/rise/decay rates such as k, p_G and S_I have non-abstract physiological meanings for interstitial transport rate, endogenous glucose removal and insulin sensitivity, which are also widely studied and can be experimentally tested [e.g. Araujo-Vilar et al., 1998; Avogaro et al., 1989; Bettini et al., 1995; Prigeon et al., 1996; Kraegen and Chisholm, 1984; Vicini et al., 1999; Pillonetto et al., 2002]. Many of these studies, although initiated with the Minimal Model, designed experiments that specifically test for insulin sensitivity, which is not explicitly expressed in Equations (2.1)–(2.3). Instead, insulin sensitivity is the ratio of $-P_3/P_2$ where P_2 is numerically negative in the original paper by Bergman et al. [1979, 1981], and can thus end up being identified with pooling errors [Caumo et al., 1999; Vicini et al., 1999], giving rise to a current ratio, but incorrect magnitudes for the transport rates P_2 and P_3.

Additional features that significantly differentiate the critical care model of Figure 2.6 from the Minimal Model of Figure 2.2 are the two saturation dynamics and suppression of endogenous insulin production in the presence of exogenous insulin. These non-linear features are also important in clinical glycemic control where exogenous insulin utilisation must be accurately captured to enable safe and precise insulin control.

In further comparison, the model developed by Salzsieder et al. [1990a] of Figure 2.3 is also simple, and had been verified in dogs [Salzsieder et al., 1985; Fischer et al., 1987], as well as humans [Salzsieder et al., 1990a,b; Fischer et al., 1990]. However, this model, being focused on Type I diabetic patients, is not particularly suitable for critical care. The implementation of model-based con-

trol by Salzsieder et al. [1990a] also required long term study of a patient's meal and exercise patterns, which is not suitable in critical care. As a result, parameter fitting is computational intensive, and therefore not suitable for real-time clinical control. Rapid, real-time parameter identification is very important in model-predictive control to address time-variability of parameters, as many recent studies have pointed out the importance of accounting for both inter- and intra-patient variabilities [Parker and Doyle, 2001; Parker et al., 2001; Hovorka et al., 2004].

The much more complex models developed by Parker et al. [1999] of Figure 2.4 has limited applicability in clinical control, as a result. Although the model has a very detailed physiological structure and offers the most precise picture of glucose-insulin metabolism, many assumptions and population parameter values need to be placed for the model to be useable in real-time clinical control. Hence, this well-structured model is no more suitable than a simpler, much more easily identified model.

The model of Hovorka et al. [2004] has a greater breakdown of the glucose and the insulin actions compared to the Minimal Model. The six compartments exhibit complex dynamics and interactions between each other. This model has recently been applied in critical care glycemic management and achieved promising results [Plank et al., 2006]. However, with 6 patient specific parameters to be identified, trade-offs between parameters must be cautiously reviewed to maintain their true physiological meanings and clinical accuracy.

In summary, the model developed in this chapter, presented in Equations (2.9)–(2.13) and Figure 2.6 is particularly developed for ready clinical applicability. Having a robust model that is adaptable to any patient, while being physiologically valid and simple, is more the focus of its development than being metabolically correct in every detail. The model features an interstitial compartment for insulin storage to account for the delay between insulin secretion, or infusion, and utilization. Saturation dynamics reflect plasma insulin pooling and saturable interstitial insulin effect, addressing these shortcomings of the Minimal Model in clinical control applications [Doran et al., 2004a,b; Hann et al., 2006]. Hence, it has all significant clinically observed and relevant linear and non-linear dynamics, without excessive terms, complexity or dynamics.

In particular, the four other models studied in this chapter all require extensive data sampling and parameter identification. This significantly disadvantages the use of these models for clinical glycemic control in a critical care environment where data sampling is generally infrequent. Parker et al. [1999] designed their model to be incorporated with a CGM system. However, current CGM technology still lacks the measurement accuracy and reliability to achieve the simulated results presented in Parker et al. [1999]. On contrast, the model developed in this chapter requires only two parameters to be identified, utilising infrequent blood glucose measurements alone. Hence, this model is particularly suitable for control application in the critical care environment.

Finally, the model has been verified using critical care patient data [Hann et al., 2006] and tested clinically [Chase et al., 2005b,c; Wong et al., 2006a,b; Lonergan et al., 2006a]. These clinical results and related parameter identification methods are presented and discussed in detail in Chapters 3 and 4. In particular, the parameter identification method developed in the next chapter further assesses the generalisability of the model, and enhances its adaptability. Overall, this model represents a balanced tradeoff of complexity and non-linearity versus simplicity with respect to the other models presented, which span a range of these tradeoffs. An overall and detailed review of models in critical care glycemic control may also be found as part of the review by Chase et al. [2006b].

Chapter 3

Parameter Identification and Dynamic System Model Validation

To better control glucose levels, model-based [Chee et al., 2003a,b; Plank et al., 2006; Chase et al., 2005c; Wong et al., 2006a,b] and titration-based or sliding-scale protocols [Van den Berghe et al., 2001, 2003; Krinsley, 2004, 2003b; Albisser et al., 1974; Goldberg et al., 2004b; Laver et al., 2004] have been clinically tested. Model-based methods can be very accurate, but require the ability to identify patient specific parameters and capture all of the observed dynamics [Chase et al., 2006b]. Currently, most common parameter identification methods are non-linear, non-convex and in some cases too computationally intense for real-time use in most clinical environments [Hovorka and Vicini, 2001]. This chapter presents an integral-based fitting method for the glucose-insulin system model in Equations (2.9)–(2.13).

This method has been used in Chase et al. [2005c] and Wong et al. [2006a,b]. The method mathematically reformulates the physiological model for critical care patients in terms of integrals or areas under the curve(s). As a result, identifying time-varying patient specific parameters within physiological constraints becomes linear and convex with minimal computation required, creating a relaxed optimisation for this parameter identification problem.

A fast, accurate identification method is important in the process of refining and testing a model as many more patients can be studied in a short time. For non-linear or non-convex methods, any fitting or prediction error can be due to the model not capturing dynamics or, instead, due to finding a local, rather than the global, minima. Hence, it can become difficult to differentiate model error or inadequacy from non-optimal local minima solutions. Using many different

starting points may find a better, more globally optimal solution, but at the cost of significantly increased computational time. However, there is still only a probability of finding the global minimum, rather than the certainty provided by a convex method. More importantly, a fast, accurate convex method enables confident application in real-time model-based control and medical decision support applications.

This chapter presents a convex parameter identification method for the nonlinear dynamic system model presented. This method is then used to validate the model's ability to fit and predict blood glucose data using nearly 1,300 hours of retrospective critical care patient data. Parameter values and their sensitivity are then analysed for robustness and the results summarised.

3.1 Integral-Based Parameter Identification Method

To simplify and linearise the optimisation problem, the parameters V_I, V_G, n, k, α_G, α_I, I_B, k_{pd} and k_{pr} in Equations (2.9)–(2.13) can be obtained a priori via the results of an extensive literature search [e.g. DeFronzo et al., 1979; Turnheim and Waldhausl, 1988; Thorsteinsson, 1990; Prigeon et al., 1996; Natali et al., 2000; Doran, 2004]. They are assumed to be non-patient-specific or population-based constants. In addition, sensitivity analysis shows these parameters are insensitive [Hann et al., 2005] or tradeoff directly with other parameters [Chase et al., 2004]. Thus, in the latter case, some must be held constant at validated population values to restrict identification error. Finally, many are also found to have tight population ranges in the literature indicating little variability between patients [Doran, 2004], and thus allowing them to be more safely held constant in this model.

The exogenous feed details $P(t)$ and exogenous insulin $u_{ex}(t)$, are control inputs in a glycemic control problem, and therefore known for parameter identification. The equilibrium glucose level, G_E, can be estimated for a patient under stable insulin and dextrose infusion as a longer term 12–24 hour moving average. Finally, p_G and S_I are left to be identified as time-varying patient specific model parameters.

This approach can be thought of as a minimal approach where the major dynamics are identified first (S_I and p_G) before secondary parameters can be modified to better fit the data if required. It is therefore important to ensure the fitting method for identifying time-varying patient specific parameters is as least demanding computationally as possible. This way other parameters can be varied (if required) without significantly affecting the overall computation time. Computational time is a significant factor to consider in real-time clinical control, as well as in the process of refining and testing the model on large numbers of patients or large retrospective data sets, as it directly impacts the turnaround time between data input and decision making.

Integrating both sides of Equation (2.9) and defining the overall saturated insulin action in the interstitial compartment as $\bar{Q}$:

$$\bar{Q} = Q/(1 + \alpha_G Q) \tag{3.1}$$

In addition, glucose appearance rate per volume of plasma is redefined as P_V:

$$P_V = P(t)/V_G \tag{3.2}$$

The following expression holds for any segment of time from t_0 to t:

$$\begin{aligned} \textstyle\int_{t_0}^{t} \dot{G} dt &= \int_{t_0}^{t} -p_G G - S_I(G + G_E)\bar{Q} + P_V \; dt \\ \Rightarrow \quad G(t) - G(t_0) &= -\int_{t_0}^{t} p_G G \; dt - \int_{t_0}^{t} S_I(G + G_E)\bar{Q} \; dt + \int_{t_0}^{t} P_V \; dt \end{aligned} \tag{3.3}$$

Substituting the total blood glucose level, G_T:

$$G_T = G + G_E \tag{3.4}$$

into Equation (3.3) results in an equivalent expression that is easy to compute numerically, given measured total glucose levels:

$$G_T(t) - G_T(t_0) = -\int_{t_0}^{t} p_G(G_T - G_E)\ dt - \int_{t_0}^{t} S_I G_T \bar{Q}\ dt + \int_{t_0}^{t} P_V\ dt \qquad (3.5)$$

To reduce computational complexity and account for variation over time, the total time interval is divided into equal segments during which p_G and S_I are defined as piecewise constant:

$$p_G = \sum_{i=1}^{N} p_{G_i} \left(H(t - t_{i-1}) - H(t - t_i)\right) \qquad (3.6)$$

$$S_I = \sum_{i=1}^{N} S_{I_i} \left(H(t - t_{i-1}) - H(t - t_i)\right) \qquad (3.7)$$

where $H(t - t_0)$ is the Heaviside function defined $H(t - t_0) = 0$ when $t < t_0$, and $H(t - t_0) = 1$, when $t \geq t_0$. Note that the value of N in Equations (3.6) and (3.7) may be different depending on the number of hours used per segment. Finally, the variation in Equations (3.6) and (3.7) can also be defined as linear or higher order, over these time periods for greater detail, at a cost of increasing the number of unknown parameters required to parameterise p_G and S_I over a given period of time. Other parameters or different length time segments may also be used with no loss of generality.

The only unknown parameters in Equation (3.5) are p_{G_i} and S_{I_i} when Equations (3.6) and (3.7) are used. However, these are constant parameters, such that after numerically integrating the data, Equation (3.5) can be written as a simple linear system in terms of these unknown values:

$$\underline{A} \begin{bmatrix} p_{G_i} \\ S_{I_i} \end{bmatrix} = \underline{b} \qquad (3.8)$$

where the number of equations for each time segment can be arbitrarily selected by integrating over different time segments. To ensure that the values obtained for p_G and S_I are within physiologically valid ranges, weighted constraints can be placed on both parameters when solving Equation (3.8).

To compute the integrals in Equation (3.5) over different time segments, the total blood glucose profile, G_T, is approximated using simple linear interpolation between the data points, forming a piecewise linear curve $G_{T-approx}$. The error between the patient's real glucose level G_{T-real} and the approximated curve $G_{T-approx}$ is defined:

$$G_{T-real}(t) = G_{T-approx}(t) + \varepsilon(t) \tag{3.9}$$

where the error term, $\varepsilon(t)$, should fall within the interval, $0 \leq |\varepsilon(t)| \leq \delta$, for small δ, and δ is a measure of the theoretically best possible fit of the model to the data.

Using Equation (3.5), G_{T-real} can be calculated in any given time interval $[t_0, t]$ with the constant parameters p_{G_i} and S_{I_i} as defined in Equations (3.6) and (3.7):

$$\begin{aligned} G_{T-real}(t) &= G_{T-real}(t_0) - p_{G_i} \int_{t_0}^{t} G_{T-real}(t) - G_E \; dt \\ &\quad -S_{I_i} \int_{t_0}^{t} G_{T-real}(t)\bar{Q}(t) \; dt + \int_{t_0}^{t} P_V(t) \; dt \\ &= G_{T-approx}(t_0) + p_{G_i}(t - t_0)G_E - p_{G_i} \int_{t_0}^{t} G_{T-approx}(t) \; dt \\ &\quad -S_{I_i} \int_{t_0}^{t} G_{T-approx}(t)\bar{Q}(t) \; dt + \int_{t_0}^{t} P_V(t) \; dt + E(t) \end{aligned} \tag{3.10}$$

where the error term $E(t)$ arises from using the approximate piecewise linear blood glucose profile. The magnitude and order of E(t) is defined as

$$\begin{aligned}
|E(t)| &= \left|\varepsilon(t_0) - p_{G_i}\int_{t_0}^{t}\varepsilon(t)\ dt - S_{I_i}\int_{t_0}^{t}\varepsilon(t)\bar{Q}(t)\ dt\right| \\
&\leq |\varepsilon(t_0)| + p_{G_i}\left|\int_{t_0}^{t}\varepsilon(t)\ dt\right| + S_{I_i}\left|\int_{t_0}^{t}\varepsilon(t)\bar{Q}(t)\ dt\right| \\
&\leq \delta + p_{G_i}\int_{t_0}^{t}|\varepsilon(t)|\ dt + S_{I_i}\int_{t_0}^{t}|\varepsilon(t)|\,\bar{Q}(t)\ dt \\
&\leq \delta + p_{G_i}\delta(t-t_0) + S_{I_i}\delta\int_{t_0}^{t}\bar{Q}(t)\ dt \\
&= O(\delta) \qquad (3.11)
\end{aligned}$$

Note that even if the time period, $[t, t_0]$, and the integral, $\int_{t_0}^{t}\bar{Q}(t)\ dt$, are both large, the piecewise patient specific parameter terms, $p_{G_i}\delta(t - t_0)$ and $S_{I_i}\delta\int_{t_0}^{t}\bar{Q}(t)\ dt$, are small compared to the integral patient specific terms, $p_{G_i}\int_{t_0}^{t}G_{T-real}(t)\ dt$ and $S_{I_i}\int_{t_0}^{t}G_{T-real}(t)\bar{Q}(t)\ dt$, when it is assumed that the glucose level is greater than 1 mmol/L, $G_{T-real}(t) > 1$ mmol/L, which should always be true for a living patient.

The first two error terms in Equation (3.11) yield

$$\left|\frac{p_{G_i}\delta(t-t_0)}{p_{G_i}\int_{t_0}^{t}G_{T-real}(t)\ dt}\right| < \frac{\delta(t-t_0)}{\int_{t_0}^{t}1\ dt} = \delta \qquad (3.12)$$

$$\left|\frac{S_{I_i}\delta\int_{t_0}^{t}\bar{Q}(t)\ dt}{S_{I_i}\int_{t_0}^{t}G_{T-real}(t)\bar{Q}(t)\ dt}\right| < \frac{\delta\int_{t_0}^{t}\bar{Q}(t)\ dt}{\int_{t_0}^{t}\bar{Q}(t)\ dt} = \delta \qquad (3.13)$$

where $G_{T-real}(t) = 1$ mmol/L has been used to show the lower limit. More specifically, δ, as defined in Equation (3.9) measures how well the model captures the measured data. Thus, the fit is not affected by the linear approximation of the glucose data when using this integral formulation. Therefore, for a general time period $[t_0, t]$ this approximation of the glucose data can be used to represent the best fit, G_{T-real}, utilising integral functions, as in Equation (3.5), to identify the parameters defining the piecewise constant definitions for p_G and S_I from Equations (3.6) and (3.7). Importantly, this approximation can be used without introducing additional error beyond any inherent model error.

The integrals in Equation (3.5) can be determined for several different time periods in a given data set to find p_G and S_I. For example, as shown in Figure 3.1, when the length of the time period is chosen to be 120 min long, $[t_0, t_0+120]$, the fractional clearance of glucose, p_G, can be defined to take on one value, p_{G_1} and the insulin sensitivity parameter, S_I, can be defined to take on two values, S_{I_1} and S_{I_2}. The end result is three unknowns for this time period, requiring integrations over three intervals.

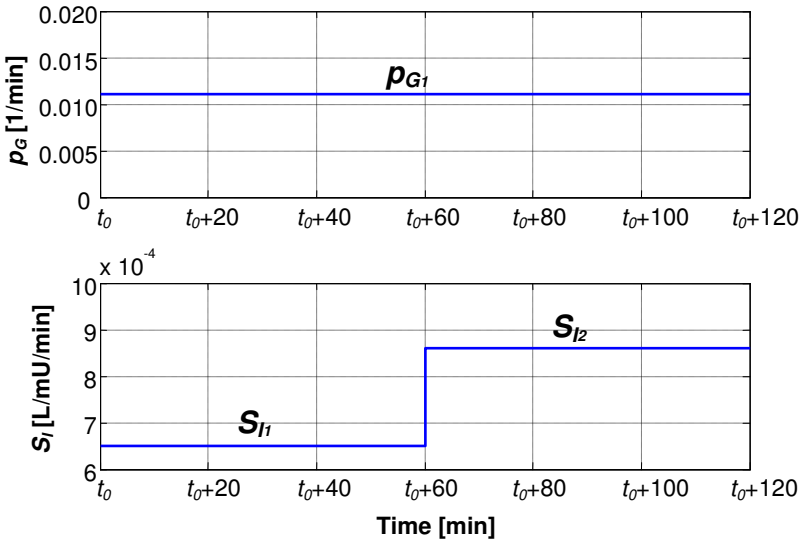

Figure 3.1 Example of functions for p_G and S_I

To find the patient specific parameter values that give the best fit to the measured glucose data in this time interval, six equations are proposed with the generic form:

$$G_{T-approx}(t_0 + 20i) - G_{T-fit}(t_0 + 20i) = 0 \qquad \text{for } i = 1, \ldots, 6 \tag{3.14}$$

To show the equations that result, the first and last of these equations, $i = 1$ and $i = 6$, are given

$$
\begin{aligned}
& G_{T-approx}(t_0+20) - G_{T-approx}(t_0) \\
& \quad - 20 p_{G_1} G_E + p_{G_1} \int_{t_0}^{t_0+20} G_{T-approx}(t)\ dt \\
& \quad + S_{I_1} \int_{t_0}^{t_0+20} G_{T-approx}(t) \bar{Q}(t)\ dt \\
& \quad - \int_{t_0}^{t_0+20} P_V(t)\ dt \\
& \quad = 0
\end{aligned} \tag{3.15}
$$

$$
\begin{aligned}
& G_{T-approx}(t_0+120) - G_{T-approx}(t_0) \\
& \quad - 120 p_{G_1} G_E + p_{G_1} \int_{t_0}^{t_0+120} G_{T-approx}(t)\ dt \\
& \quad + S_{I_1} \int_{t_0}^{t_0+60} G_{T-approx}(t) \bar{Q}(t)\ dt + S_{I_2} \int_{t_0+60}^{t_0+120} G_{T-approx}(t) \bar{Q}(t)\ dt \\
& \quad - \int_{t_0}^{t_0+120} P_V(t)\ dt \\
& \quad = 0
\end{aligned} \tag{3.16}
$$

where the integrals in Equations (3.15) and (3.16) can be readily evaluated numerically. The unknowns in these equations are p_{G_1}, and S_{I_1} and S_{I_2} . Therefore, for $i = 1, \ldots, 6$, Equation (3.14) defines a least squares system of six linear equations with three unknowns. The convex solution of these parameters consequently defines the time-varying profile for p_G and S_I for that time period. Finally, using integrals, instead of derivative based fitting methods, has the additional advantage of being robust to noise in the measured glucose data, by effectively providing a low-pass filter in the summations involved in numerically integrating.

3.2 Model Parameter Values and Ranges

There have been numerous studies on a wide variety of metabolic rates, providing references for glucose-insulin metabolic system parameter values. A comprehensive study was performed by Doran [2004], summarising reported parameter values throughout the literature. A quick summary of reported ranges for the

parameters used in the model defined in Equations (2.9)–(2.13) is presented in Table 3.1, with full referencing to the relevant literature within the table.

Table 3.1 Reported range of parameter values

Parameter	Reported Range		Reference
p_G	0.0059 – 0.0466	1/min	Avogaro et al. [1989] Bergman et al. [1981] Bettini et al. [1995] Cobelli et al. [1999] Furler et al. [1985] McDonald et al. [2000] Pillonetto et al. [2002] Vicini et al. [1999]
S_I	0.02 – 2.26 (majority between [0.02–1.11]$\times 10^{-3}$)	$\times 10^{-3}$ L/mU/min	Araujo-Vilar et al. [1998] Avogaro et al. [1989] Bergman et al. [1981, 1985, 1987] Cobelli et al. [1999] DeFronzo et al. [1979] Duncan et al. [2003] McDonald et al. [2000] Natali et al. [2000] Pillonetto et al. [2002] Vicini et al. [1999] Prigeon et al. [1996]
k	0.0053 – 0.0139	1/min	Kobayashi et al. [1983] Nestler et al. [1988] Natali et al. [2000] Kraegen and Chisholm [1984] Turnheim and Waldhausl [1988]
n	0.02 – 0.3 (majority between 0.02–0.16)	1/min	Nestler et al. [1988] Turnheim and Waldhausl [1988] Thorsteinsson [1990] Bergman et al. [1981] Kraegen and Chisholm [1984] Ferrannini and Cobelli [1987a]
α_G	0.001 – 0.04	L/mU	Natali et al. [2000] Prigeon et al. [1996] Nestler et al. [1988] Transberg et al. [1981] Turnheim and Waldhausl [1988] Duckworth and Kitabchi [1981]
α_I	0.0005 – 0.0043	L/mU	Thorsteinsson [1990] Prigeon et al. [1996] Ellemann et al. [1987] Kuehn and Blundell [1980]
I_B	4 – 19	mU/min	Ferrannini and Cobelli [1987a] Ferrannini et al. [2005] Ellemann et al. [1987] Van Cauter et al. [1992] Sherwin et al. [1974] Bergman et al. [1981]

3.3 Model Validation

After studying the reported parameter values, the generic values used in the glucose-insulin model validation are summarised in Table 3.2. These chosen values are the mean from the reported range, or the most supported literature values. The distribution volume for this initial model validation is set to 12 L for both glucose and insulin [Bergman et al., 1981]. The constant C that defines endogenous insulin suppression under the presence of exogenous insulin is set to 1.0.

Table 3.2 Fitting method verification model parameters

Parameter	Value	
k	0.0099	[1/min]
n	0.16	[min-1]
α_I	0.0017	[L/mU]
α_G	0.004	[L/mU]
I_B	9.6	[mU/min]
$V_G = V_I = V$	12.0	[L]

3.3.1 Model Validation Method and Cohort

The generic model in Equations (2.9)–(2.13) and the integral-based parameter identification method are used on data from a random selection of 18 patients from a 201 patient data audit at Christchurch Hospital [Shaw et al., 2004, 2005; Doran, 2004]. Each patient record had a period greater than 1 day with intervals between measured data points of 4 hours or less. The data density of 4 hours was selected to ensure enough measurements to enable a good model evaluation. The entire length of stay was not always considered, as many patients only had a shorter period of data that fitted these criteria. This cohort broadly represents the cross-section of patients seen in the ICU, regarding medical condition, age, sex, APACHE II scores and mortality, as summarised in Table 3.3. Type 1 and Type 2 diabetes is somewhat over-represented because these patients were often more frequently measured. Note that body mass index (BMI) is not typically recorded in most ICUs and was therefore not retrospectively available, limiting patient specificity in estimating some population parameter values. Ethical consent was obtained from the Canterbury Ethics Committee for this audit.

Table 3.3 Retrospective patient cohort background information

Patient ID	Medical Subgroup	APACHE II Score	Age	Sex	Mortality	Diabetes
R24	Other Medical	25	47	M	Y	Type 1
R87	Other Medical	26	62	F		
R130	Trauma	11	21	M		Type 1
R229	Cardiac	15	73	F		
R278	Other Medical	20	78	M		Type 2
R289	Cardiac	18	70	M		
R468	General Surgical	32	76	M		
R484	Other Medical	34	30	F		
R486	General Surgical	22	76	F		Type 2
R519	General Surgical	29	69	M		Type 2
R554	Other Medical	26	20	F		Type 1
R666	Cardiac	8	44	F		Type 2
R847	Other Medical	17	67	F		
R1016	General Surgical	20	37	F		Type 2
R1025	Pulmonary	36	48	M		Type 2
R1090	General Surgical	Unknown	37	F		
R1099	Pulmonary	Unknown	24	M	Y	
R1125	Other Medical	Unknown	72	F	Y	

For patient specific parameter identification, the endogenous glucose removal, p_G, is held constant over 2-hour periods and the insulin sensitivity, S_I, varies every hour, creating piecewise constant time-varying model parameters. Fitting bounds on p_G are [0.01, 0.02] [1/min], and on S_I are [1.0×10^{-5}, 2.5×10^{-3}] [L/mU/min]. Dextrose input is simply modelled as a step-wise function in this initial validation because it does not vary much through time in this patient data, because it was not being varied to control glucose. Thus, its value remained largely constant. It is thus defined:

$$P(t_i \leq t < t_{i+1}) = \bar{P}_i \tag{3.17}$$

3.3.2 Results

The average patient data interval was 3.0 days, with the longest at 12.3 days. The absolute average blood glucose fitting error over all patients was 4.57%, with a range of 0.87–8.83%. These values are close to or within the experimental glucose measurement error, and match the expectations of other non-linear fitting

methods [Hovorka and Vicini, 2001]. The summarised results with inter-quartile range (IQR) are shown in Table 3.4

Table 3.4 Retrospective blood glucose fitting error

Patient Number	Mean Percentage Error (%)	Percentage Error Standard Deviation (%)	Time Interval (days)	Number of Measurements	
				Total	Per Day
R24	4.66	6.84	2.0	32	16.0
R87	2.35	2.69	6.4	48	7.5
R130	7.42	6.17	1.4	31	22.0
R229	5.65	9.72	10.0	78	7.8
R278	8.83	11.17	1.6	13	8.1
R289	6.56	7.68	1.7	13	7.7
R468	5.46	6.10	1.7	17	10.0
R484	2.41	2.04	1.7	18	10.6
R486	6.43	6.89	1.6	16	10.0
R519	3.04	2.55	12.3	82	6.7
R554	5.11	4.58	2.3	40	17.4
R666	3.50	2.38	1.6	15	9.4
R847	4.26	4.36	1.5	12	8.0
R1016	3.87	5.05	1.6	13	8.1
R1025	4.12	4.74	1.7	15	8.8
R1090	0.87	0.80	1.6	10	6.3
R1099	4.47	3.90	1.6	14	8.3
R1125	3.17	2.69	1.7	11	6.5
Average	*4.57*	*5.02*	*3.0*	*26.6*	*10.0*
IQR	*3.34–5.56*	*2.69–6.51*	*1.6–2.2*	*13.0–31.5*	*7.7–10.0*

Figure 3.2 shows the fitted results for Patient R519. To reduce the impact of noise and erroneous measurements, the fitted values of p_G and S_I were replaced by their smoothed, zero-phase (zero-lag) three-point moving average to produce the fitted model simulated curve in the figure. Specifically, S_I is fitted hourly, and p_G is fitted every two hourly. Therefore, the three-point moving average of S_I at hour n would be the average of fitted S_I from hours $n-1$, n and $n+1$. The three-point moving average of two-hourly fitted p_G at hour n and $n+1$, where n is an odd number, would be the average of fitted p_G of hours $n-2$ to $n+3$. The result is a less accurate fit (slightly larger least square error), but a smoother more physiological time-varying profile for these parameters. Comparisons of smoothed and raw fitted p_G and S_I are shown in Figure 3.3.

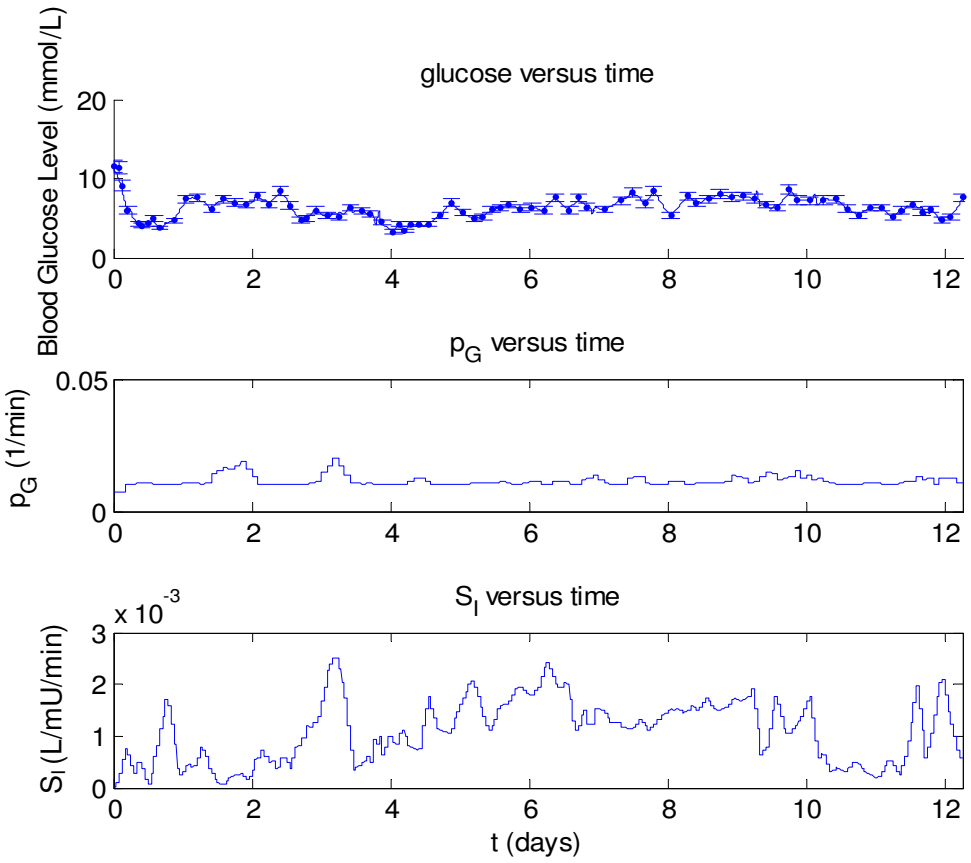

Figure 3.2 Patient R519 blood glucose data fit (top), corresponding endogenous glucose removal p_G (middle) and corresponding insulin sensitivity parameter S_I (bottom)

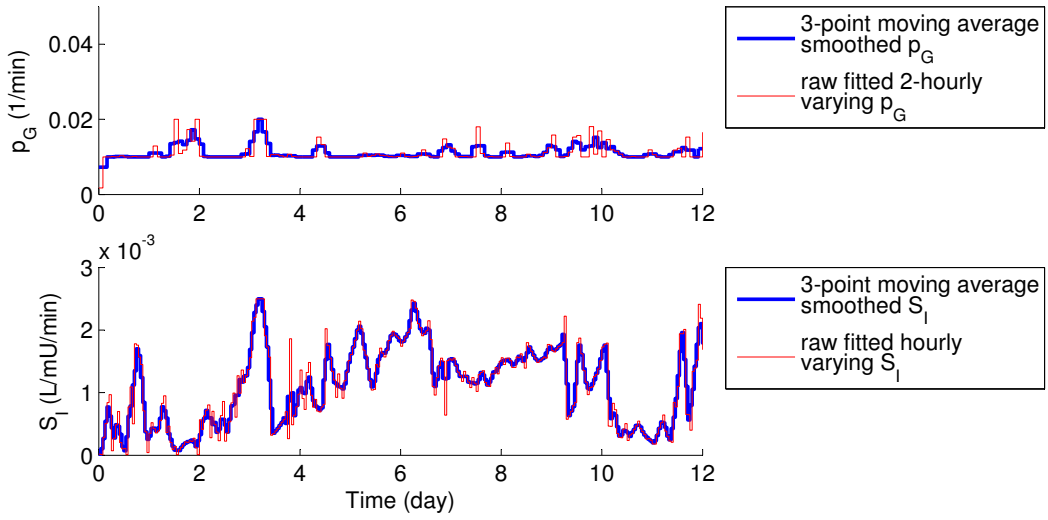

Figure 3.3 Patient R519 fitted p_G and S_I

Patient R519 had a total length of stay close to 2 weeks and shows the effectiveness of the model and integral fitting method as the model fitted blood glucose curve goes through every error bar. The patient specific parameter value for p_G was quasi-constant and S_I varied significantly. Both parameters were well within reported physiological ranges [e.g. Avogaro et al., 1989; Cobelli et al., 1999; Bergman et al., 1981, 1987; Prigeon et al., 1996; Doran, 2004].

Table 3.5 summarises the p_G and S_I values found for all the patients. The standard deviations for p_G are all approximately 5–10 times smaller than the mean value indicating that p_G remains relatively constant. This result validates the use of 2-hour, or longer, and even constant values for p_G [Hann et al., 2005]. Similarly, S_I is much more variable, indicating the 1-hour, or shorter, window as appropriate. These results also match clinical expectations and observations [McDonald et al., 2000; Hovorka et al., 2003; Chase et al., 2005c].

Table 3.5 Retrospective fitted p_G and S_I

Patient	p_G [1/min]		S_I [L/mU/min]	
Number	Mean	std	Mean	std
R24	0.0101	0.0002	0.00048	0.00016
R87	0.0109	0.0013	0.00076	0.00044
R130	0.0106	0.0010	0.00045	0.00028
R229	0.0111	0.0014	0.00110	0.00060
R278	0.0134	0.0030	0.00130	0.00035
R289	0.0100	0.0010	0.00110	0.00040
R468	0.0108	0.0008	0.00047	0.00024
R484	0.0108	0.0011	0.00049	0.00014
R486	0.0107	0.0010	0.00052	0.00032
R519	0.0114	0.0019	0.00110	0.00060
R554	0.0107	0.0012	0.00084	0.00054
R666	0.0101	0.0002	0.00032	0.00017
R847	0.0114	0.0013	0.00150	0.00060
R1016	0.0112	0.0015	0.00042	0.00019
R1025	0.0109	0.0011	0.00088	0.00045
R1090	0.0114	0.0026	0.00091	0.00017
R1099	0.0123	0.0019	0.00140	0.00040
R1125	0.0101	0.0014	0.00064	0.00037
Average	*0.0110*	*0.0013*	*0.00082*	*0.00036*
IQR	*0.0107–0.0113*	*0.0010–0.0015*	*0.00049–0.00110*	*0.00022–0.00045*

Comparing the computational effort between the integral-based fitting method to the traditionally preferred NRLS (non-linear least square) method on Patient R87, the integral fitting method found a global solution within 30 sec, producing a mean error of 2.35% (std 2.69%). The NRLS method took over 8 hours on the same computer, with both methods using MATLAB®, and only found a local minima, producing a mean error of 4.68% (std 5.52%).

Overall, the integral fitting method is approximately 1,000 times faster, because it does not require extensive iterations, and guarantees to find the global solution. This significant computational advantage over the traditionally favored NRLS method makes the integral-based fitting method a better choice for real-time clinical control applications where fast identification is required. In addition, adjustments in other minor parameters can then be quickly tested if necessary in clinical situations, given the very fast (initial) identification of p_G and S_I.

3.4 Model Prediction

For control applications, it is essential to know how well the fitted model can predict glycemic response to an intervention. If the fitted patient specific model is able to capture the immediate future glycemic changes, it also verifies that the fitted parameters reflect clinical physiology, and are not merely "molded" to fit collected data. More specifically, accurate prediction is a significant model and fitting method validation requirement.

Ten patients were used to test the 1 hour predictive ability of the identified model. To make a forward prediction from a given point, the model fit from the data over the previous 8 hours was used. Note that predictions are insensitive to the length of time fitted prior to prediction, as long as it is greater than 2 hours or 3–4 measurements. The 2 hours or 3–4 measurements criteria are used because these patient data are generally 2–3 hours apart.

The prediction is made by holding the current identified patient specific parameters, p_G and S_I, and the equilibrium glucose level, G_E, constant over the next hour. The resulting model predicted value is compared to the actual data and the percentage absolute error, e_i, calculated. For patients where there was insufficient consecutive data every hour, the intermediate blood glucose targets

were obtained via interpolation between data points. This process was repeated in moving 9-hour blocks, generating 13–76 predictions per patient.

The results in Table 3.6 show that 1-hour predictions have an average absolute error of 2–11%, which is close to the measurement error with the Glucocard^{TM} sensor of 7–12% over the glycemic ranges in the data [Arkray, 2001]. Most average errors are $< 6\%$ and well within measurement error. These errors are also within the clinically acceptable "A" range for glycemic control of approximately $\pm 20\%$ using the Clarke Error Grid [Clarke, 2005].

Table 3.6 Fitted model prediction errors

Patient	Number of predictions	Average prediction error e (%)	Standard deviation (%)
R24	22	5.86	4.00
R87	41	4.71	5.21
R130	18	10.12	9.55
R519	76	5.25	5.98
R554	24	10.90	8.89
R666	13	4.66	3.01
R1016	13	7.01	6.27
R1025	14	5.09	4.54
R1090	13	1.86	0.87
R1125	14	6.83	4.78
Average	*24.8*	*6.23*	*5.31*
IQR	*13.0–23.0*	*4.69–6.92*	*3.51–6.13*

3.5 Parameter Sensitivity Study

A sensitivity analysis was done on the population constant parameters k, n, α_I and α_G for Patient R87, using variations in individual parameters of -50%, -10%, $+10\%$ and $+50\%$ from the assumed values. Table 3.7 shows the resulting percentage change in the mean and standard deviation of the fitted S_I values. The parameter p_G was not included as it was essentially constant and did not change more than 1%.

Variations of k and α_I gave very little change to the identified S_I. This result suggests that k and α_I can be fixed at the population values, and that

Table 3.7 Sensitivity analysis on S_I (expressed in % change in S_I) for Patient R87

Parameter	Percentage change from population value used							
	-10		+10		-50		+50	
	Mean	std	Mean	std	Mean	std	Mean	std
k	2.6	3.3	0.9	2.0	4.5	3.7	2.5	3.3
n	6.9	2.6	6.0	1.5	32.8	4.9	30.0	8.9
α_I	0.2	0.2	3.1	4.7	1.2	1.8	4.1	4.7
α_G	6.6	5.1	4.3	2.2	19.3	4.6	17.6	7.2

the resulting errors will have little effect on the identified values of S_I or p_G. The standard deviation of S_I from changing n is small compared to the mean, showing that the S_I curve is effectively scaled up or down but not changed in shape. Therefore, n can effectively be fixed at the population value, too. Figure 3.4 demonstrates this scaling effect.

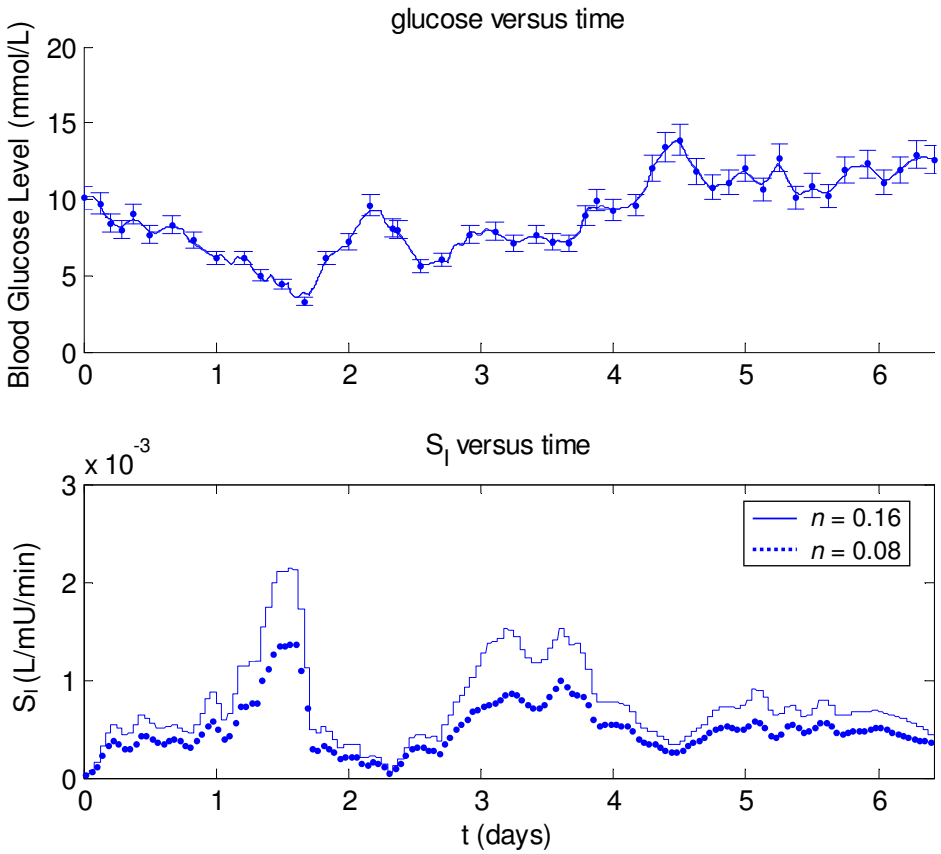

Figure 3.4 The effect of changing n on Patient R87. The dotted curve of S_I corresponds to $n = 0.16 \times (1 - 0.5)$ and the solid curve of S_I corresponds to $n = 0.16$. The blood glucose curves are essentially overlaid.

One parameter that does produce a significant change is α_G, as shown in Figure 3.5 and Table 3.7. Note in Figure 3.5 that changes in α_G resulted in several data points being missed in days 4–6, unlike in Figure 3.4, where α_G is at its assumed reported population value for Patient R87. Change in α_G also has a scaling effect on S_I, however, as indicated by the poor fit in days 4–6, these S_I values identified are not physiologically accurate. In particular, the S_I curve is reduced as α_G is lowered because a lower α_G leaves more effective insulin $\bar{Q}$ for action. This result suggests a need to further identify α_G, but also that it trades off at higher insulin values with S_I [Chase et al., 2004].

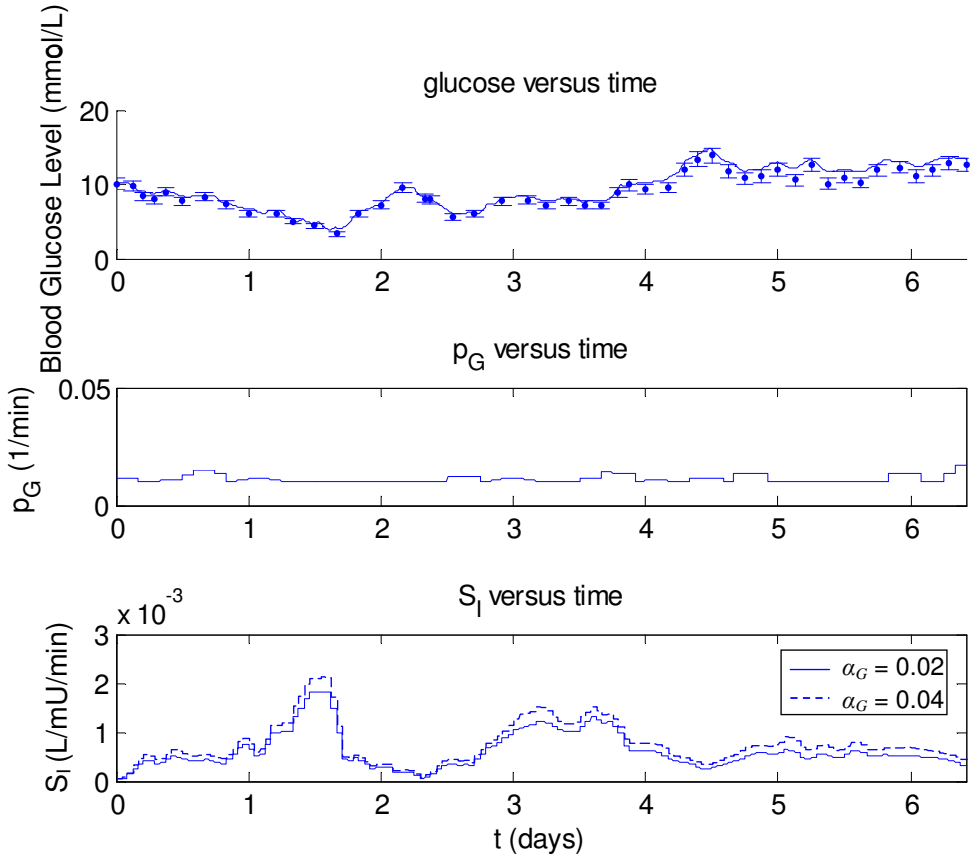

Figure 3.5 The effect of changing α_G for Patient R87. The dashed curve of S_I corresponds to $\alpha_G = 0.04$ and the solid curve of S_I corresponds to $\alpha_G = 0.04 \times (1 - 0.5)$. Fitted blood glucose curve where $\alpha_G = 0.04$ not shown.

All the results in the fitting suggest that p_G is essentially constant for each patient at a patient specific value. In addition, Table 3.5 shows very little variation in the value of p_G over all the patients in the cohort. Thus, the effect of holding $p_G = 0.01$ [1/min] constant at its approximately average value over the cohort is examined.

Fitting error does not significantly differ whether p_G is fitted or held at a constant. The mean fitting error across all 18 patients when p_G is fitted is 4.57%, with a standard deviation of 5.02% in Table 3.4. When p_G is held constant at 0.01, the mean fitting error is 4.43%, with a standard deviation of 5.02%. The nearly identical fitting quality suggests that p_G can be held at a population value ($p_G = 0.01$) similar to k, n and α_I.

3.6 Adjustment in Model Parameters

As indicated in the sensitivity studies in Section 3.5, further studies were carried out on some parameters to "fine tune" the glucose-insulin model presented in Equations (2.9)–(2.13), as suggested previously in Section 3.1. In addition, many variables might be more exactly defined with no loss of fitting or prediction error, all else equal. Finally, such an analysis provides further insights into the modelled dynamics, critical parameters and parameter sensitivity.

3.6.1 Distribution Volume V_G and V_I

Initially, one common distribution volume was used for both the glucose and the insulin compartment, and the value of 12 L was taken as the average value over all physiological compartments, as reported in Bergman et al. [1981]. The Minimal Model of insulin kinetics in Bergman et al. [1981] did not deal with exogenous insulin input or an explicit insulin interstitial distribution space, as the study was focused on IVGTT (Intravenous Glucose Tolerance Tests). This difference occurred in part because the IVGTT did not involve exogenous insulin administration.

In the earlier stage of physiological model development, Doran et al. [2004b] simplified the Minimal Model into a two-compartment model. The two compartments were glucose and insulin respectively. As Equation (2.10) was introduced into the physiological model, the interstitial space distribution volume needs to be reviewed. In particular, many studies on insulin kinetic modelling suggest different volumes for glucose and insulin distribution [Ferrannini and Cobelli, 1987a; Van Cauter et al., 1992; Sherwin et al., 1974; Insel et al., 1975].

The insulin distribution volume, which is the plasma volume, is found to be around 4.5 % body weight, with little variation between individuals [Ferrannini and Cobelli, 1987a]. However, the estimated total plasma equivalent space for glucose can vary up to 5-fold depending on modelling methods [Ferrannini and Cobelli, 1987a], and ranges from 14–27% body weight [e.g. Ferrannini and Cobelli, 1987a; Sherwin et al., 1974; Insel et al., 1975].

Taking V_G in Equation (2.9) as 19% of body weight and V_I in Equation (2.11) as 4.5% of body weight for a 70 kg average body weight (as ICU patients' weights are generally unavailable), the re-fitted S_I distribution for the 18-patients is shown in Figure 3.6. The average fitting error from using $V_G = 13.3$ L and $V_I = 3.15$ L is 4.31% (std = 5.57%), which is very similar to the results when $V_G = V_I = 12$ L (4.57%, std = 5.02%) in Table 3.4. Comparing the fitted S_I, changing the volumes for V_I and V_G resulted in a much lower mean S_I (3.12×10^{-4} v.s 9.22×10^{-4}) due to the lower volume and resulting higher insulin concentrations. However, the relative covariance of hour to hour variations is still similar (0.66 v.s 0.60), indicating the variations from hour to hour are very similar, and that little change in profile shape has occurred.

In conclusion, changing the volumes did not change the quality of fit. This result suggests that the fitting method and the parameter S_I are very robust to these volumes although not insensitive. The S_I fitted with more physiologically correct volumes obtained from more in-depth insulin kinetic modelling studies is now one step closer to indicating the "true" tissue sensitivity to insulin that the S_I parameter represents.

3.6.2 Effective Insulin Half-Life k and Saturation α_G

Insulin sensitivity can tradeoff with the parameter for the effective half-life of insulin (k) and the effective insulin saturation limit (α_G) [Chase et al., 2004]. Although frequent re-evaluation of S_I can generally produce a good fit to the data, if its variation is not a realistic reflection of the "true" overall insulin sensitivity, the use of the model in dynamic patient specific glycemic prediction will be poor. Therefore, other minor parameters that can tradeoff with S_I must be carefully examined, to minimise unwanted mitigating or compromising effects.

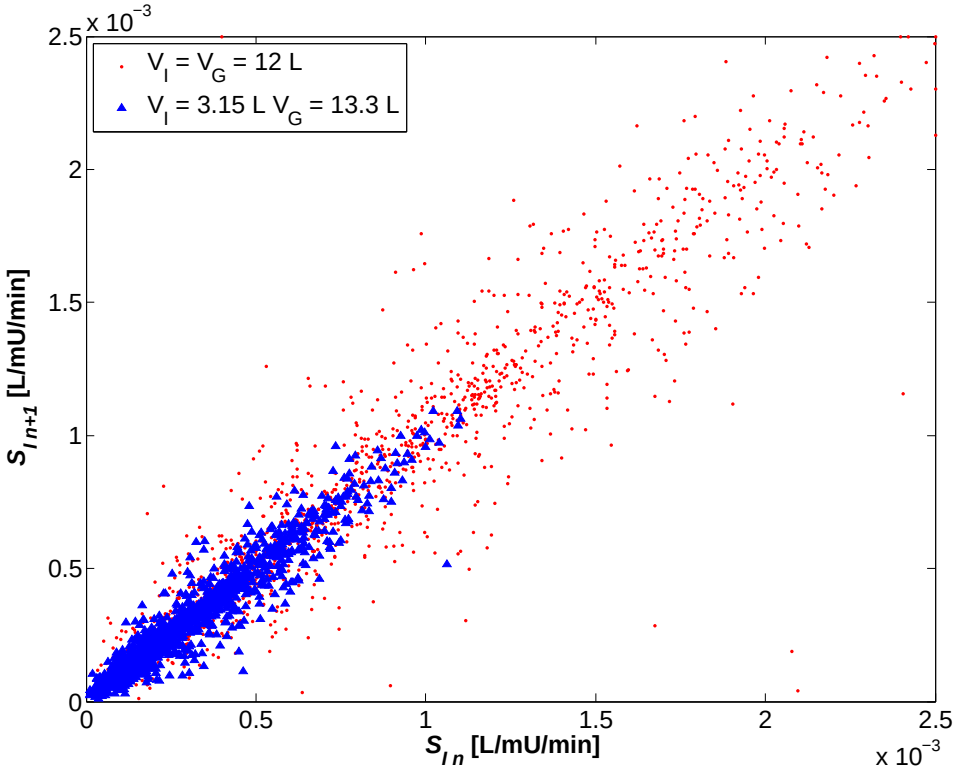

Figure 3.6 Fitted S_I and distribution volumes for 18 retrospective patients

The level of effective insulin saturation, α_G, can also have a significant detrimental impact on model-based glycemic control. Exacerbating this issue, its value can vary widely between individuals (0.001–0.04 [L/mU]) [Natali et al., 2000; Prigeon et al., 1996; Nestler et al., 1988; Transberg et al., 1981; Turnheim and Waldhausl, 1988; Duckworth and Kitabchi, 1981; Chase et al., 2004]. However, real-time identification is difficult because its detection is available only when significant saturation occurs, followed by a large prediction error, and its ultimate refection in overall poor control [Chase et al., 2004, 2005c].

For patient safety, α_G is chosen to be 1/65 L/mU, corresponding to the highest reported average saturation level [Prigeon et al., 1996]. If the modelled saturation level is too low, the risk of administering excess insulin increases, due to seeing the patient as near the saturation limit and requiring insulin for a given predicted change in blood glucose levels. If a patient does have a low saturation limit, the patient will then be seen as more insulin resistant, but will not be at risk of hypoglycemia due to administering excess insulin [Chase et al., 2004, 2005c]. Hence, this selection is primarily made with respect to control safety in

the absence of any other data. Finally, note that clinical identification of α_G in critical care would require extensive non-therapeutic interventions that are not ethically possible or likely in regular care and glycemic control.

When k is not approximated correctly, the impact on model dynamics is transferred into the value of S_I. This effect is not observable in the 18-patient data, because its impact is only seen when data frequency is greater than once every hour. When data frequency is greater than once every hour, a 1st order linear S_I produces a better fit and can reveal faster dynamics [Chase et al., 2005c]. Under this circumstance, an incorrect k value results in the non-physiological sawtooth S_I profile, as shown in the lower panel of Figure 3.7(a).

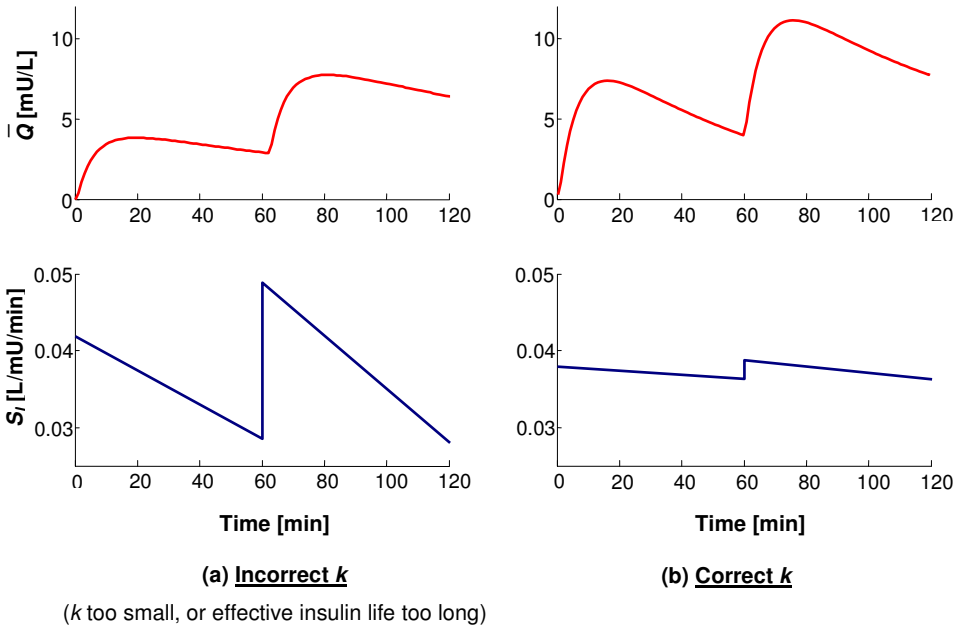

Figure 3.7 S_I resembling saw tooth profile

Figure 3.7(a) shows a value of k that is too small, or an effective insulin half-life that is too long. Therefore, the modelled curve of saturated or effective interstitial insulin effect, $\bar{Q}$ in the top panel of Figure 3.7(a) is too "flat", forcing the model to require the system to be more insulin sensitive at first, and then significantly less sensitive later. This effect creates the sawtooth profile in S_I in the lower panel in Figure 3.7(a). Figure 3.7(b) shows the situation when k is correctly modelled. In this case, S_I in the lower panel is relatively constant because $\bar{Q}$ in the top panel has the correct shape and decay to match (frequent) blood glucose data, where the slight sawtooth is likely due to measurement noise.

If zero order S_I is fitted when k is incorrect and the data sampling frequency is high, the quality of fit can be poor. In the clinical control studies of Chase et al. [2005c] where data frequency is greater than once every hour, the value of k is adapted in clinical control trials when sawtooth behaviour in S_I is observed. This approach allowed an adaptation in k that better reflected the true value of k in those trials. However, such high data density with measurement intervals less than hourly is not clinically feasible outside a (brief) research study. Thus, better understanding and a useful population value is still required.

Fitting S_I to the 18-patient data with $k = 0.0198$ (corresponding to $t_{1/2} =$ 35 min) and $\alpha_G = 1/65$ produced very similar error as when $k = 0.0099$ (corresponding to $t_{1/2} = 70$ min) and $\alpha_G = 1/25$ (4.27, std 5.70% v.s 4.31, std 5.57%). In both cases, $V_I = 3.15$ L and $V_G = 13.3$ L were used.

Although changing k and α_G did not noticeably improve the fitting quality in the 18-patient cohort, a k corresponding to an effective insulin half-life of 35 min captures better short term dynamics in 2 of the 3 patients reported in Chase et al. [2005c], and the 7 patients reported in Wong et al. [2006a], where blood glucose levels were sampled every 30 min. The median fitting error decreased from 5.75% to 5.32% when the effective insulin half-life decreased from 70 to 35 min ($k = 0.0099 \rightarrow 0.0198$) for all the patients in Wong et al. [2006a]. Finally, having α_G set to a lower saturation level (1/65 as opposed to 1/25 1/min) ensures better patient safety during a glycemic control trial [Chase et al., 2004, 2005c].

3.6.3 Final Model Parameter Summary

The final decision on parameter values are shown in Table 3.8. Values for k_{pr} and k_{pd} for the rise and decay of enteral dextrose inputs appearing from the gut and intestines are set to 0.0347 min^{-1} and 0.0068 min^{-1}, respectively, corresponding to half-lives of 20 and 100 min to reflect published results [Kiwanuka et al., 2001; Ludvik et al., 1997; Radziuk et al., 1978; Nielsen et al., 1998; Basu et al., 2001, 2004; Firth et al., 1985]. The constant C in Equation 2.11 is set to $C = 3.15$ that produces good approximation to the 18-patient data.

Table 3.8 Population and generic model parameters

Parameter	Value	
k	0.0198	[1/min]
n	0.16	[min-1]
α_I	0.0017	[L/mU]
α_G	0.0154	[L/mU]
V_G	13.3	[L]
V_I	3.15	[L]
k_{pd}	0.0069	[1/min]
k_{pr}	0.0347	[1/min]
I_B	9.45	[mU/min]

3.7 Summary

The integral-based fitting method presented in this chapter is effective in reducing a typically non-linear, non-convex optimization problem to a simple convex, linear system. The integral fitting method is ∼1,000+ times faster than traditional non-convex NRLS fitting methods for these kinds of non-linear, non-convex dynamic systems because it does not require extensive iterations, nor multiple starting points to ensure accurate optimal solutions.

The validation of the integral-based fitting method on retrospective data from the 18 long term patient cohort produced good quality fits, with errors within the reported measurement accuracy. All fitted values for p_G and S_I are within physiologically valid ranges reported in the literature, while other minor parameters are fixed at population values. This result verifies the effectiveness of the fitting method developed, as well as the physiological validity and adequacy of the glucose-insulin model of Equations (2.9)–(2.11).

Endogenous glucose removal p_G remained nearly constant throughout all patients and tests, suggesting it can be held constant. The insulin sensitivity parameter S_I, showed much greater variation. Some of this variability is due to the highly variable condition of the critical care patients, which can induce large variation in the level of counter-regulatory hormones present and hence in insulin sensitivity [Hann et al., 2005; Chase et al., 2006b]. In addition, drug therapies such as beta-blockers or vaso-dilators can also have an impact on insulin sensitivity [Chase et al., 2005c; Wong et al., 2006b].

Sensitivity analysis supports the assumption that p_G and S_I are the only crucial parameters that drive the dynamics of the glucose-insulin system. Changing the parameters k, n, and α_I from the initially assumed population values did not significantly affect the fits and the trends of the primary parameters p_G and S_I. However, k was later modified based on higher frequency data revealing shorter term dynamics. The effective insulin saturation parameter α_G was also lowered as a precaution to ensure better patient safety when considering the application of this physiological model in glycemic control trials.

Forward prediction of glucose values for a period of one hour ahead were within 2–11% of the measured values, further validating the p_G and S_I values obtained. This error is also within the clinically acceptable "A" range for glycemic control and is also within the 7–12% sensor error.

All of these results demonstrate the potential of this model for clinical control. More specifically, given the patient specific parameters at any point in time, the amount of insulin can be directly calculated to regulate a patient's blood glucose level to a target level in the next hour. This process could be continued every hour so that a patient's glucose level is tightly controlled over their entire stay at the ICU with minimal variation. Note that holding p_G and S_I constant during the prediction interval only presents the simplified targeted glycemic control scheme, as it ignores the potentially hidden stochastic behaviours of the parameters. Analysis of the stochastic behaviour in these parameters would further enhance the capability of the physiological model and fitting method as used in glycemic control to predict the glycemic response to an intervention, as Chapters 5–7 later show.

Chapter 4

Critical Care Glycemic Control

The physiological model developed for critical care glycemic control in Chapter 2 and the integral-based parameter identification method presented in Chapter 3 have been tested in clinical control trials in three stages [Chase et al., 2005b,c; Wong et al., 2006a,b; Lonergan et al., 2006a]. These trials were carried out in the Christchurch Hospital Intensive Care Unit, with ethical consent obtained from the Canterbury Ethics Committee and the South Island Regional Ethics Committee.

The control algorithms implemented are adaptive and predictive. The first stage of clinical trials used insulin-only control [Chase et al., 2005b,c], and the second stage added carbohydrate enteral infusion control [Wong et al., 2006a,b]. These first and second stages employed computerised control algorithms, where a computational unit is used on site. The third stage of the clinical trials, having proved that the algorithm and overall approach is safe and effective in the first two stages, transformed the insulin and nutrition adaptive, predictive control algorithm from computerised into tabulated form. This change made large-scale clinical implementation simple, and readily adaptable to any intensive care unit [Lonergan et al., 2006a].

This chapter briefly presents the protocols and results for each stage of the clinical control trials.

4.1 Insulin Only (Bolus) Control

The first stage of the clinical trials utilised insulin-only control to test the efficacy of the physiological model of Equations (2.9)–(2.11). Three patients were admitted to this stage of clinical trials.

Protocol

These proof-of-concept clinical trials span five hours, including an insulin challenge hour, and four hours of tight blood glucose control. At the end of each hour during the controlled phase, the blood glucose target to be achieved in the next hour is set according to both the current blood glucose level and level of insulin resistance. Generally a 10–20% hourly reduction is chosen. The minimum target level is 4.5 mmol/L.

All patients were undergoing a constant, unit standard enteral nasal-gastric feed of approximately 1000 calories of glucose per day, which was the current standard for the Christchurch Hospital ICU. Selected patients had to be stable, hyperglycemic and representative of typical ICU conditions. Specific inclusion criteria include: the presence of constant naso-gastric feed; random blood glucose concentration being greater than 8 mmol/L; the patient being over 16 years old; and the presence of an in situ arterial cannula. Exclusion criteria include: the absence of a naso-gastric tube or arterial catheter; the patient being moribund or not expected to survive more than 72 hours; patients receiving neuromuscular blockade; and patients having body mass index above 35 kg/m^2.

Trials begin at 0700 hours, at which time any insulin infusion is held constant with constant naso-gastric feed maintained. Christchurch Hospital ICU patients are given Isosource$^{\text{TM}}$ enteral feed at a known constant rate (typically 70 ml/hr) throughout the trial via the naso-gastric tube, which is standard procedure at this ICU. Blood glucose readings are taken hourly to determine the patients' equilibrium blood glucose level, G_E, at 1000 hours. At 1000 hours, patients are injected with a fixed 1500 mU bolus of Actrapid$^{\text{TM}}$ insulin via an intravenous cannula using a Graseby 3500 syringe pump. Plasma glucose is measured at 15 min intervals until 1100 hour. Paired blood samples are taken and analysed using a bedside Glucocard$^{\text{TM}}$ Test Strip II glucose testing kit, with 7% absolute error in readings at typically elevated blood glucose levels [Arkray, 2001].

Patient specific parameters, p_G and S_I, are fitted as discontinuous first order functions using the first hour of data. Based on these values, an insulin bolus size is calculated by the controller to achieve the target blood glucose level set for the end of the following hour. Blood glucose is monitored every 30 min, and patient specific parameters are re-evaluated every hour using the data obtained in the previous hour. Following each re-evaluation, the controller determines the insulin bolus required to achieve the targeted blood glucose reduction.

The overall approach is a bolus driven, patient specific adaptive control method that uses prior data to regularly update the patient specific parameters. The overall clinical trial procedure is outlined in Figure 4.1.

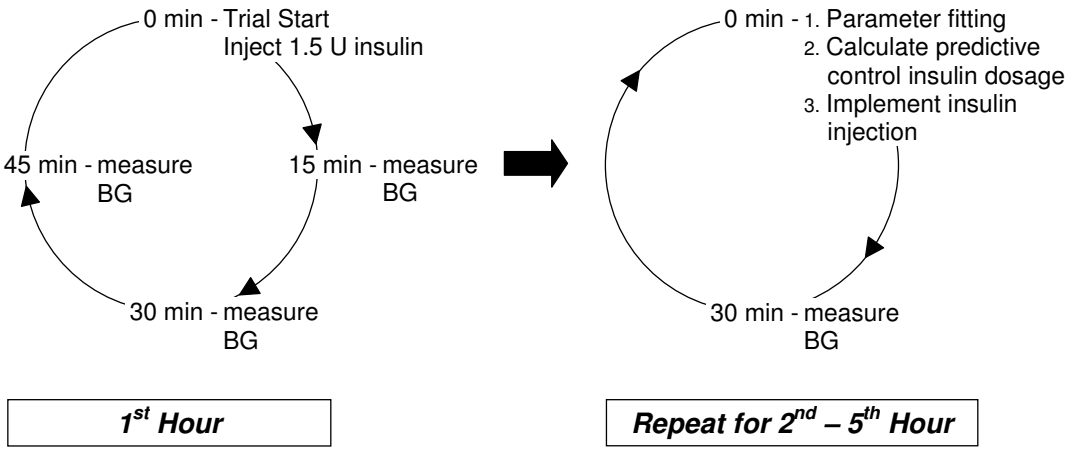

Figure 4.1 Insulin bolus glycemic control procedure

A bolus-based approach is seen as being potentially safer than continuous infusions when used in a semi-automated fashion with medical staff in the loop. More specifically, if medical staff are detained or busy, a bolus-based approach does not infuse more insulin at a rate that is potentially too high for that upcoming hour [Chase et al., 2005b].

For patient safety, a limit of 6 U/hr is placed on the insulin bolus to be administered. In addition, the controller limits saturated interstitial insulin $Q - Q/(1 + \alpha_G Q) \leq 30$ mU/L to avoid excess insulin effect saturation. The glucose and insulin distribution volumes are assumed to be $V_G = V_I = 12$ L for these trials. Blood glucose fluctuations greater than 10% of the blood glucose level in a given hour are also undesirable. When a patient is predicted to exhibit a large fluctuation over the next hour, the controller sets an intermediate target

to be achieved in 30 min using a smaller bolus to eliminate large fluctuations that result from large boluses.

Trial Results

Figure 4.2 shows the trial results of Patient C301, demonstrating the progression of a trial. The controller used k corresponding to an effective insulin half-life of 70 min, and $\alpha_G = 1/25$ $[L/mU]$. Modification of these generic constant parameter values were considered after this trial to better patient safety (changing α_G to 1/65 L/mU), and minimise sawtooth effect seen in S_I in the bottom panel of Figure 4.2, as explained in Section 3.6.2 of Chapter 3. A detailed review on parameter modification of Patient C301 can be found in Chase et al. [2005c]. Specific predictive control target acquisition error for Patient C301 is presented in Table 4.1.

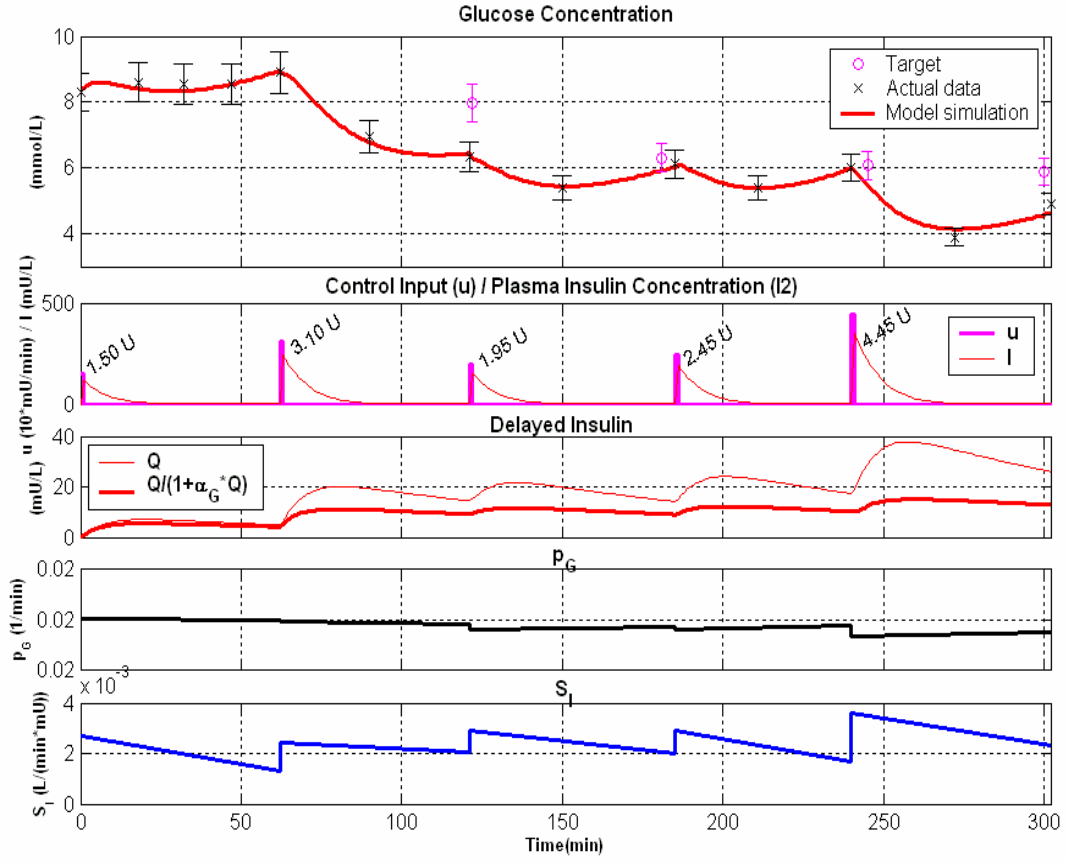

Figure 4.2 Insulin bolus glycemic control trial of Patient C301. The top panel displays the glycemic progression of the controlled patient. The second panel shows the insulin boluses given. The third panel shows the interstitial insulin and its saturable action. The forth and last panels are the fitted patient parameters p_G and S_I.

Table 4.1 Effectiveness of predictive insulin bolus control represented in target error for Patient C301

Time (min)	Target glucose (mmol/L)	Achieved glucose (mmol/L)	% Error (abs)	% Revisited trial predicted error (abs)[a]
120	7.97	6.35	20 (−1.62)	6 (−0.43)
180	6.31	6.13	3 (−0.18)	2 (−0.11)
240	6.08	6.00	1 (−0.08)	3 (0.17)
300	5.89	4.90	17 (−0.99)	8 (−0.40)

[a] Prediction error from post-trial simulation (k changed from 0.0099 to 0.0198 1/min and $\alpha_G = 1/65$ L/mU).

As Figure 4.2 shows, even though the originally assumed k and α_G did not provide the best fit, the blood glucose level was reduced systematically in a safe manner. When the parameter values were modified, the predictive control target acquisition error reduced significantly, as shown in Table 4.1.

Two other trial results are presented in Table 4.2. Most of the larger prediction errors were a result of insulin utilisation saturation, which the controller predicted. These patients' detailed trial review and analysis can be found in Chase et al. [2005b,c]

Table 4.2 Effectiveness of predictive insulin bolus control represented in target error for Patient C302–3

Patient	Time (min)	Target glucose (mmol/L)	Achieved glucose (mmol/L)	Error (%) (abs)
C302	120	9.81	9.10	7%
	180	8.39	8.75	4%
	240	7.61*	6.00	21%
	270	6.54	6.85	5%
	300	6.00*	7.20	20%
C303	120	8.58	10.40	21%
	180	10.98*	8.70	21%
	240	7.64	7.35	4%
	300	6.92*	6.90	0%

* Target value was compromised because the desired glucose reduction was restricted by saturation.

In summary, these three first proof-of-concept predictive target glycemic control trials in the ICU verified the applicability of the physiological model of Equations (2.9)–(2.11) and the integral-based parameter identification method presented in Chapter 3 for critical care glycemic control. The controller reduced

the three patients' blood glucose from 6.35 → 4.90, 9.10 → 7.20 and 10.40 → 6.90 mmol/L respectively during the 5 hour trials. The mean predictive target acquisition accuracy was 6.7%, which is less than the typical 7–12% measurement error [Arkray, 2001], excluding occasions where insulin effect saturation limited the achievable glycemic reduction.

4.2 Insulin and Nutrition Control

Seeing the proven short term benefits from the insulin-only predictive target glycemic control in the first stage of clinical trials, the second stage proposed the use of an additional dextrose control input as well as longer trials. As the first stage trials showed, insulin-only control has limited performance in the presence of significant insulin effect saturation, which occurs due to extreme insulin resistance in some of these patients. More specifically, critically ill patients generally have heightened secretion of counter-regulatory hormones which stimulates endogenous glucose production and increases effective insulin resistance [Mizock, 2001; McCowen et al., 2001; Chase et al., 2005c; Wong et al., 2006b]. Under this already severely compromised situation, high glucose nutritional regimes often result in excess glucose [Patino et al., 1999; Weissman, 1999; Woolfson, 1980; Elia et al., 2005], exacerbating hyperglycemia. As a result, only limited reductions might be available with insulin alone, necessitating this second control input. In addition, several recent studies encouraged review of clinical nutrition regimes because many current practices have hidden adverse effects [Iyer, 2002; Krishnan et al., 2003; Dickerson et al., 2002; Dickerson, 2005].

Simulated control results using insulin only and insulin plus nutrition control in Figure 4.3 shows that insulin-nutrition control can better combat insulin resistance. These trials were simulated using the retrospective patient cohort used for validating the integral-based parameter identification method. The hospital control data were real clinical data collected for these patients during their stay in the ICU. Insulin only control only approaches similar control performance when insulin sensitivity is high. At very low insulin sensitivity, insulin only control appeared even less effective than hospital control data. This result occurs because the clinicians usually would resort to reducing dextrose feed to severely hyperglycemic patients if they did not respond to large doses of insulin. This action

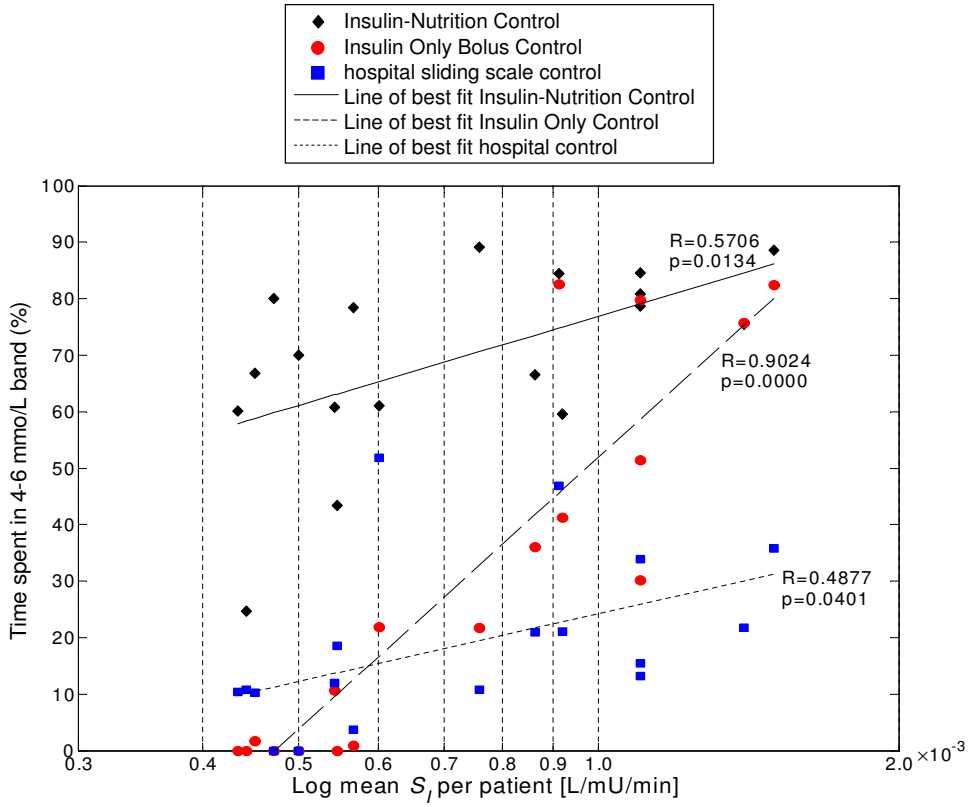

Figure 4.3 Simulated insulin-only and insulin-nutrition control performances v.s hospital control data

essentially incorporates some basic nutrition control in the clinical sliding scale protocol used when insulin sensitivity is low.

Protocol

The trial procedure follows the same outline as the insulin-only trials, with the addition of controlling dextrose. Patient selection, inclusion and exclusion criteria are also the same as for the insulin-only control trials, and specific details can be found in Wong et al. [2006b]. The outline for the insulin-nutrition control control procedure is shown in Figure 4.4.

Insulin is still administered in boluses for safety from infusions being left on, and dextrose is given at a constant feeding rate until the controller advises adjustment. Equations (2.12)–(2.13) define the dynamics resulting from the dextrose interventions. Minimum dextrose is set at 280 kcal/day of glucose or approximately 30% of goal feed. The goal feed rate is an ideal feed rate determined by the clinician on admission to the insulin-nutrition glycemic control protocol. This

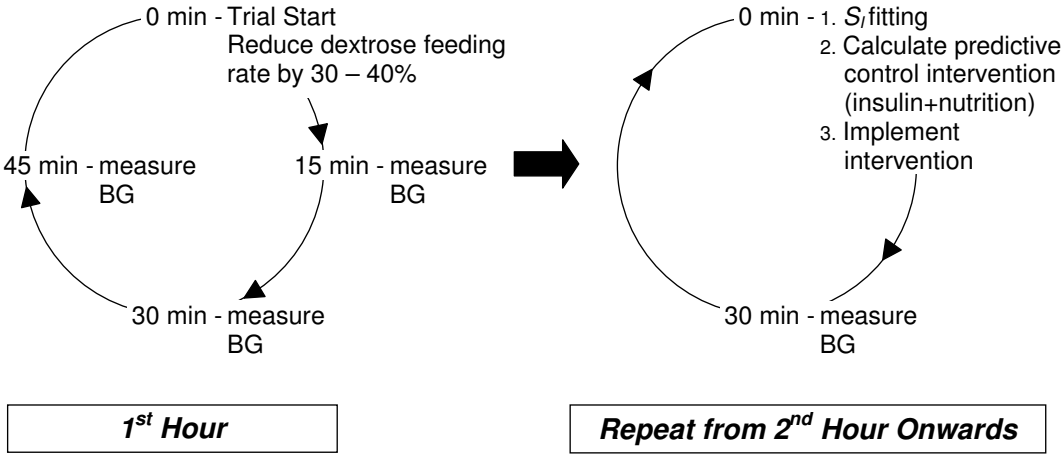

Figure 4.4 Insulin-nutrition glycemic control procedure

lower limit on feed rate is placed to avoid increased risk of nosocomial infections [Rubinson et al., 2004]. Wong et al. [2006b] includes a complete description of the insulin-nutrition glycemic control protocol.

Trial Results

Eight patients participated in the insulin-nutrition glycemic control trials in the Christchurch Hospital ICU. The background information of these patients are summarised in Table 4.3. These patients represent a heterogeneous cross-section in age and sex. The median APACHE II score is 23 with interquartile range [19, 25], which represents a more critically ill cohort compared with other critical care hyperglycemia control studies [Van den Berghe et al., 2001; Krinsley, 2003a]. The high proportion of septic patients stems from their severity of condition and, hence, likelihood of hyperglycemia.

Patients C401–7 had trials spanning 10 hours, and Patient C408 spanned 24 hours. Patient C408 only had data collected hourly from the 2$^{\text{nd}}$ hour onwards. Trials results, expressed in predictive control target acquisition ability, are summarised in Table 4.4. Boxplots for the prediction error for each individual patient are shown in Figure 4.5.

Overall, 41.9% of targets are achieved within ±5% target acquisition error. Seven out of $n = 86$ targets had error $> 20\%$, resulting in 90.7% of all mea-

Table 4.3 Background information on insulin-nutrition control trial patients

Patient number	Medical subgroup	APACHE II score	APACHE II ROD (%)	APACHE III	SAPS II	SAPS II ROD (%)	Age	Sex	Mortality	Diabetes
C401	Sepsis	17	14.3	40	15	2	56	M	N	Type 2
C402	Sepsis	24	49.7	59	35	16.7	64	M	N	
C403	Pulmonary	31	73.3	85	45	34.8	60	M	N	
C404	Sepsis	26	59.7	91	62	71.9	75	F	N	
C405	Sepsis	21	33.2	58	34	15.3	73	M	N	Type 2
C406	Other medical	17	14.3	44	44	32.6	57	M	N	
C407	General surgical	23	62.3	84	57	61.9	73	F	N	Type 2
C408	Other medical	20	38.1	67	47	39.2	60	M	N	

Table 4.4 Predictive insulin-nutrition glycemic control trial results

	Mean target absolute error	
Patient	%	mmol/L
C401	12.6	0.8
C402	9.9	0.9
C403	7.2	0.3
C404	10.0	0.6
C405	2.4	0.1
C406	7.6	0.4
C407	7.5	0.4
C408	10.5	0.6
average	*7.2*	*0.5*

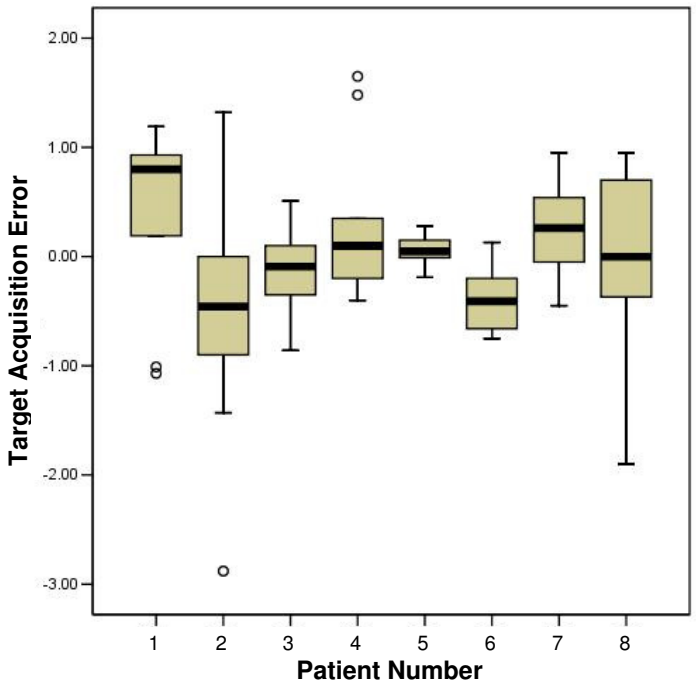

Figure 4.5 Target acquisition error in insulin-nutrition control trials

surements having a target acquisition error within ±20%. The larger errors are attributed to significant and rapid changes in patient condition, such as Patient C402 who suffered from atrial fibrillation [Wong et al., 2006b], which caused the outlying errors in that case as their condition changed suddenly. Overall, the outlying errors in each case are small compared to the measurement error and/or can be ascribed to clinically verified, acute or sudden changes in patient conditions.

This 8 patient cohort has a significant level of illness as measured by APACHE II score. With a median APACHE II score of 23 (range [17, 31]), the insulin-nutrition predictive target glycemic control algorithm showed tight control to less than 5.5 mmol/L. In comparison, Van den Berghe et al. [2001] achieved similarly tight control with median APACHE II score of 9 (interquartile range [7, 13], which represents a much lower level of illness. For a more comparable ICU population, Krinsley [2003a] showed tight control to a higher 7–7.5 mmol/L target (average 7.3 mmol/L) for a cohort with median APACHE II of 16 (interquartile range [10, 23]). Both these studies used insulin alone to control glucose levels. Hence, the added control obtained by modulating nutrition, as well as insulin, to control glycemic levels is seen in the ability to achieve tight control to a level similar to that of Van den Berghe et al. [2001], but for a more critically ill ICU cohort.

In conclusion, this stage of insulin-nutrition predictive target glycemic control trials demonstrates the potential for accurate reduction and tight regulation of glucose levels despite significant inter-patient variability and time-variant physiological condition. The average absolute error was 0.5 mmol/L, which is small compared with the 4–6 mmol/L desired range. In addition, the outlying target errors of 15–20% are not considered clinically significant in the glucose ranges involved in this ICU clinical environment.

Finally, the clinically verified effective glucose-insulin physiological model of Equations (2.9)–(2.13), the integral-based parameter identification method presented in Chapter 3, and the insulin-nutrition predictive algorithm presented here can, in combination, provide safe and effective glycemic control. Extended to long-term control studies, it has the potential to reduce ICU mortality and the risk of severe complications with relatively limited clinical effort and labour. The next step is larger scale trials to validate these effects.

4.3 Specialized Relative Insulin and Nutrition Tables (SPRINT)

A robust, easy-to-use protocol "SPRINT" (Specialized Relative Insulin Nutrition Tables) that employs both insulin and feed modulation is developed from the computerized insulin-nutrition predictive target glycemic control protocol [Wong

et al., 2005, 2006b] used in the 2nd stage of the clinical trials. Its goal is to maintain blood glucose levels in the target band of 4.0–6.1 mmol/L, as well as being easy to use with performance equivalent to the computerized predecessor protocol. Thus, SPRINT is implemented through 2 look-up tables in a wheel-based format, making it simple to use, and readily and widely adaptable in ICU. Overall, it is designed to mimic the computerised protocol, while providing a simple interface for easy, large-scale clinical implementation.

Protocol

The SPRINT protocol consists of two wheels dedicated to enteral nutrition optimization and insulin bolus administration, as shown in Figures 4.6 and 4.7. The SPRINT algorithm requires the current and previous blood glucose measurements, previous hour's nutrition feed rate, and previous hour's insulin bolus size to determine the nutrition and insulin interventions for the coming interval. The insulin bolus and feed rate for the next hour are then obtained with the wheels and instructions in Figures 4.6 and 4.7. SPRINT is used hourly with blood glucose samples taken from the arterial cannula for patient comfort. If no arterial cannula is present, blood is only taken every 2 hours via pin-stick from the toes or fingers. Specific limitations on dextrose and insulin adminstration are outlined in Lonergan et al. [2006a] and Shaw et al. [2006].

When a patient is glycemically stable, measurement frequency is changed from every hour to every 2 hours. Glycemic stability is defined as 3 hours in the 4.0–6.1 mmol/L band with 3 U or less of insulin/hr and 60% or more of the patient specific goal feed rate. Such a patient is not significantly insulin resistant and is in the target band, making sudden changes potentially less likely to occur and that allows less frequent measurement. In the hour between 2-hourly measurements, the nurse administers an insulin bolus of the same size as the previous hour, and leaves the feed rate unchanged.

Any patient who has two consecutive blood glucose measurements greater than 8 mmol/L over a time period of at least 4 hours is eligible to go on the SPRINT protocol. At entry, a patient specific percentile conversion sticker is created and attached to the feed wheel in Figure 4.6. This sticker converts absolute percentage goal feed (e.g. 30–100%) to an enteral feed pump rate in ml/hr. The values on the feed conversion sticker are computed based on the patient's age,

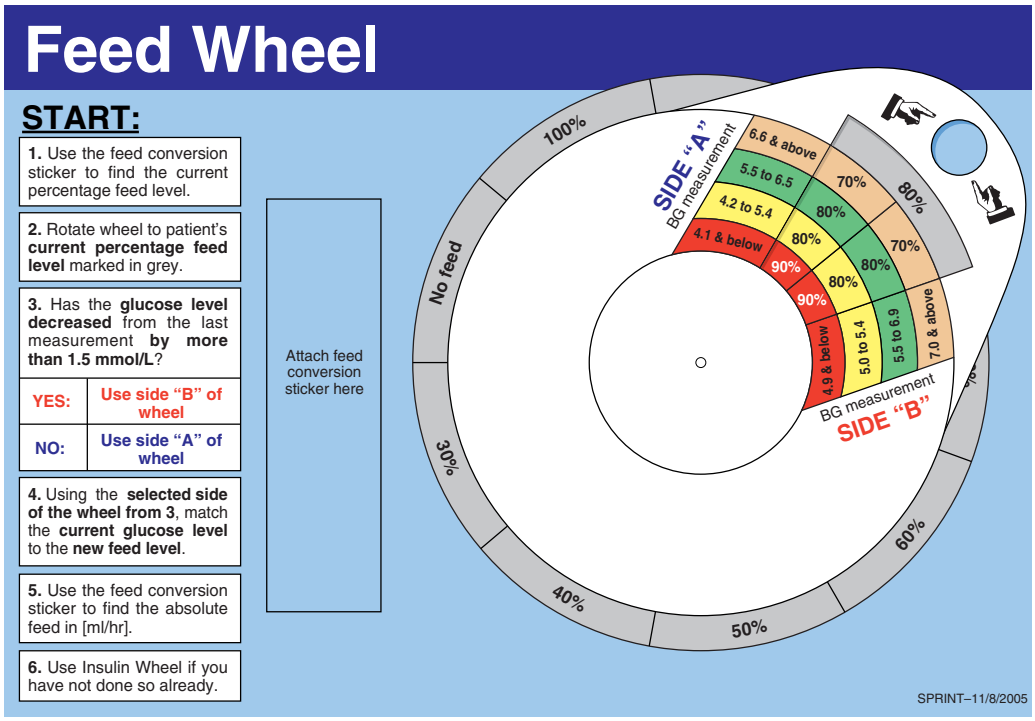

(a)

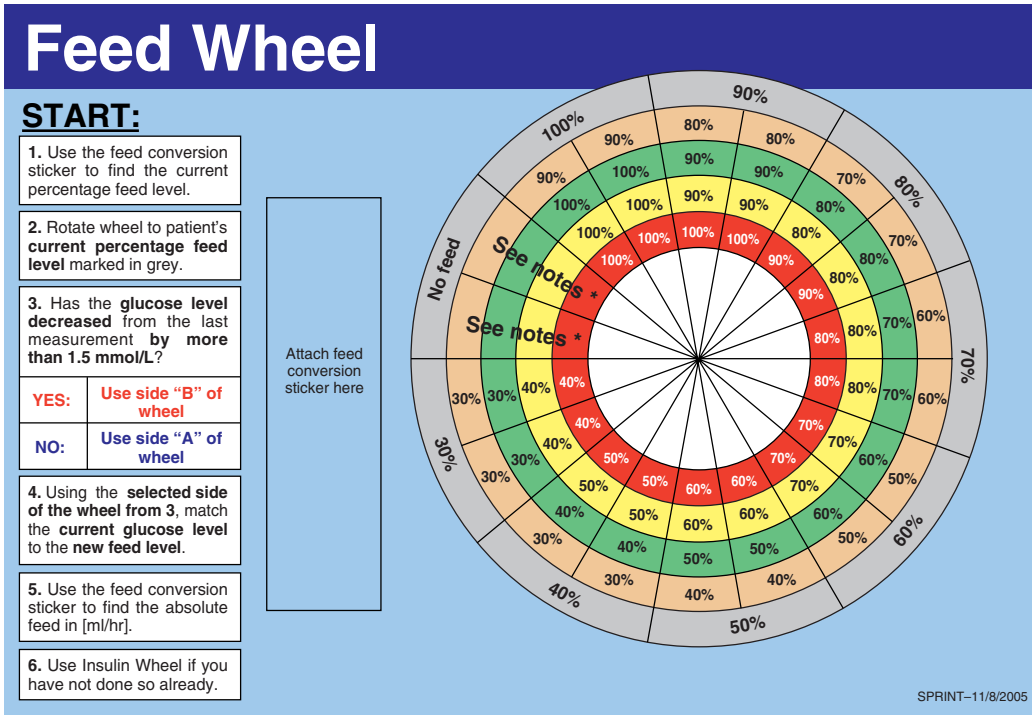

(b)

Figure 4.6 SPRINT feed wheel with dial (a) and with dial removed (b). Blood glucose (BG) values are in mmol/L. Reproduced with permission from Lonergan et al. [2006b].

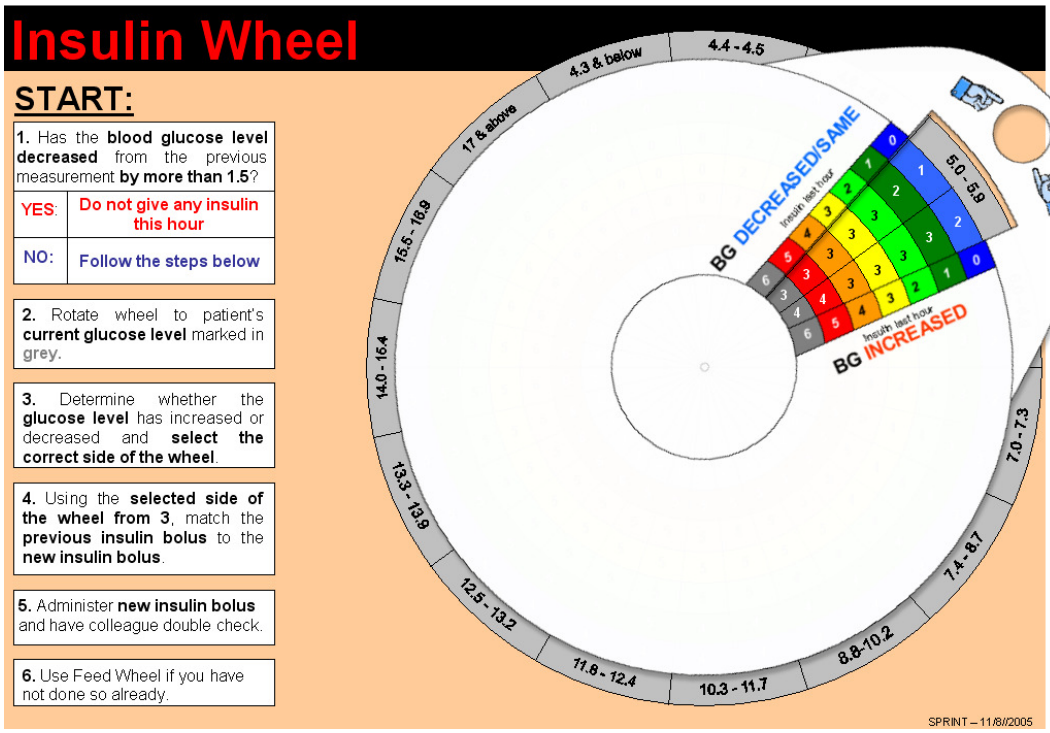

(a)

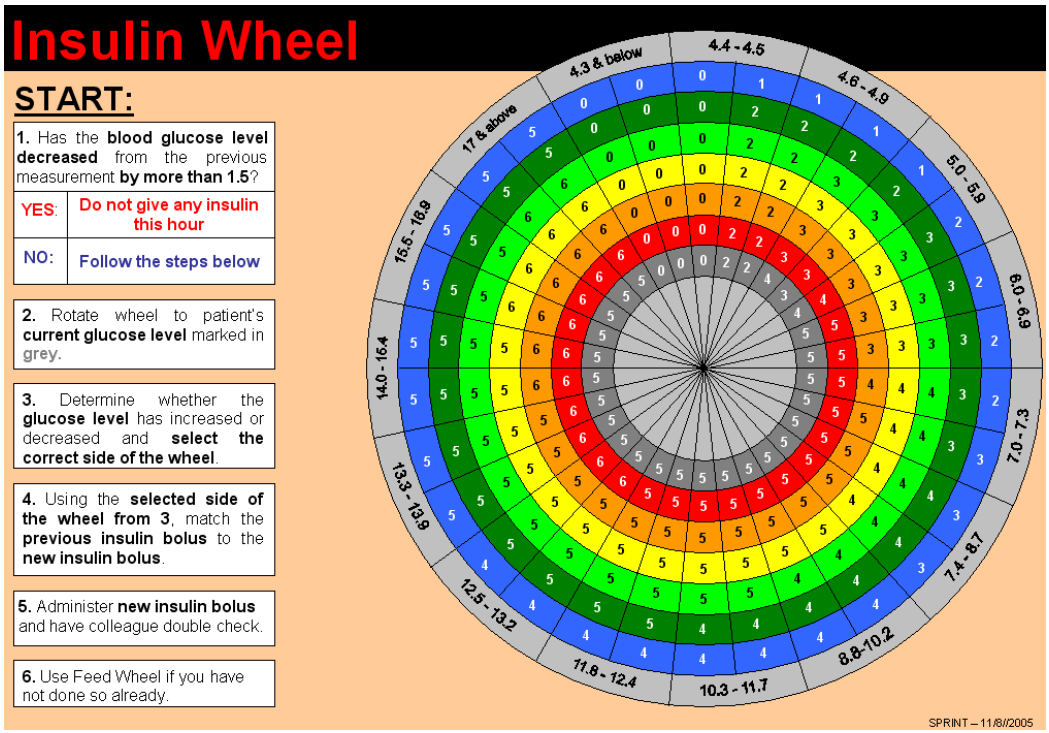

(b)

Figure 4.7 SPRINT insulin wheel with dial (a) and with dial removed (b). Blood glucose (BG) values are in mmol/L. Reproduced with permission from Lonergan et al. [2006b].

body frame size, and gender. The range of goal nutrition rates is 50–100 mL/h [Shaw et al., 2006]. Details are found in Lonergan et al. [2006a] and Chase et al. [2006a].

Trial Results

A total number of 165 patients were enrolled in SPRINT during this study. Over 15,000 measurements were recorded for over 23,000 hours of patient control. Patients were measured 2-hourly for 64% of their stay indicating significant periods of stable control. Table 4.5 presents a summary of glycemic control on the SPRINT protocol for the 165 patients.

Table 4.5 SPRINT trial results (Data are expressed as median [5^{th}–95^{th} percentile range] as appropriate)

Overall data		
Number of patients	165	
Hours of control	23,324	hours
Total *BG* measurements	15,874	
BG mean*	5.9 [4.1–8.3]	mmol/L
BG standard deviation*	1.3	mmol/L
Percentage between 4–6.1 mmol/L	61%	
Percentage between 4–7.0 mmol/L	82%	
Percentage between 4–7.75 mmol/L	89%	
Percentage $<$ 4 mmol/L	3.3%	
Percentage $<$ 2.5 mmol/L	0.1%	
Per-patient data		
Hours of control	95 [12–447]	hours
Number of measurements	68 [10–271]	
BG mean*	5.9 [5.0–7.4]	mmol/L
BG standard deviation*	1.1 [0.7–2.3]	mmol/L
Median hourly insulin	2.5 [1.3–4.1]	U
Median nutrition rate (RESOURCE® Diabetic)	37.5 [0–80.3]	ml/hr
(assuming 1.06 cal/mL [Novartis, 2005])	954 [0–2043]	kCal/day
Median percentage of goal feed	52.7% [29.7–70.3%]	

*Lognormal distribution

Overall, 61% of all measurements were in the 4.0–6.1 mmol/L desirable glycemic band. Average glycemia was 5.1 ± 1.7 mmol/L. Only 3.3% of all measurements were below 4 mmol/L with 6 hypoglycemic events below 2.2 mmol/L. Figure 4.8 shows the SPRINT controlled blood glucose measurement distribution in all trials.

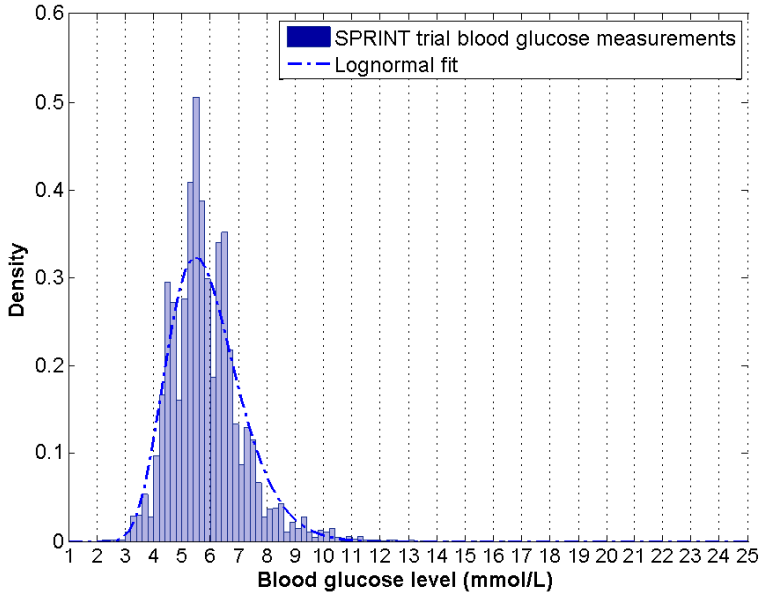

Figure 4.8 SPRINT trials blood glucose distribution

In conclusion, SPRINT provided successful glycemic management in a highly dynamic environment. This protocol is implemented by the nursing staff without the need for physician intervention or interpretation. Because it was developed using the models and methods for computerised control, SPRINT effectively furthers and mass validates the physiological model of Equations (2.9)–(2.13), the parameter identification method presented in Chapter 3, and the previously computerised predictive target glycemic control protocol. It did so by converting these methods to a simpler discretised protocol with minimal labour and hardware requirements to enable this large-scale clinical study.

4.4 Protocol Comparison

The final protocol at the third stage of protocol development, SPRINT, provided enough data to be compared with the published ICU protocols listed in Table 4.6 [Lonergan et al., 2006b]. These protocols all have a target average glucose level less than 7.8 mmol/L. SPRINT and the computerised insulin-nutrition control modulate both feed and insulin, while the remaining protocols utilize insulin only. The Mayo protocol was designed to maintain blood glucose below 7.8 mmol/L [Krinsley, 2004]. The Leuven protocol is from the landmark study by Van den Berghe et al. [2003] with a 6.1 mmol/L target average. The Bath and Yale pro-

tocols are from other recent ICU glycemic control studies [Laver et al., 2004; Goldberg et al., 2004b]. The "Canterbury District Health Board (CDHB) Standard Insulin Sliding Scale" is a standard insulin sliding scale previously used in the Christchurch ICU, and the "Aggressive Insulin Sliding Scale" protocol is a more aggressive form [Lonergan et al., 2006b]. Detailed methods for comparison using simulation on the same long-term patient cohort used for parameter identification validation presented in Section 3.3 are presented in Lonergan et al. [2006b].

Table 4.6 Protocols compared in virtual patient simulations

SPRINT Protocol
Insulin-Nutrition Control Protocol [Wong et al., 2006b]
Mayo Clinic Protocol [Krinsley, 2004]
Leuven Protocol [Van den Berghe et al., 2001]
Bath University Protocol [Laver et al., 2004]
Yale University Protocol [Goldberg et al., 2004b]
CDHB Standard Insulin Sliding Scale Protocol
Aggressive Insulin Sliding Scale Protocol

Figure 4.9 shows the simulated controlled blood glucose distribution from all protocols. SPRINT provided performance comparable with the computerized insulin-nutrition control protocol. SPRINT and the insulin-nutrition control protocol both display much tighter control within the target bands and less incidence of hypoglycemia. The goal of these two protocols is to maximize time within a band, not just a limit or average at the edge of the band. Both protocols avoid insulin saturation, deal with measurement error, and account for inter-patient variability.

The noticeable outlying protocol was from the Mayo Clinic [Krinsley, 2003a]. However, it was designed to be less intensive with a target average of 7.8 mmol/L, which it essentially meets. The results in Figure 4.9 are summarized in Table 4.7 using log-normal distributions as the best fit to the resulting data ($p<0.005$). A two-sample Kolmogorov-Smirnov Test was carried out on all permutations of simulation data sets. The results of these non-parametric tests indicate that none of the data sets can be drawn from the same distribution ($p<0.005$).

The log median blood glucose values for SPRINT and the insulin-nutrition control protocol are comparable with the Leuven protocol [Van den Berghe et al., 2001, 2003]. However, the 2 std range of 3.5–9.6 mmol/L for SPRINT compared

Table 4.7 Protocol comparison summary

							Sliding scale	
	SPRINT	Insulin-Nutrition	Mayo Clinic	Leuven	Bath	Yale	Standard	Aggressive
Log median	5.8	5.9	8.6	5.6	6.2	6.7	6.9	6.6
Multiplicative std	1.3	1.4	1.3	1.7	1.5	1.4	1.4	1.3
1 std range	(4.5–7.5)	(4.4– 8.0)	(6.7–11.1)	(3.4– 9.2)	(4.3– 9.0)	(4.8– 9.4)	(5.1– 9.3)	(5.0– 8.8)
2 std range	(3.5–9.6)	(3.3–10.8)	(5.2–14.2)	(2.1–15.2)	(2.9–13.1)	(3.4–13.2)	(3.8–12.7)	(3.8–11.6)
Blood glucose time								
In 4.0–6.1 band	61.7 %	62.2 %	11.2 %	35.8 %	45.5 %	22.3 %	41.9 %	43.8 %
In 4.0–7.8 band	83.5 %	82.9 %	27.4 %	51.0 %	70.0 %	64.8 %	60.0 %	65.2 %
Less than 3.9	4.4 %	1.1 %	9.6 %	23.6 %	7.1 %	5.9 %	2.4 %	2.8 %
Less than 3.3	0.50%	0.57%	0.15%	11.60%	1.90%	3.30%	0.34%	0.34%
Higher than 7.8	12.1 %	16.1 %	72.0 %	25.3 %	22.9 %	29.3 %	37.5 %	32.0 %
Average insulin [U/h]	2.4	2.6	1.6	3.0	5.8	4.6	1.9	2.1
Average % goal feed	61.9 %	75.8 %	67.7 %	67.7 %	71.8 %	71.4 %	67.7 %	67.7 %

All blood glucose values are in mg/dL.

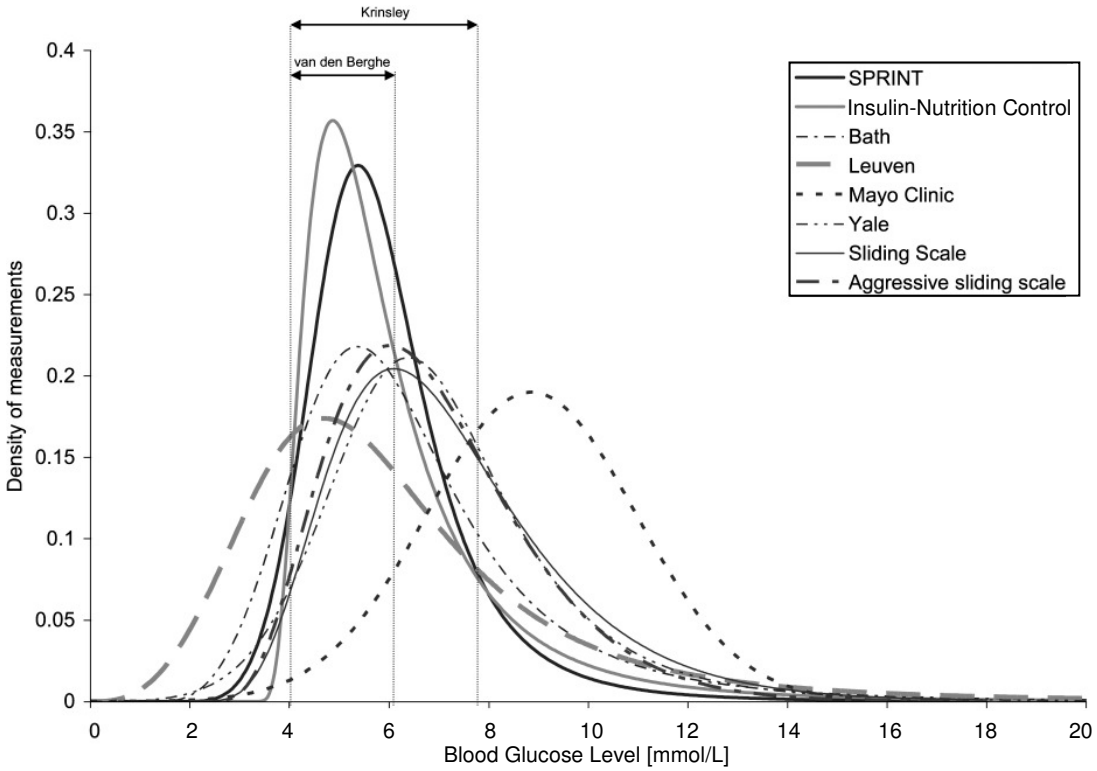

Figure 4.9 Glycemic control protocol comparison. Target bands by Van den Berghe et al. [2003] and [Krinsley, 2003b] are indicated.

with that of 2.1–15.2 mmol/L for the Leuven protocol shows much tighter control, with similar results for the ±1 standard deviation range. The other insulin-only protocols gave similar larger spreads with higher average levels compared with SPRINT and the insulin-nutrition control protocol, as seen in Table 4.7. This result shows that SPRINT and the computerised insulin-nutrition control protocol can tightly regulate blood glucose without significant risk of hypoglycemia, with 0.50% and 0.057% of patient time, respectively, spent at a blood glucose level less than 3.3 mmol/L, shown in Table 4.7. The study by Van den Berghe et al. [2001] details the clinical significance of maintaining normoglycemia, and indicates that averages outside the target range are associated with poorer outcomes [Van den Berghe et al., 2003]. This is significant as many of the protocols in Table 4.7 had simulated averages above the 6.1 mmol/L target limit.

All protocol simulations assumed the same ideal, or goal, feed. SPRINT had the lowest feed at 61.9% of goal feed. However, there was no evidence to suggest that feeding patients at this level is associated with adverse outcomes. In particular, Krishnan et al. [2003] showed that feeding at a level of 33–66%

of the American College of Chest Physicians (ACCP) goal feed (approximately 9–18 kcal/kg/day) was associated with improved mortality and outcomes compared with the 67–100% rate. Note that the ACCP goal feed rate guidelines are effectively identical to these used in SPRINT [Shaw et al., 2006].

Finally, Lonergan et al. [2006b] showed that the simulated results compare well with reported average values, suggesting that the computer simulation method produced realistic results compared to clinical data. This belief is validated in comparing simulated and clinical SPRINT data in Figure 4.10. Overall, SPRINT is seen to be a safe and effective glycemic control protocol through large scale clinical trials and simulated protocol comparisons. In addition, modulating both insulin and nutrition is seen to deliver more effective and tighter control. In addition, the protocol can adapt to both intra- and inter-patient variability.

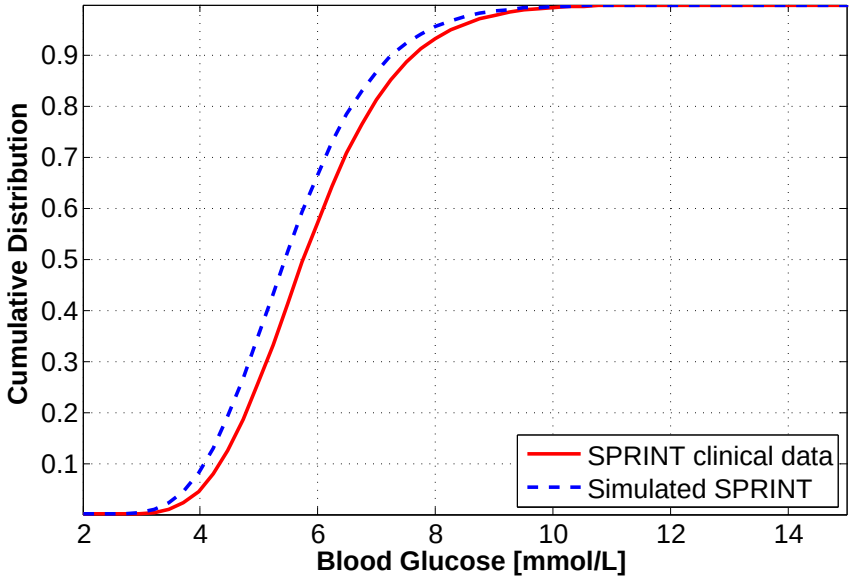

Figure 4.10 SPRINT clinical v.s simulated results

4.5 Summary

Through the three stages of protocol development using the glucose-insulin model of Equations (2.9)–(2.13) and the parameter identification method presented in Chapter 3, it is clear that an adaptive algorithm that uses both insulin and nutrition as control means delivers safer and more effective glycemic control.

The final protocol, SPRINT, is presented in two wheel-based look-up tables, further enhancing the adaptive insulin-nutrition control algorithm's adaptability in critical care environments.

Effectively, the computerised insulin-nutrition control algorithm is mass validated via SPRINT for its minimal labor and hardware requirements. In simulations, the computerised protocol still shows superior glycemic control performances compared to existing protocols. Thus, the computerised predictive target glycemic control algorithm will be the benchmark and the platform for further enhancements.

The previously developed computerised algorithms presented in this chapter, use frequent parameter fitting to closely track patient dynamic and parameter variation. Therefore, the algorithms are adaptive to different patients as well as evolving patient conditions. The frequent parameter fitting thus enables accurate predictive control.

Further study into the stochastic behaviour of parameter variations, especially insulin sensitivity, would add insight into control algorithm development and possibly enable the controller to be "one step ahead" of the observable patient dynamics. In addition, a "clinical event predictor" capable of foretelling at least some clinically significant events or their likelihood, such as atrial fibrillation which occurred in two computerised insulin-nutrition control trials [Wong et al., 2006b], can take protocol development to a higher level. It is for capturing this variability that this thesis develops a stochastic model in the following chapters to augment and optimise these methods and control approaches to provide better glycemic control and patient care.

Chapter 5

Stochastic Modelling and Initial Insulin Sensitivity Model

The control algorithms presented in Chapter 4 all determine interventions by assuming that the identified p_G and S_I values are constant between the control intervention and the one-hour time interval to a pre-selected target. However, identified profiles of p_G and S_I have shown that both variables can evolve significantly through time based on patient condition [Hann et al., 2005; Chase et al., 2005b,c; Wong et al., 2006b]. In particular, sudden variations may also occur due to the acute onset of conditions such as atrial fibrillation [Wong et al., 2006b]. A verified model of the variability of p_G and S_I overtime would thus significantly assist clinical control intervention decision making.

Intensive care units are highly dynamic in terms of volatility of patient conditions and rigorous drug therapies. While diurnal variation in glucose tolerance is evident in healthy and diabetic individuals [Lee et al., 1992; Verrillo et al., 1989; Radziuk and Pye, 2006; Carroll and Nestel, 1973; Arasaradnam et al., 2002], there is currently no evidence of this phenomenon in critically ill patients. Being unconsciously sedated most of the time in an ICU, it is debatable if critically ill patients experience day and night. Constant enteral or IV nutrition support further removes any sense of time, or metabolic variation associated with it. In addition, onset of many acute medical events such as atrial fibrillation do not have clear known causes. Therefore, deterministic means of predicting a change in a critically ill patient's metabolic status is ill suited.

In contrast, a stochastic model that lumps all randomness together, can deliver a holistic picture of the metabolic dynamics under critical illness. While it is often tempting from a medical research point of view to understand and model all

possible drug therapies and hormones interactions and effects, it is unrealistic for such model to be used for control applications. A stochastic model that captures critical illness dynamics as a whole, while being "fuzzy", can provide the most realistic view by probability.

Therefore, the proposed stochastic model will reflect, as well as provide insight into, the clinically observed dynamic behaviour of p_G and S_I, and thus aid control protocol design. The stochastic knowledge can further act as a patient simulator. Finally, it can be used to provide probabilistic predictions in clinical intervention outcome. In particular, for control uses, a probability density distribution in blood glucose levels can be produced for each clinical intervention, allowing different intervention possibilities to be explored. The most desirable, probabilistically favorable blood glucose outcome can then be chosen. In summary, the stochastic model will enhance clinical glycemic control in the following major aspects:

1. Provide probabilistic predictions and blood glucose probability intervals for the outcome of clinical interventions.
2. Minimise the risk of unexpected glycemic excursion, particularly hypoglycemia.

The overall outcome will be added safety and better knowledge to glycemic control protocol design and decision making.

5.1 Model Cohort

An initial proof-of-concept stochastic model was developed from the set of long term retrospective clinical data from 18 critical care patients in the Department of Intensive Care Medicine, Christchurch Hospital. These 18 patients are a selection from a 201-patient data audit at the Christchurch Hospital [Shaw et al., 2005, 2004; Hann et al., 2005; Doran, 2004], and have been presented in Section 3.3. These patients have a minimum stay in ICU of 1.4 days, with intervals between measured data points of four hours or less. A summary of this cohort's background information is presented in Table 3.3 in Section 3.3. This cohort broadly

represents a typical cross section of ICU patients, regarding medical condition, age, sex, APACHE II scores and mortality. The average APACHE II score for this cohort is 22.6, with a range of 8–36. Diagnosed Type 1 and Type 2 diabetes are slightly over-represented because they often received greater monitoring.

5.2 Initial Insulin Sensitivity Stochastic Model

Glucose-insulin model (Equations (2.9)–(2.13)) fitted patient values for p_G and S_I were used to develop the initial stochastic model. Zero-order piecewise linear functions are used to define the modelled p_G and S_I, with a discontinuity every two hours for p_G and every hour for S_I using the integral-based parameter identification method presented in Section 3.3. Constant generic parameter values are summarised in Table 3.8. This choice of intervals provides 1,278 fitted hourly S_I values and 635 fitted 2-hourly p_G values.

The fitted p_G and S_I profiles from these 18 long term critical care patients revealed non-uniform variation patterns with respect to the parameter values themselves. The variation distribution of fitted S_I from the 18 patients, plotted as S_{In+1} against S_{In}, is shown by the dots in Figure 5.1. A similar plot for 2-hourly p_G variation is shown in Figure 5.2.

It is clear in both Figures 5.1 and 5.2 that the variability of both parameters over any given fitting time frame is dependent on its present value, and that the stochastic behaviour or distribution of these variations also depends on their current state. Thus, a 2-dimensional kernel density estimation method was chosen for constructing the stochastic model that describes the transition of parameter values from one fitting time frame to the next, with respect to the parameter values. The method has the advantage of producing a smooth, continuous function across the parameter range [Simonoff, 1996; Scott, 1992]. The overall result is a bivariate probability function for the potential parameter values.

Essentially, kernel density estimation methods enable data extrapolation to the entire population given this type of sample from the population. The 2-dimensional kernel estimation method provides an approximation to the parameter variation behaviour according to how the existing or current data behaves. Where there is higher density of data, more certainty can be drawn on the “true”

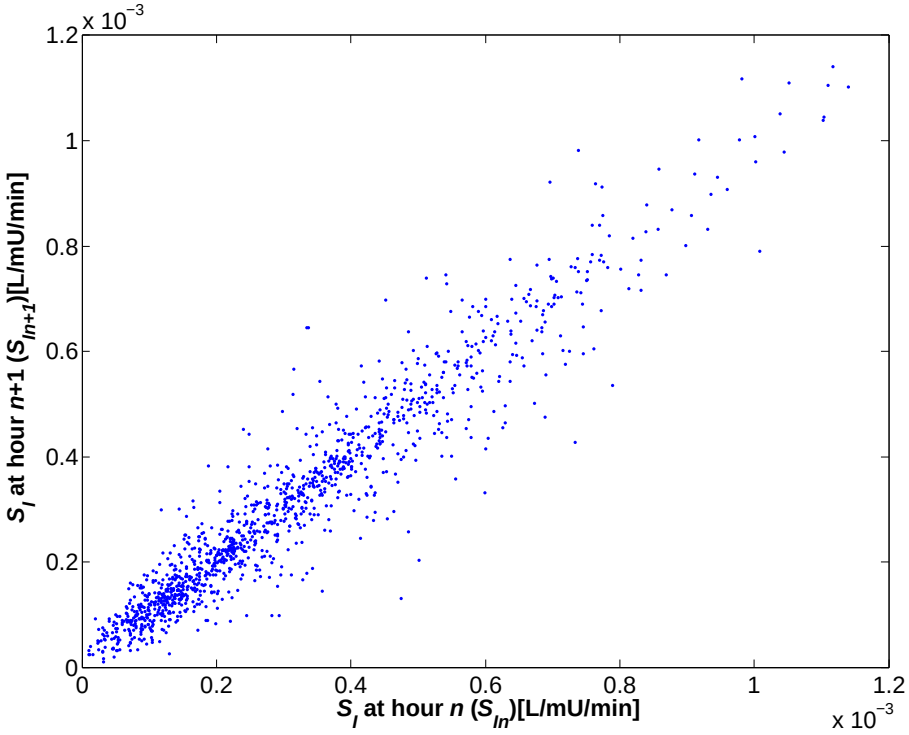

Figure 5.1 Retrospectively fitted hourly S_I variation on 18 ICU patients

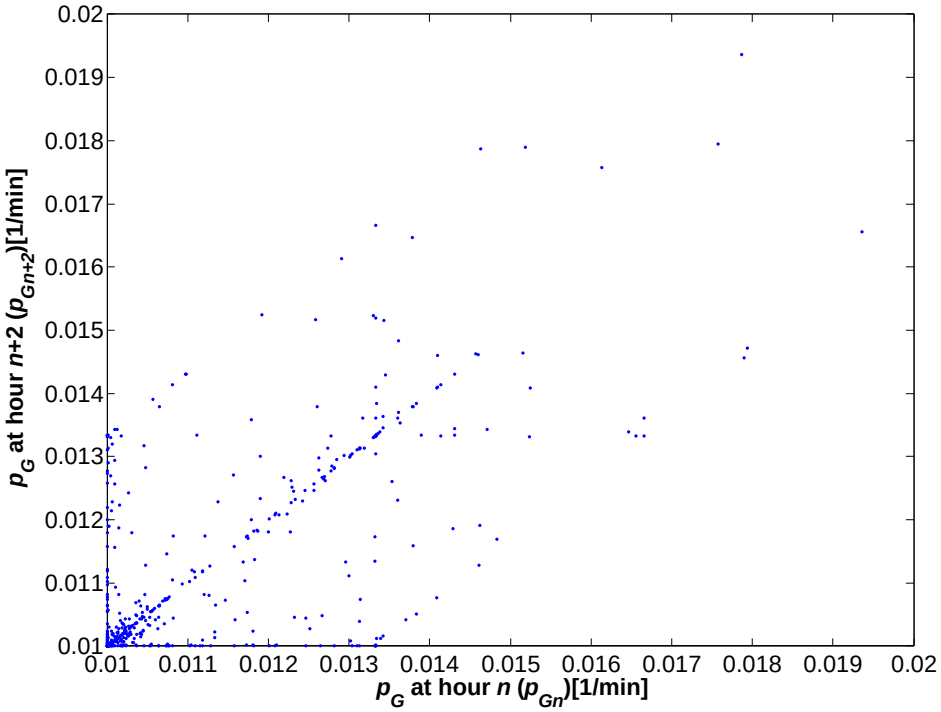

Figure 5.2 Retrospectively fitted hourly p_G variation on 18 ICU patients

behavioural pattern of the variant.

An example of a visually and conceptually simpler one-dimensional kernel density estimation method is shown in Figure 5.3. The kernel density estimate $\rho(x)$ is the solid line and the kernel functions that add up to $\rho(x)$ are dashed. Six sample points were considered in this illustrative example. Note that where the points are denser, the density estimate has higher values. Hence, these approximations are more certain and thus more accurate in the presence of significant data points. In contrast, a lack of data cannot be remedied by this approximation, as might be expected.

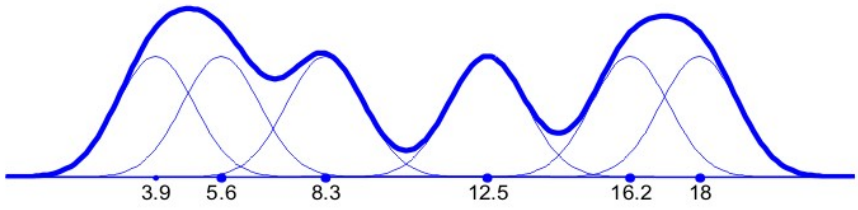

Figure 5.3 One-dimensional kernel density estimation (The kernel density estimate $\rho(x)$ is the solid line; the kernel functions which add up to $\rho(x)$ are dashed.)

On the same principle, the 2-dimensional kernel density estimation process can be thought of as a sand building exercise for visualisation. If a pile of sand is dropped onto every data point dot in Figure 5.1, then the resulting sand sculpture is the simple representation of the kernel density estimate across the $S_{In} - S_{In+1}$ plane, much like the solid line in Figure 5.3. However, in this case, the sand sculpture is physically constrained to the positive first quadrant. Thus, the probability of non-positive, physiologically invalid S_I values is eliminated with this added boundary on the density estimate.

Since the probability distribution of a possible future S_{In+1} value depends on S_{In}, time-varying S_I profiles or trajectories can be treated as a Markov chain. A Markov chain constitutes a sequence of random variables, $X_0, X_1, X_2, X_3, \ldots$, with the value X_n being the state of the process at time n. The Markov property states that the conditional probability density functions of future states of the process, given the present state, depends only upon the current state. Therefore, the conditional probability density function of X_{n+1} given past states is a function

of X_n alone:

$$p(X_{n+1}|X_0, X_1, X_2, \ldots, X_n) = p(X_{n+1}|X_n) \tag{5.1}$$

Additionally, the conditional probability has the statistical property:

$$p(A|B) = \frac{p(A,B)}{p(B)} \tag{5.2}$$

Therefore, given the Markovian stochastic behaviour of S_I, the conditional probability of S_{In+1} taking on a value y can be calculated by knowing or having identified $S_{In=x}$:

$$p(S_{In+1} = y|S_{In} = x) = \frac{p(S_{In} = x, S_{In+1} = y)}{p(S_{In} = x)} \tag{5.3}$$

Equation (5.3) is the conditional probability function that will provide the stochastic information needed on potential S_I variation. The numerator on the right hand side, which is the 2-dimensional kernel density estimated joint probability density $p(x, y)$, is constructed based upon or using the available clinical data.

$$p(x,y) = \frac{1}{n}\sum_{i=1}^{n} \frac{\phi(x; x_i, \sigma_{x_i}^2)}{p_{x_i}} \frac{\phi(y; y_i, \sigma_{y_i}^2)}{p_{y_i}} \tag{5.4}$$

where

$$p_{x_i} = \int_0^\infty \phi(x; x_i, \sigma_{x_i}^2) \tag{5.5}$$

$$p_{y_i} = \int_0^\infty \phi(y; y_i, \sigma_{y_i}^2) \tag{5.6}$$

and x_i and y_i are the coordinates of each dot in Figure 5.1. Equation (5.4) is the 2-dimensional kernel density estimator function. Each $\phi(x; x_i, \sigma_{x_i}^2)$ and $\phi(y; y_i, \sigma_{y_i}^2)$ is a normal probability distribution function centred at corresponding

x_i and y_i. To force non-negativity in x and y, Equations (5.5) and (5.6) provide normalisation in the positive domain, where each p_{x_i} and p_{y_i} represents the area under each $\phi(x; x_i, \sigma^2_{x_i})$ and $\phi(y; y_i, \sigma^2_{y_i})$ between zero and infinity.

Since $p(B)$ is defined:

$$p(B) = \int p(A, B) dA \tag{5.7}$$

The denominator on the right hand side of Equation (5.3) can be calculated by integrating Equation (5.4):

$$\begin{aligned} p(x) &= \int p(x, y) dy \\ &= \frac{1}{n} \sum_{i=1}^{n} \frac{\phi(x; x_i, \sigma^2_{x_i})}{p_{x_i}} \frac{\phi(y; y_i, \sigma^2_{y_i})}{p_{y_i}} dy \\ &= \frac{1}{n} \sum_{i=1}^{n} \frac{\phi(x; x_i, \sigma^2_{x_i})}{p_{x_i}} \cdot 1 \end{aligned} \tag{5.8}$$

Therefore, Equation (5.3) can be calculated from Equations (5.4) and (5.8):

$$\begin{aligned} p(S_{In+1} = y | S_{In} = x) &= \frac{\sum_{i=1}^{n} \frac{\phi(x; x_i, \sigma^2_{x_i})}{p_{x_i}} \frac{\phi(y; y_i, \sigma^2_{y_i})}{p_{y_i}}}{\sum_{i=1}^{n} \frac{\phi(x; x_i, \sigma^2_{x_i})}{p_{x_i}}} \\ &= \sum_{i=1}^{n} \omega_i(x) \frac{\phi(y; y_i, \sigma^2_{y_i})}{p_{y_i}} \end{aligned} \tag{5.9}$$

where

$$\omega_i(x) = \frac{\phi(x; x_i, \sigma^2_{x_i}) / p_{x_i}}{\sum_{j=1}^{n} \phi(x; x_j, \sigma^2_{x_j}) / p_{x_j}} \tag{5.10}$$

In conclusion, Equations (5.9) and (5.10) define the 2-dimensional kernel density estimation in conditional S_I variability. Note that S_{In+1} variability is "conditional" because it depends on the prior state S_{In}. More specifically, knowing S_I at any hour n, $S_{In} = x$, the probability of S_I at hour $n+1$, $S_{In+1} = y$, can be calculated from Equation (5.9).

The step-by-step description for how $p(S_{In+1} = y|S_{In} = x)$ in Equation (5.9) is computed is given as follows:

1. For every fitted S_I data point, as shown by the dots in Figure 5.1 and identified as (x_i, y_i) where $i = 1, 2, \ldots, n$, calculate p_{x_i} and p_{y_i} using Equations (5.5) and (5.6). The variance σ_{x_i} and σ_{y_i} at each (x_i, y_i) depends on the local data density and is calculated directly. Details of the derivation of σ are shown in Appendix A.

2. Knowing or identifying the value $S_{In} = x$, calculate $\omega_i(x)$ for $i = 1, 2, \ldots, n$ using Equation (5.10).

3. Calculate the probability that $S_{In+1} = y$ given $S_{In} = x$, $p(S_{In+1} = y|S_{In} = x)$, by substituting $\omega_i(x)$ for $i = 1, 2, \ldots, n$ into Equation (5.9).

Step 1 only needs to be carried out once, because it depends solely on the existing data set used to construct the stochastic model. The calculated p_{x_i} and p_{y_i} can then be stored for use in steps 2 and 3.

A better illustration of the construction of the (conditional) stochastic model can be shown by the following example using a data set of only 8 samples for simplicity, as shown in Figure 5.4. Panel A shows the 8 data points and the contours of the individual kernels for them. Each kernel is a 2-dimensional Gaussian skewed by a weighting function $\omega_i(x)$ as defined in Equation (5.10). The weighting function skews the Gaussian kernels in the x direction with respect to the x axis data density at each data point, as shown in panel B. The overall kernel density estimation function is then the sum of the individual kernels as defined in Equation (5.9), shown in panel C.

In summary, the 2-dimensional kernel density estimation method creates a smooth, continuous model surface that reflects the sample data pattern. Note

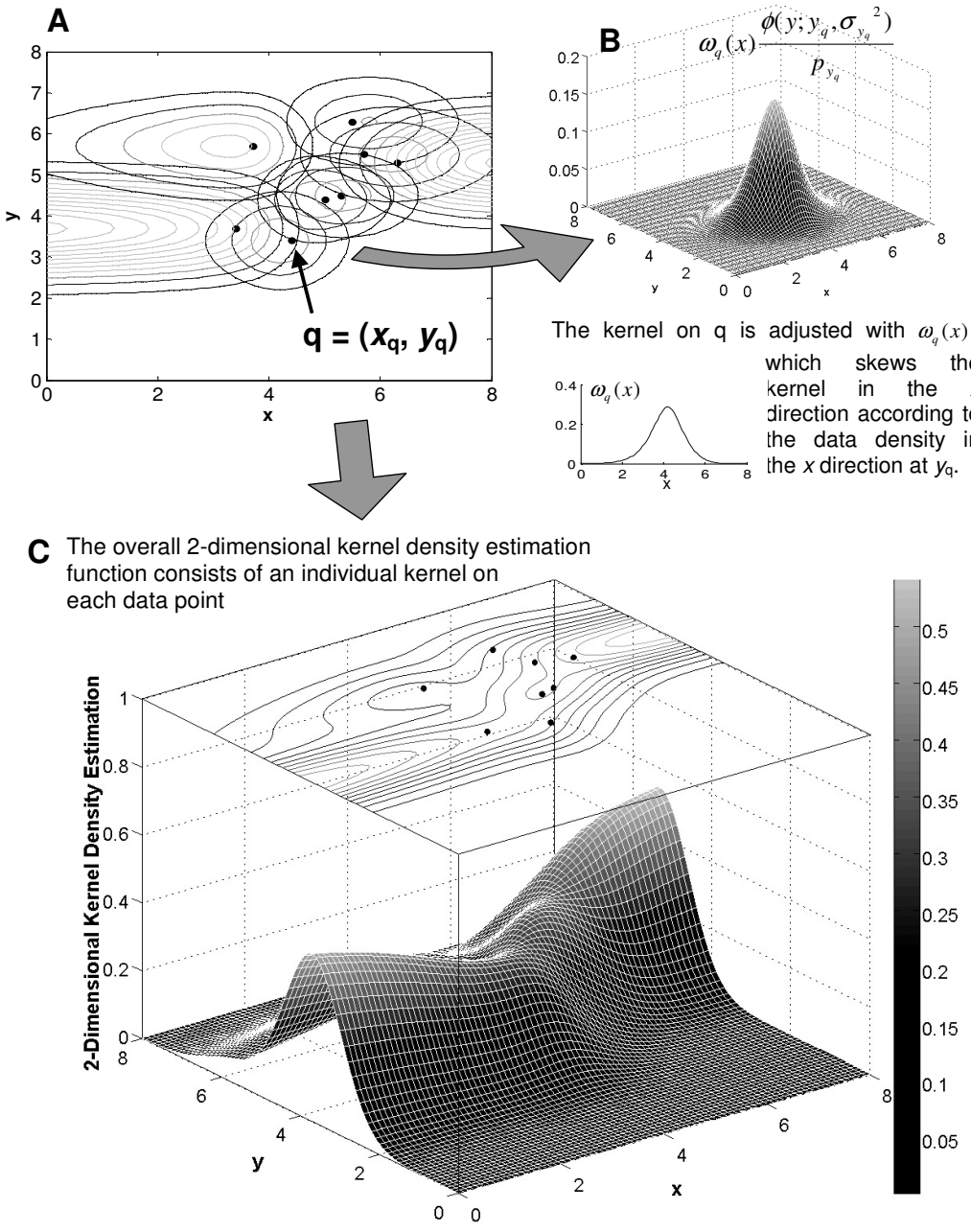

Figure 5.4 Example of 2-Dimensional Kernel Estimation Function

that the example shown is the "conditional" 2-dimensional kernel density estimate function as defined in Equation (5.9). Every slice of the surface in panel C along the y axis is the probability distribution in y (S_{In+1}) given x (S_{In}), and therefore its area under the curve along the y axis sums to 1.0. In comparison, the kernel density estimation joint probability function defined in Equation (5.4) has the volume under the 3-D surface equal to 1.0. The final 3-D S_I stochastic model is thus developed and shown in Figure 5.5 for the data set used for this study.

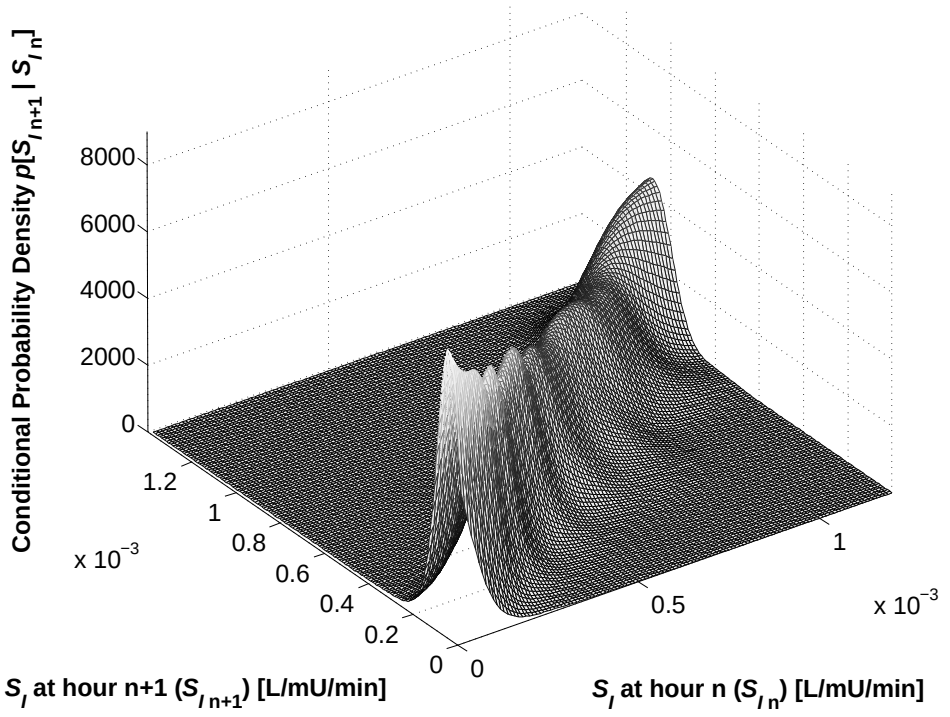

Figure 5.5 Initial 3-dimensional stochastic model of S_I variability. Each slice of the surface along the S_{In+1} axis has its area under the curve summing to 1.

Having constructed the S_I stochastic model, a grid of data that describes the surface shown in Figure 5.5 can be stored and used as a look-up table. Having an identified hourly S_I value in clinical situations [Chase et al., 2005b,c; Wong et al., 2006a,b], the probability distribution, and hence the probability intervals, can be gathered, as shown in Figure 5.6. The solid line is the kernel density estimate surface sliced along $S_{In} = 0.6 \times 10^{-3}$. This line represents the probability distribution for potential S_{In+1}, one hour after having identified the current hour $S_{In} = 0.6 \times 10^{-3}$. From this distribution, probability intervals are also obtained, giving the most likely S_I value in an hour at 0.58×10^{-3}, inter-quartile range

$[0.51\times10^{-3}, 0.65\times10^{-3}]$, and the 0.90 probability interval $[0.39\times10^{-3}, 0.75\times10^{-3}]$. This probabilistic information can then be used to assist in the assessment of patient condition and clinical decision making regarding the optimal glycemic control intervention over the next hour.

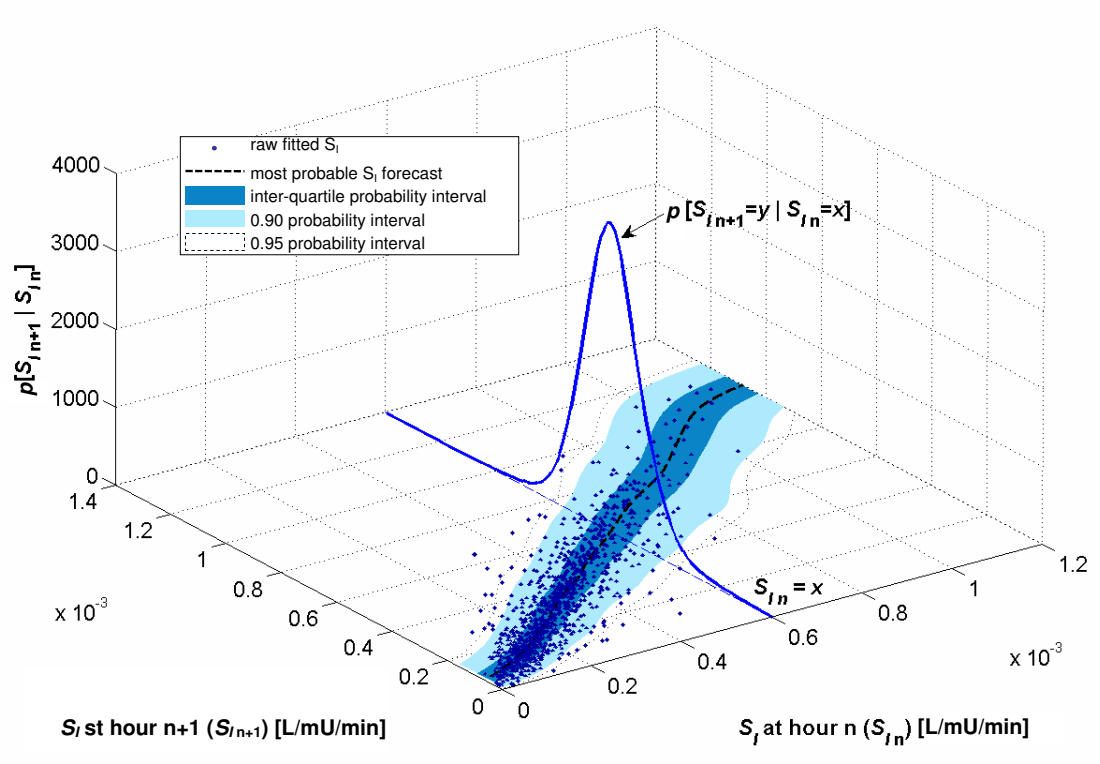

Figure 5.6 S_I probability density function from the initial stochastic model

The same kernel density estimation operations described were also applied to the endogenous glucose removal parameter p_G. However, the probability density across the $x-y$ plane is highly concentrated along the line $y = x$, and particularly at the point [0.01, 0.01]. This behaviour is evident in the scatter plot in Figure 5.2. This result reinforces that endogenous clearance, as modelled by p_G, generally stays constant at a patient specific value [Hann et al., 2005]. From Hann et al. [2005], the variation of P_G, when it occurs, is over days rather than hours, and thus is not as amenable to this approach or as necessary in 1–4 hourly interventions.

Hence, the variability of p_G is neglected from here on with regard to stochastic parameter models and behaviours. In addition, calculating the joint probability distribution between p_G and S_I requires significantly more computational effort and time than considering S_I alone for potentially little gain in this instance.

Finally, as this research is focused on clinical glycemic control, computational simplicity is essential in permitting fast real-time clinical control interventions.

5.3 Initial Stochastic Model Validation

The stochastic parameter model can be integrated into the glucose-insulin system model of Equations (2.9)–(2.13). This step allows the blood glucose level probability distribution one hour following a known insulin [Chase et al., 2005b,c] and/or nutrition [Wong et al., 2006a,b] intervention to be defined based on the stochastic model defined distribution of S_{In+1}.

5.3.1 Initial Validation

Method

The stochastic model developed from the 18-patient cohort was evaluated on 8 previous clinical control trials in the ICU [Wong et al., 2006b]. These 8 patients have the same median APACHE II score and a narrower range compared to the 18-patient cohort (median [range]: 22 [17–31] v.s 22 [8–36]). The background information on these 8 patients is presented in Table 4.3. Importantly, these trial data are independent from the 18-patient cohort used to develop the stochastic model. The trials were performed according to the protocol presented in Section 4.2.

To assess the stochastic model developed on its clinical control validity, these 8 trials are numerically performed using the following modified cycle of steps:

1. Fit p_G and S_I to an hourly cycle of blood glucose data using integral-based parameter identification. (Control inputs are as given in the clinical trial.)

2. Generate probability intervals of potential S_I from the time-average identified S_I of the evaluated cycle using the stochastic model developed for S_I.

3. Calculate blood glucose probability intervals for a given intervention based on the S_I probability intervals. This task is performed using the numerical model of Equations (2.9)–(2.13), and the S_I probability interval values.

4. Compare blood glucose probability intervals to real blood glucose trial measurements.

Results

Blood glucose probability intervals produced at each control intervention are compared against the measured values one hour later. These results are summarised in Table 5.1. The S_I stochastic model can account for 84% of measurements over time with a 0.90 probability, and 45% with a 0.50 probability, over the 8 clinical control trials used for analysis in the retrospective study.

The simulated result for Patient C402 is shown in Figure 5.7. The top panel displays blood glucose, where the crosses are the actual clinical measurements with 7% measurement error, the solid line is the fitted blood glucose profile, and the circles are the most likely probabilistic blood glucose predictions following control interventions. The 0.90 and inter-quartile probability intervals are also shown with each most probable blood glucose forecast. The bottom panel shows the fitted 1^{st} order linear S_I, its constant average hourly value for comparison to the S_{In+1} bounds, and the probabilistic bounds on S_{In+1} produced from the stochastic model.

Patient C402 represents a typical insulin resistant critical care patient, whose fitted S_I value tends to be in the lower physiological population range. The fitted S_I between 120 and 180 minutes departed significantly from the predicted S_I, reflecting a sudden hyperadrenergic event that extensively altered the patient condition. In this specific case, this event occurred as part of an episode of atrial fibrillation that was clinically observed and recorded around 150 minutes. Consequently, the probabilistic prediction made for 180 minutes fails to agree with the actual measurement.

The results from this patient demonstrated the sufficiency of the stochastic model. Most blood glucose levels were within the 0.90 probability intervals. The outlying events at 120 and 180 minutes were due to more extreme variations, which are not uncommon in the critically ill. However, to capture these

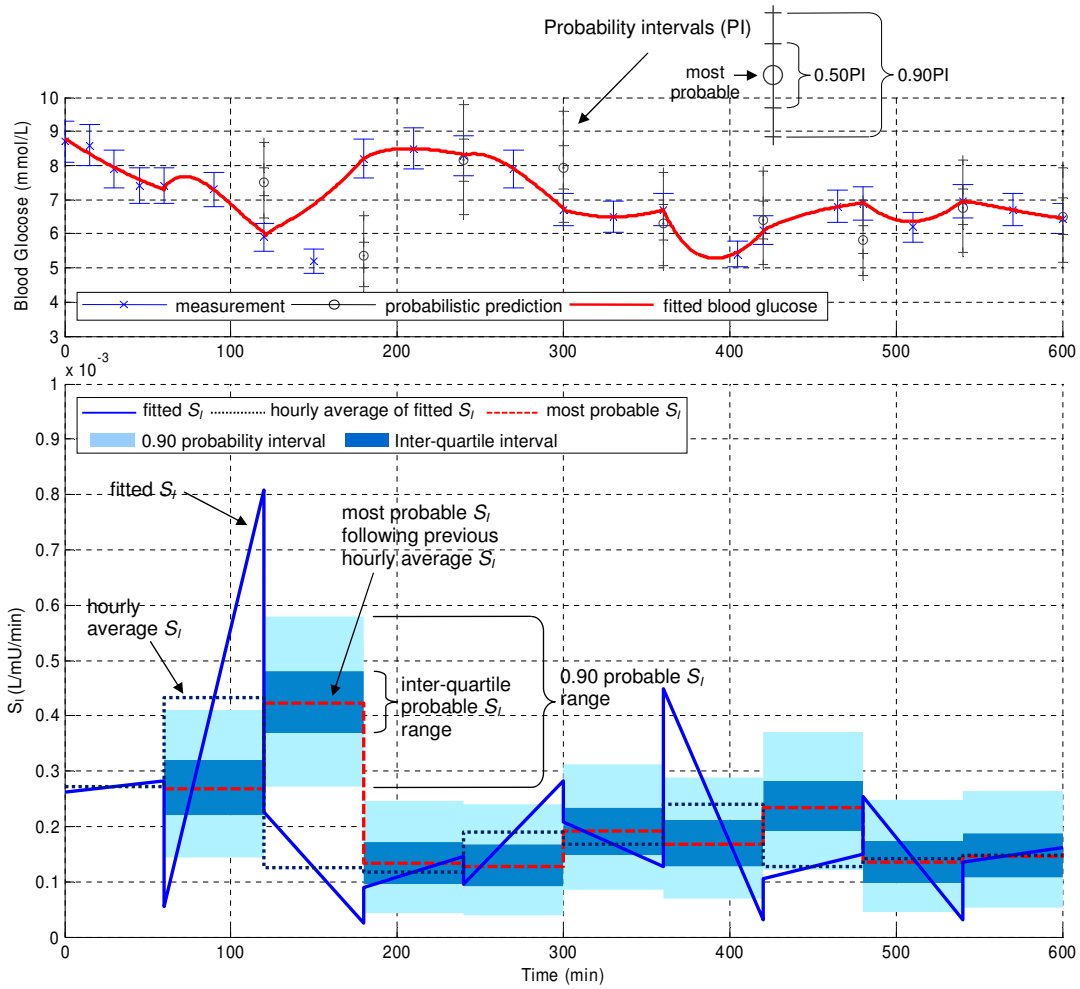

Figure 5.7 Simulated clinical control trial on Patient C402

Table 5.1 Retrospective probabilistic assessment on clinical control trials

Controlled patient ID	Number of interventions	Measurement error within inter-quartile probability interval	Measurement error within 0.90 probability interval
C401	9	2 (22%)	7 (78%)
C402	9	5 (56%)	7 (78%)
C403	9	1 (11%)	7 (78%)
C404	9	1 (11%)	6 (67%)
C405	9	7 (78%)	9 (100%)
C406	9	8 (89%)	8 (89%)
C407	9	5 (56%)	9 (100%)
C408	23	10 (43%)	19 (83%)
total	86	39 (45%)	72 (84%)

events, the probability intervals would become meaninglessly wide. Hence, the 0.90 probability level was employed for practicality and usefulness in decision support.

Figure 5.8 shows the same form of results for Patient C402. This patient began the blood glucose regulation trial at a normoglycemic level. The blood glucose briefly dropped below 4 mmol/L during the clinical trial, which was not initially accounted for with the probabilistic forecast. All other results matched (qualitative) expectations.

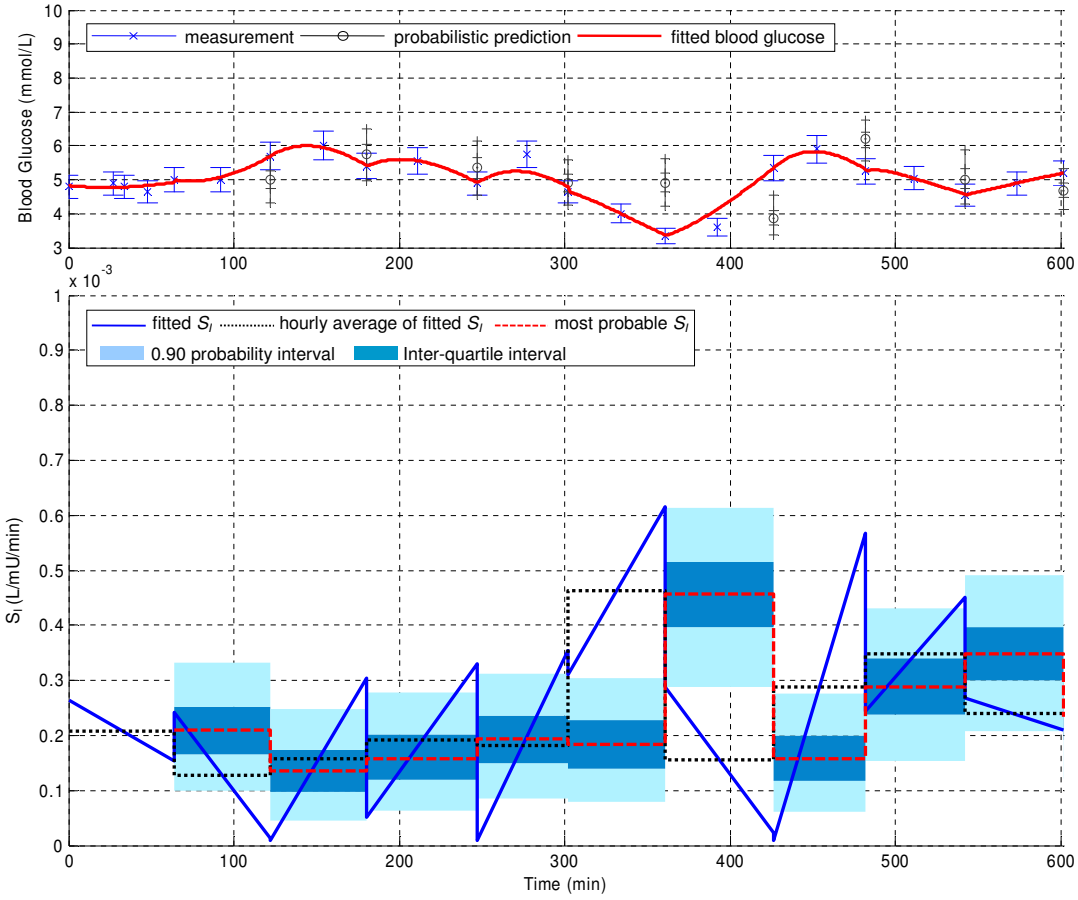

Figure 5.8 Simulated clinical control trial on Patient C404

Different control interventions to manage the low (∼3.2 mmol/L) glucose value were then explored in Figure 5.9. More specifically, the low glucose occurs due to variability. Therefore, the S_I stochastic model was used to assist decision making in re-simulating the trial. A comparison between the clinical trial (panels

A and C) and the new control interventions determined using the probability intervals (panels B and D) is shown in Figure 5.9. These panels indicate that using the distribution of S_I enables more effective decision making and control that can better account for, and more aggressively remedy, the sudden change.

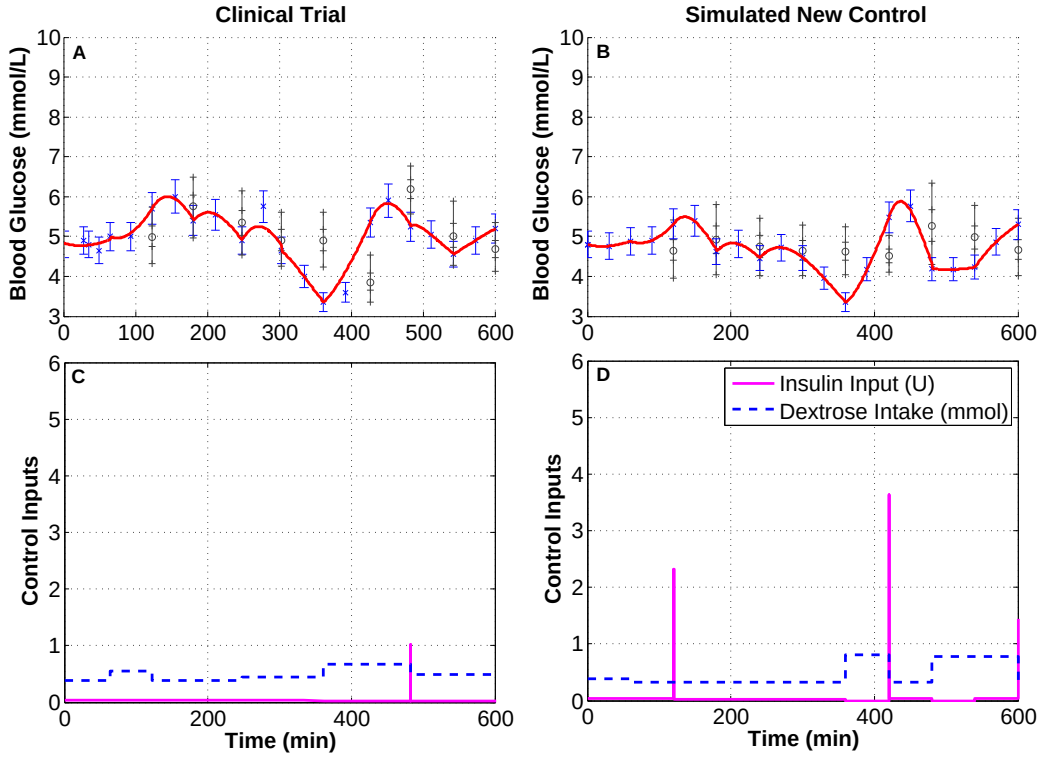

Figure 5.9 Clinical trial vs. simulated new control results on Patient C404

The simulated new control protocol aimed to maintain the 0.90 probability intervals above 4 mmol/L. More aggressive control interventions were thus taken in the first half of the trial, resulting in the blood glucose levels more tightly maintained at a lower level up to 300 minutes. The brief blood glucose excursion below 4 mmol/L was still unavoidable because the change in the patient's S_I exceeded the 0.90 probability interval limit of the created S_I stochastic model. However, a more vigorous remedy action was taken at 360 minutes in using the stochastic model probability intervals to result in the blood glucose levels having a 0.90 probability of being above 4 mmol/L in one hour. Overall, the application of the S_I stochastic model in control protocols, as in this case, delivers tighter, safer and more responsive glycemic management.

Figure 5.10 shows the simulated results for Patient C408. This patient was the first 24-hour clinical control trial performed, with a measurement interval of

one hour [Wong et al., 2006b]. Out of 23 predictions, 7 were outside of the inter-quartile range, but within the 0.90 probability interval. The fitted S_I profile shows the evolution of the patient condition through a day. The Markovian S_I stochastic model successfully predicts the S_I variation trend, shown by the shifting of the S_I probability intervals closely following the identified S_I.

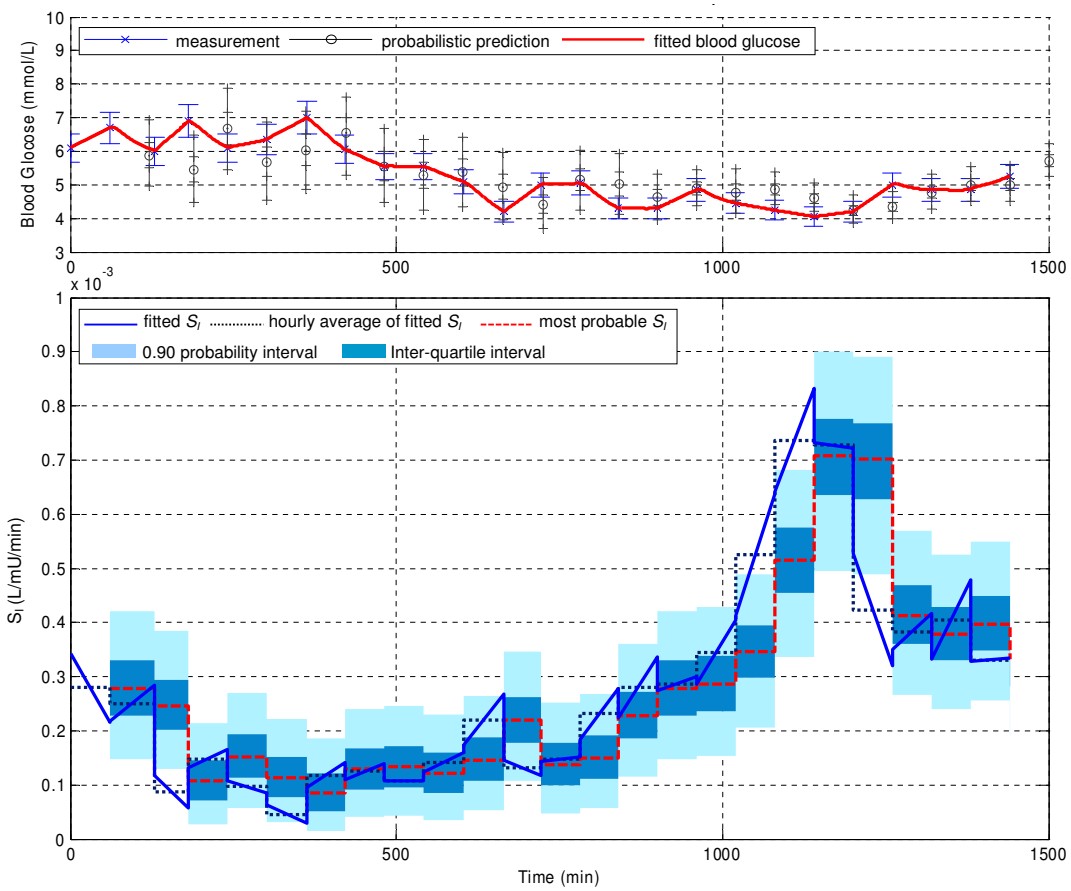

Figure 5.10 Simulated clinical control trial on Patient C408

In this patient, note that when S_I increases, the probability interval for the resulting blood glucose levels also tightens. This tightening is due to the model of Figure 5.5 having narrower distribution of S_{In+1} at (relatively) higher S_{In}. Hence, tighter S_{In+1} profiles generally result in tighter glucose bounds.

In contrast, the wide range of uncertainties in blood glucose levels associated with very low S_I values reflects a common problem in critical care, where highly insulin resistant patients with high insulin inputs, as often seen in intensive insulin therapy, can experience a sudden plunge in blood glucose levels and become

hypoglycemic [Amiel et al., 1987; Bolli et al., 1984; Raskin, 1984]. This type of situation was also encountered by Patient C404 in Figures 5.8 and 5.9, whose S_I profile also was in the lower physiological range [Hann et al., 2005; Doran, 2004]. Similarly, sudden large drop in S_I over 1 hour, as at 120 min in Patient C402 of Figure 5.7, can result in equally large sudden rises. In summary, the wider S_{In+1} distribution of lower S_{In} thus reflects the clinically observed greater variability of the more critically ill [Chase et al., 2006b, 2007].

Overall, the stochastic model is well reflected in the 8 patients. However, these 8 patients' data are very limited, spanning only 104 hours in total. Further larger-cohort studies or analyses could further verify the generality of the model and the method of creating the stochastic model.

5.3.2 Further Validation

Method

Further validation was carried out against the larger data set from the SPRINT trials presented in Section 4.3. The percentage of model fitted S_I for these 165 patients within the initial stochastic model probability intervals was assessed. These patients also have a similar median APACHE II score to the 18-patient cohort and the 8-patients tested in the initial validation (median [range]: 19 [1–43] v.s 22 [8–36] and 22 [17–31]). The range of APACHE II score is significantly greater, as would be expected for this much larger cohort. The main difference to note about these patients is that their data were collected while they are on long term intensive glycemic control. These patients have mostly one-hourly data, and may thus potentially reflect dynamics that would otherwise not appear in less frequently measured 3–4+ hourly data.

Results

The fitted S_I for these 165 patients are within the 0.90 probability interval 87.26% of the time, and inter-quartile interval 53.70% of the time. These percentages are comparable to the previous analysis on the 8 insulin-nutrition control patients in Table 5.1. A further study of these 165 patients' metabolic dynamics under intensive glycemic control may reveal other, currently hidden dynamics.

5.4 Summary

The initial S_I stochastic model has been verified with 2 other different, independent cohorts. Stochastic modelling of S_I using the 2-dimensional kernel density method presented has great potential in delivering probability prediction assisted glycemic control when incorporated into the glucose-insulin system model of Equations (2.9)–(2.13) utilising the integral-based parameter identification. This "package" can effectively capture the highly dynamic metabolic dynamics of the critical care patients. The stochastic model also further enhances the ability to predict, as well as imitate, typical critical care patient dynamics. Sudden metabolic changes can be better accounted for, and more aggressively remedied. Finally, tighter, safer and more responsive glycemic management is delivered.

Chapter 6

Higher Dynamic Stochastic Model and Model Comparison

The availability of data from 165 patients on the SPRINT protocol presented in Section 4.3 provides the basis for a more comprehensive and detailed study of hyperglycemic patient dynamics. These patients were all under intensive glycemic control, and had data collected primarily 1-hourly. Their data may reveal deeper, more subtle dynamic behaviour that may otherwise not be observable for data collected at a lesser frequency. A stochastic model created from this cohort will thus add dynamics that may be hidden in the initial stochastic model built on a smaller cohort with lower data density. In addition, these patients represent the target patient group to which the final stochastic model-based glycemic control protocol will be applied.

6.1 Higher Dynamic Model Cohort

The 165 SPRINT controlled patients have controlled glycemic data totalling 23,324 hours (over 27,500 hours of total length of patient stay in the ICU). By comparison, the initial model was only built on close to 1,300 hours of data over 18 patients, none of whom were on intensive glycemic control. Another major difference between these two sets of data was that the SPRINT blood glucose data were primarily collected hourly, whereas the blood glucose data for the initial model of Chapter 5 was generally collected every 3 to 4 hours. Therefore, SPRINT data provides a potentially better and more complete understanding of the highly dynamic critically ill metabolism that is more suitable for intensive glycemic control. Moreover, the SPRINT patients are the exact target group for

such a stochastic model to be used with glycemic control in the ICU.

A background comparison between these 165 SPRINT controlled patients is made with 485 hyperglycemic patients from the Christchurch Hospital ICU between September 2004 and August 2005. The goal is to ensure that the cohort used to create the model is representative of the cohort to which the model may be applied in a clinical setting. Thus it is an evaluation of the generality or representativeness of the cohort, and thus, of the stochastic model that would result.

As shown in Tables 6.1 and 6.2, the SPRINT cohort is a broad representation of typical hyperglycemic ICU patients. There is no significant difference between cohorts for age, sex and APACHE II scores for those patients that had an ICU stay greater than 3 days ($p >= 0.15$). There is a difference ($p<0.01$) between cohorts by APACHE III diagnosis code, as the retrospective cohort has a larger proportion of operative cardiac patients with short ICU stay. There is less difference between the cohorts ($p=0.12$) for those patients that stay in ICU for at least 3 days, which is the main target group for long term glycemic control, and consists of 73% of the 165 patients and 96% of the control hours. Note that the SPRINT patients who stayed in the ICU for less than 3 days were still also included to broaden the generalisability of the group. Overall, there is no significant statistical difference in composition between the SPRINT cohort and the long-staying (>= 3 days) general ICU cohort in Christchurch.

6.2 Higher Dynamic Model

The same parameter fitting method introduced in Chapter 3 was used to fit hourly constant S_I profiles in the glucose-insulin model defined by Equations (2.9)–(2.13), using the clinically recorded patient data. The endogenous glucose removal parameter, p_G, was kept at a constant level of 0.01 [1/min], which is the average of the fitted p_G levels for the 18-patient cohort used to create the initial stochastic model. As explained in Section 5.2, the computational benefits of leaving p_G as a constant largely outweigh the otherwise very little clinically observable data fitting improvement that might be obtained. Therefore, this stochastic model, like the initial model, only focuses on S_I.

Table 6.1 Comparison of SPRINT and retrospective 485-patient cohorts

	All patients			Length of stay $\geq$ 3 days		
	Retro.	SPRINT	p-value	Retro.	SPRINT	p-value
No. of patients	485	165		168	120	
% Male	61	66	0.25	61	66	0.38
Age (yr)	64 [52–74]	65 [50–74]	0.46	61 [46–73]	65 [49–74]	0.25
APACHE II score	16 [13–21]	19 [15–25]	< 0.01	20 [16–24]	19 [15–26]	0.44
APACHE II risk of death (%)	21 [10–42]	29 [15–55]	< 0.01	31 [14–52]	31 [16–56]	0.15

*Only 74% of APACHE II data for the retrospective cohort was available. Data are expressed as median [inter-quartile range] where appropriate.

Table 6.2 Diagnosis breakdown by APACHE III code of SPRINT and retrospective cohorts (p<0.01 for difference in total distribution for all patients, p=0.12 for difference in total distribution for patients with length of ICU stay at least 3 days, chi-squared test)

	All patients					
	Retrospective			SPRINT		
	Operative	Non-operative	Total	Operative	Non-operative	Total
Cardiovascular	139 (39%)	33 (9%)	172 (48%)	24 (15%)	15 (9%)	39 (24%)
Respiratory	7 (2%)	51 (14%)	58 (16%)	3 (2%)	28 (17%)	31 (19%)
Gastrointestinal	42 (12%)	3 (1%)	45 (13%)	26 (16%)	14 (8%)	40 (24%)
Neurological	5 (1%)	18 (5%)	23 (6%)	3 (2%)	12 (7%)	15 (9%)
Trauma	5 (1%)	18 (5%)	23 (6%)	4 (2%)	19 (12%)	23 (14%)
Sepsis	0 (0%)	12 (3%)	12 (3%)	0 (0%)	9 (5%)	9 (5%)
Other						
(Renal, metabolic, orthopaedic)	4 (1%)	20 (6%)	24 (7%)	1 (1%)	7 (4%)	8 (5%)
Total	202 (57%)	155 (43%)	357	61 (37%)	104 (63%)	165

	Length of stay ≥ 3 days					
	Retrospective			SPRINT		
	Operative	Non-operative	Total	Operative	Non-operative	Total
Cardiovascular	27 (21%)	10 (8%)	37 (29%)	12 (10%)	9 (8%)	21 (18%)
Respiratory	3 (2%)	33 (26%)	36 (28%)	2 (2%)	25 (21%)	27 (23%)
Gastrointestinal	14 (11%)	1 (1%)	15 (12%)	16 (13%)	10 (8%)	26 (22%)
Neurological	3 (2%)	9 (7%)	12 (9%)	2 (2%)	8 (7%)	10 (8%)
Trauma	4 (3%)	11 (9%)	15 (12%)	4 (3%)	17 (14%)	21 (18%)
Sepsis	0 (0%)	8 (6%)	8 (6%)	0 (0%)	9 (8%)	9 (8%)
Other						
(Renal, metabolic, orthopaedic)	1 (1%)	3 (2%)	4 (3%)	1 (1%)	5 (4%)	6 (5%)
Total	52 (41%)	75 (59%)	127	37 (31%)	83 (69%)	120

Where there are no blood glucose measurement entries for more than 5 consecutive hours, S_I is not fitted. With SPRINT, this gap only occurred due to removal of the patient from the ICU for surgery or other clinical procedures. Fitted S_I is constrained between physiological limits of 1×10^{-5} and 1×10^{-3} [L/mU/min] [e.g. Doran, 2004; Chase et al., 2004; Natali et al., 2000; Prigeon et al., 1996]. The 2-dimensional kernel density estimation method presented in Section 5.2 is then used to construct the stochastic S_I model that describes the transition of parameter values from one hour to the next.

Figure 6.1 shows the distribution of the fitted hour to hour S_I and the 2-dimensional kernel joint probability density. The new 3-dimensional S_I stochastic model is shown in Figure 6.2. This model has a more dynamic structure, where there are many local peaks and troughs, especially in the higher S_{In} – lower S_{In+1} quadrant (lower right corner in Figure 6.2), compared to the initial stochastic model of Figure 5.5.

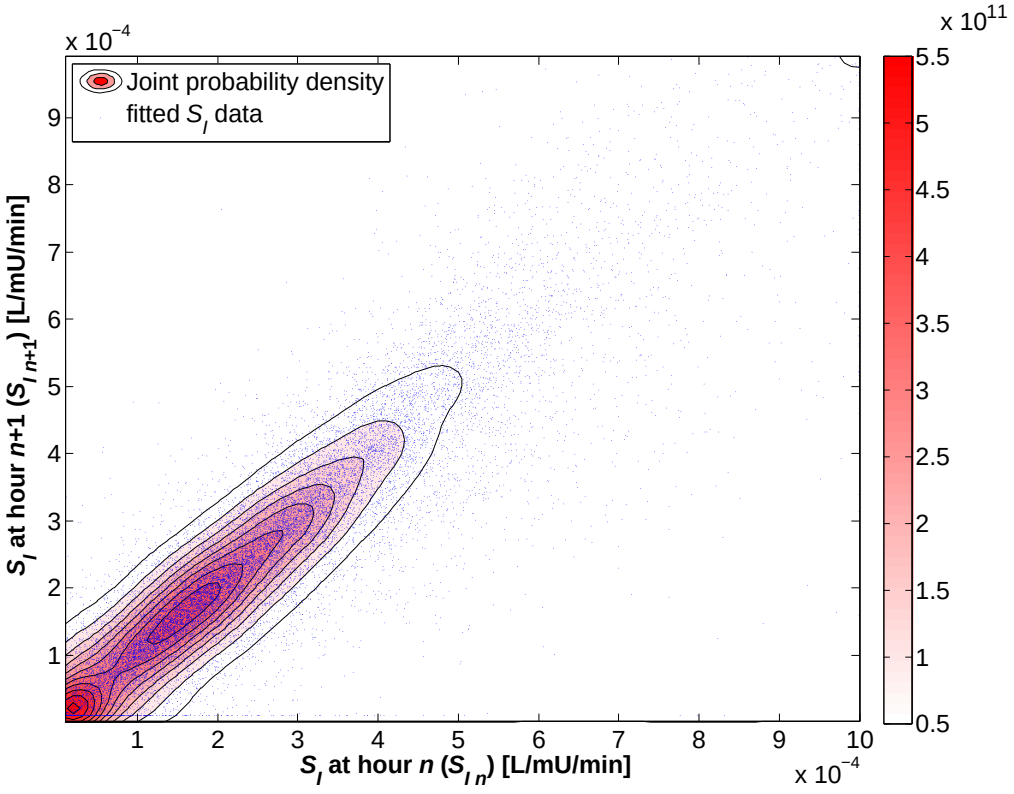

Figure 6.1 Fitted hourly S_I variation and joint kernel probability density for SPRINT patients

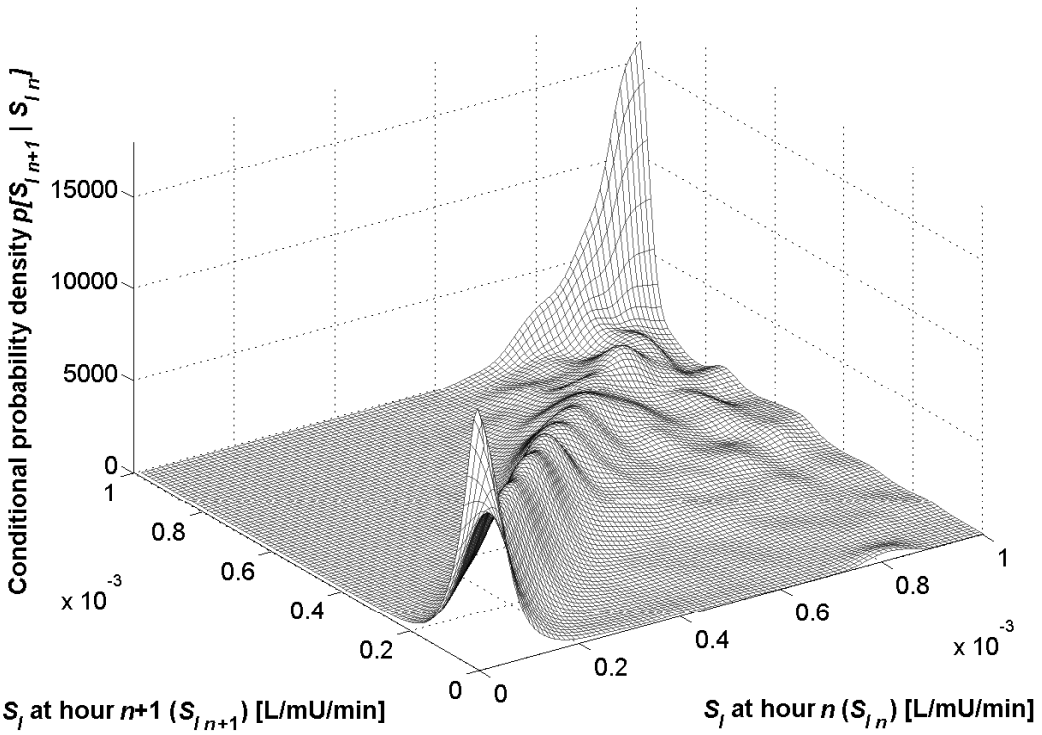

Figure 6.2 Higher dynamic stochastic model of S_I variability

Across the fitted range of S_I, the conditional probability density function is largely uni-modal and symmetric. However, as shown in the cascade plot of conditional S_{In+1} probability density functions across the S_{In} model range in Figure 6.3, there are some numerical artefacts near the boundaries of the fitted range. Probability density functions for S_{In} peak at boundary values because of the fitting constraints. For $S_{In} = [1 \times 10^{-5}, 1 \times 10^{-4}]$ and $[0.75 \times 10^{-3}, 1 \times 10^{-3}]$ at the edges of Figure 6.3, the percentile values away from the median do not consistently or monotonically decrease in probability. These ranges span 34% of the fitting range $[1 \times 10^{-5}, 1 \times 10^{-3}]$, in which 20% of the SPRINT data falls (18% between $S_{In} = [1 \times 10^{-5}, 1 \times 10^{-4}]$ and 2% between $[0.75 \times 10^{-3}, 1 \times 10^{-3}]$ in Figure 6.1).

Note that Figures 6.2 and 6.3 show the conditional probability density functions which are scaled to have the area under each function summing to 1. Thus, the asymmetry becomes very pronounced in Figures 6.2 and 6.3. The probability of S_I taking on these asymmetric conditional probability density functions is in fact very low in the overall joint probability density function shown in Figure 6.1, where the probability density sums to 1 over the entire fitting surface.

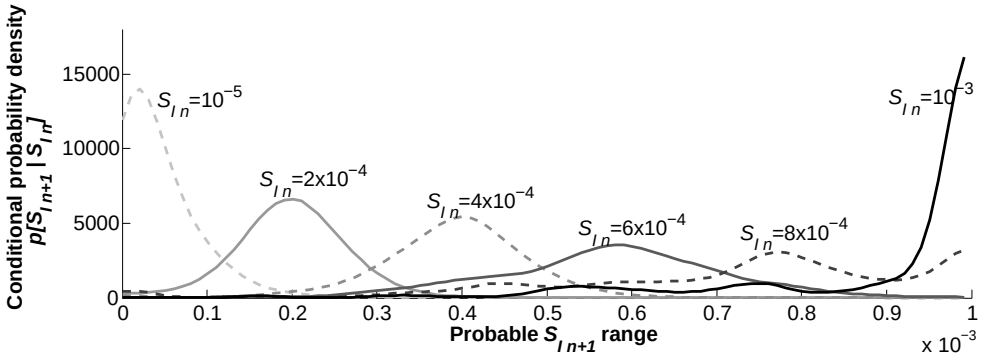

Figure 6.3 Cascade plot of S_I probability density functions over fitted S_I range. The area under each curve sums to 1.0

The asymmetric S_I probability density functions could perhaps be due to other not explicitly modelled physiology, such as variations in endogenous glucose production. More specifically, "bumpy" areas of S_I probability density function in Figure 6.3 may be a sign of S_I absorbing physiology that is unmodelled or undermodelled in Equations (2.9)–(2.13). However, this unmodelled physiology represents uncommon sudden, or extreme, dynamics, evident by the low overall joint probability density in these areas in Figure 6.1. Practically, to include all such variations in the glucose-insulin model would make it overly complicated and it would thus lose clinical feasibility. Such additions would also require added assumptions for endogenous insulin or glucose production that are not clinically measured in real-time.

Assumptions for these responses could also compromise control accuracy, as both endogenous insulin and glucose productions are known to vary significantly between patients [Sherwin et al., 1974; Ellemann et al., 1987; Van Cauter et al., 1992; Ferrannini and Cobelli, 1987b; Ferrannini et al., 2005] and over time. In addition, endogenous glucose production is suppressed with significant insulin administration in both normal and stressed states [Thorell et al., 2004], which is the case for critically ill patients under insulin therapy for glycemic management. Similarly, the endogenous insulin production is effectively removed or significantly reduced in the presence of significant exogenous insulin [Insel et al., 1975; DeFronzo et al., 1979; Transberg et al., 1981; Ellemann et al., 1987], not to mention its inhibition in stress hyperglycemia [e.g. McCowen et al., 2001]. It is therefore in the interest of this model-based clinical control applications, to have these effects mitigated into S_I. The result is a much more clinically feasible control model, where S_I accounts for critically ill population's overall sensitivity

to insulin and/or its utilisation.

In Figure 6.1, the lower bound for S_I has greater influence on the overall stochastic model than the upper bound. However, no patients have fitted S_I staying at the lower bound for a prolonged period, again suggesting that these occasions are more sudden, short term conditions, such as suppressed insulin sensitivity or utilisation due to drug therapies, rather than long term, or gradual changes, such as increased glucose production. During numerical fitting, if the fitted S_I stays at the lower bound for a prolonged period of 5 hours, the fitting method recognises a gradual evolution, and adjusts G_E to address factors such as endogenous glucose production. During the total of 23,324 control hours, only 39 such occurrences were observed, which equals to 0.17% of the time.

The short term changes due to significant drug effects or acute medical conditions such as atrial fibrillation [Wong et al., 2006b] can often cause the fitted S_I to hit the lower bound. However, if unconstrained, these situations often result in negative, unphysiological S_I. In addition, increased endogenous production with inhibited glucose production can result in an effectively zero or negative modelled S_I. These cases are too wide ranged to be accounted for in the physiological model. Note that an evolving G_E that is too high leads to a reduction in modelled endogenous glucose production, and a higher S_I may also result in the model due to a lower $-p_G G$ term. Mitigating the impact of these events into the fitted S_I simplifies the model to be clinically control feasible.

In addition, incorrect modelling of these conditions, which are difficult to account for, can severely compromise patient safety. More specifically, underestimating S_I can lead to excess insulin being given. With the aim of applying the physiological and stochastic models in clinical control, the lower bound of S_I thus plays an important role. Finally, the fitted S_I, with higher data concentration around the lower bound, realistically reflects the highly variable dynamics in the critical care environment, where drug therapies and acute medical conditions that result in highly resistant patients are common.

6.3 Clinical Use of Stochastic Model Probability Intervals

Having constructed this denser and more dynamic S_I stochastic model, a grid of data that describes the surface shown in Figure 6.2 can be stored and used as a look-up table, as introduced for the initial stochastic model in Section 5.2. Given an identified hourly S_I value in clinical situations [Chase et al., 2005b,c; Wong et al., 2006a,b], the probability density, and hence the probability intervals, can be obtained, as demonstrated in Figure 6.4. The solid line is the kernel density estimate surface sliced along $S_{In} = 0.6 \times 10^{-3}$. This line represents the probability density for potential S_{In+1}, one hour after having identified the current hour $S_{In} = 0.6 \times 10^{-3}$. From this density function, probability intervals are also obtained, giving the median of probable S_I values in an hour at a very similar 0.58×10^{-3}, inter-quartile range $[0.49 \times 10^{-3}, 0.66 \times 10^{-3}]$, and the 0.90 probability interval $[0.33 \times 10^{-3}, 0.79 \times 10^{-3}]$.

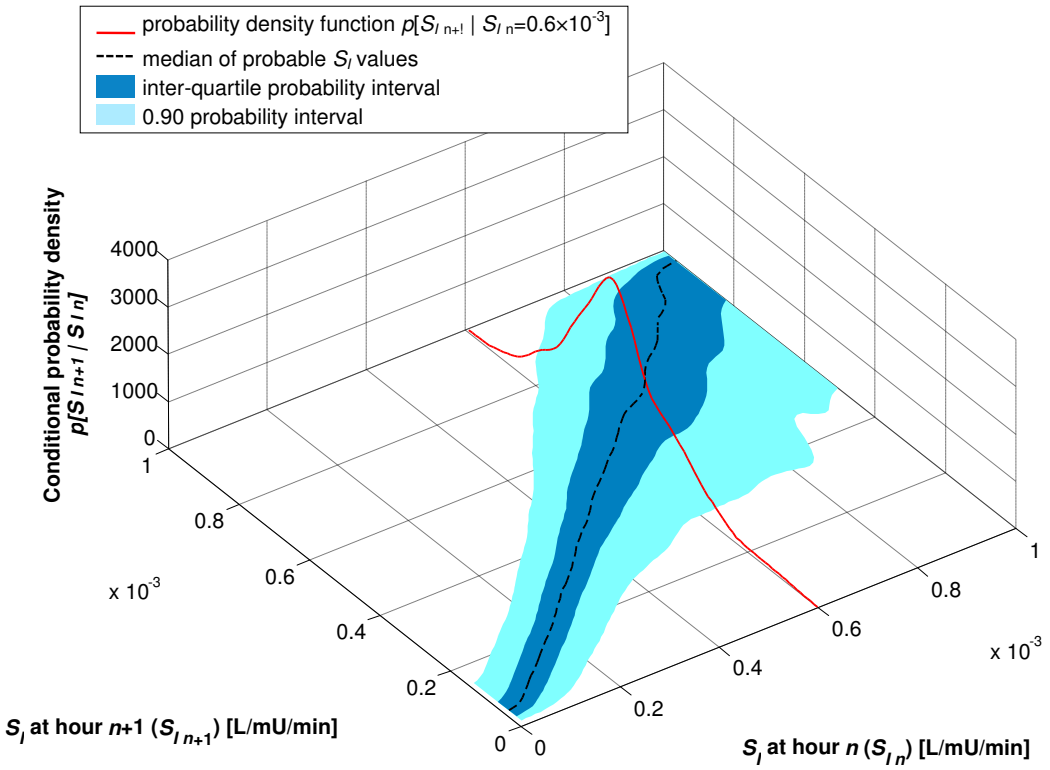

Figure 6.4 S_I probability density function from the higher dynamic stochastic model

This more dynamic model does not have as smooth a probability density function $p[S_{In+1}|S_{In} = 0.6 \times 10^{-3}]$ as the initial model. This difference is a result of the denser and greater amount of data used to create the model, and is evident in Figure 6.5. However, the resulting probability intervals are not very different. The initial model gives the median as 0.58×10^{-3} with inter-quartile range $[0.51 \times 10^{-3}, 0.65 \times 10^{-3}]$, and the 0.90 probability interval $[0.39 \times 10^{-3}, 0.75 \times 10^{-3}]$. In comparison, the model presented in this chapter yields a median of 0.58×10^{-3}, an inter-quartile range of $[0.49 \times 10^{-3}, 0.66 \times 10^{-3}]$, and the 0.90 probability interval of $[0.33 \times 10^{-3}, 0.79 \times 10^{-3}]$.

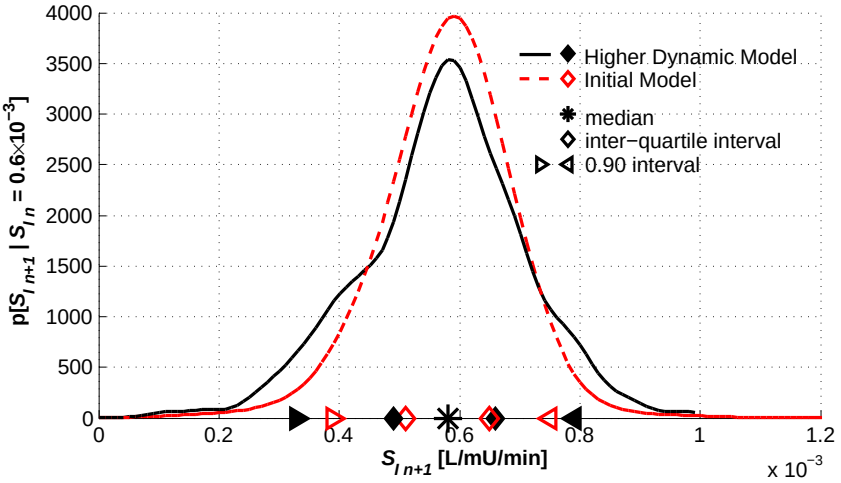

Figure 6.5 Comparison of stochastic model probability density functions $p[S_{In+1}|S_{In} = 0.6 \times 10^{-3}]$

The probability intervals used here for clinical decision making, as shown in Figure 6.4, are equal-tailed. "Equal-tailed" means that the 0.90 probability interval is between the 5^{th} percentile and the 95^{th} percentile in the probability density function. Equal-tailed probability intervals are based on the assumption and observation that the probability density function is (largely) uni-modal and symmetric. Thus, the values outside the interval are assumed to have a lower probability of occurring than the values within the interval, and represent "tails" of that distribution. Note that this assumption is only valid if the distribution, as in Figure 6.5, is monotonically or consistently decreasing moving away from its median.

6.3.1 Probability Interval Calculation

Using the interval boundary values for S_I in Equations (2.9)–(2.13), the corresponding probability intervals in blood glucose levels for a given intervention and current state can be calculated. This statistical approach holds for any strictly monotone physiological systems [Casella and Berger, 2002]. More specifically, in this case, a higher S_I value always produces lower blood glucose than a lower S_I value for a given input and state over the time S_I is defined.

In the cascade plot of the conditional S_{In+1} probability density functions across the S_{In} range in Figure 6.3, it is evident that the assumption that the conditional probability density function is largely uni-modal and symmetric is true for the bulk of the fitted S_I range, but does not hold near the boundaries. Therefore, in these regions, equal-tailed probability intervals may not give an accurate representation of the highest probability ranges. More simply, the 5^{th} and the 95^{th} percentile in the resulting blood glucose level probability distribution may not contain the 90% most probable blood glucose levels. In particular, due to the asymmetric boundary density functions in S_I, blood glucose levels outside this range may have a higher probability density than parts within the 0.90 probability interval.

To accurately obtain the probability density function in blood glucose resulting from a known probability density function in S_I, Monte Carlo simulation is the only method. In particular, while the percentile values in S_I correspond to percentile values in blood glucose levels, the "rank" of probability does not [Casella and Berger, 2002].

This situation is illustrated in Figure 6.6, where the left hand side and right hand side demonstrate the difference between the 0.90 equal-tailed blood glucose probability intervals and the probability intervals generated from Monte Carlo simulations. Panels A and B display the same probability density function (pdf) (right axis) and the cumulative distribution functions (cdf) (left axis) in S_{In+1}, when $S_{In} = 8 \times 10^{-4}$ is known. Panels C and D show the resulting pdf (right axis) and cdf (left axis) in blood glucose levels at hour $n+1$ (BG_{n+1} [mmol/L]) through Monte Carlo Simulation of the model in Equations (2.9)–(2.13). The pdf and cdf shown in panels C and D are identical and are the solution for the BG_{n+1} probability density function given $S_{In} = 8 \times 10^{-4}$. Note that in panels A

and B, the x-axes are decreasing from left to right, producing a similar shaped probability density function in blood glucose levels in panels C and D with blood glucose levels increasing as S_{In+1} decreases.

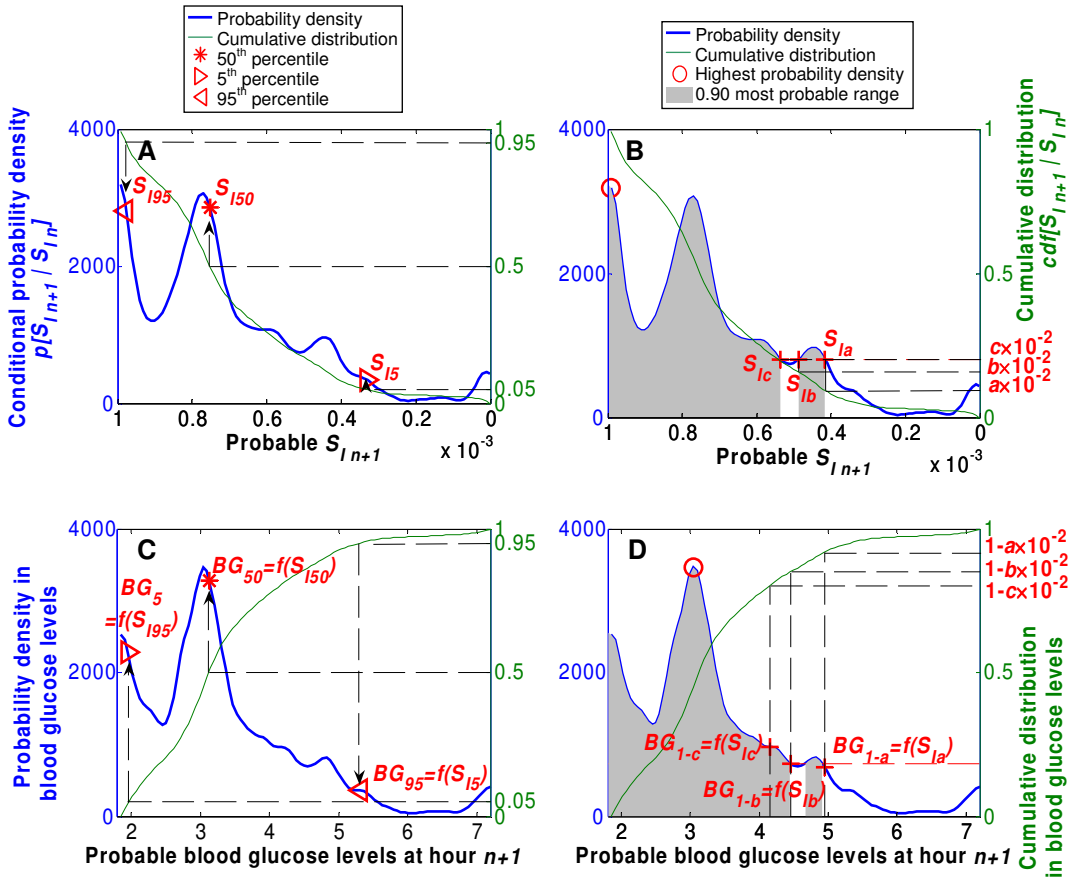

Figure 6.6 Probability density transition from S_I to blood glucose levels. Panels A and B show the pdf (right axis) and the cdf (left axis) in S_{In+1}, when $S_{In} = 8 \times 10^{-4}$ is known. Panels C and D show the resulting pdf (right axis) and cdf (left axis) in blood glucose levels at hour $n+1$ (BG_{n+1} [mmol/L]) through Monte Carlo simulation. The transformation through Equations (2.9)–(2.13) from upper panels to lower panels is denoted by f. The shaded areas in panel B and D have the highest 90% probability. The 90% most probable S_{In+1} intervals in panel B are between cdf = [a$\times 10^{-2}$, b$\times 10^{-2}$] and [c$\times 10^{-2}$, 1.0]. Note that higher S_I values in the left hand side of the reversed x-axis in panels A and B results in higher BG values on the right hand side in panels C and D.

The left hand side of Figure 6.6, panels A and C illustrate how equal-tailed probability intervals in S_{In+1} are translated into the equal-tailed probability intervals in BG_{n+1}. Let f be the transformation function between S_{In+1} to BG_{n+1}, which is the physiological model shown in Equations (2.9)–(2.13), then

$$BG_{[100-\text{percentile}]} = f(S_{I[\text{percentile}]}) \tag{6.1}$$

Thus, the percentile values of S_{In+1} in panel A corresponds to the reversed (100−percentile) values in BG_{n+1} in panel C. Or more simply, solving Equations (2.9)–(2.13) using the 5^{th} percentile value in S_{In} produces the 95^{th} percentile blood glucose levels, $BG_{95} = f(S_{I[5]})$ given that f is strictly monotone [Casella and Berger, 2002]. Therefore, the S_{In+1} probability interval between the 5^{th} and the 95^{th} percentile ($S_{In+1} = [0.33 \times 10^{-3}, 0.98 \times 10^{-3}]$ between $\triangleright$ and $\triangleleft$ in panel A) consequently gives the BG_{n+1} probability interval between the 5^{th} and the 95^{th} percentile ($BG_{n+1} = [1.9, 5.4]$ between $\triangleright$ and $\triangleleft$ in panel C). More simply, as shown in the left hand side of Figure 6.6:

- Equal-tailed 0.90 probability interval in $S_{In+1} = [S_{I[5]}, S_{I[95]}]$
- Equal-tailed 0.90 probability interval in $BG_{n+1} = [f(S_{I[95]}), f(S_{I[5]})]$

However, as illustrated in panel C, the BG_{n+1} probability interval between the 5^{th} and the 95^{th} percentile ($\triangleright$ and $\triangleleft$) includes values that have lower probability density than some BG_{n+1} values outside this interval. More specifically, $\triangleright$ has a lower probability density than the region to its left. This higher probability density region outside the 5–95% range is very narrow and at the very extreme end, however, it shows the discontinuity from a simple equal-tailed assumption.

On the right hand side of Figure 6.6, the 90% most probable S_{In+1} values are identified by the shaded areas in panel B. These values are discontinuous, and have higher probability of occurring than values outside the shaded areas. However, taking the boundary values for the 90% most probable S_{In+1} values, and then putting them into Equations (2.9)–(2.13), does not provide the 90% most probable BG_{n+1} intervals. More simply, as shown in the right hand side of Figure 6.6:

- The 0.90 probability interval of highest probability density in S_{In+1} = shaded intervals in panel B = $[S_{I[\mathrm{a}]}, S_{I[\mathrm{b}]}]$ and $[S_{I[\mathrm{c}]}, S_{I[100]}]$, where a, b and c are percentile values of $S_{I[\mathrm{a}]}$, $S_{I[\mathrm{b}]}$ and $S_{I[\mathrm{c}]}$, and

$$\mathrm{pdf}(S_{I[\mathrm{a}]}) = \mathrm{pdf}(S_{I[\mathrm{b}]}) = \mathrm{pdf}(S_{I[\mathrm{c}]}) \tag{6.2}$$

$$\mathrm{cdf}(S_{I[k]}) = k \quad \text{for } k = \mathrm{a},\ \mathrm{b},\ \mathrm{c} \tag{6.3}$$

$$(100 - \mathrm{c}) + (\mathrm{b} - \mathrm{a}) = 90 \tag{6.4}$$

- The 0.90 probability interval of the most likely BG_{n+1} = shaded intervals in panel D $\neq [f(S_{I[100]}), f(S_{I[\mathrm{c}]})]$ and $[f(S_{I[\mathrm{b}], f(S_{I[\mathrm{a}]})]}$, or

$$\mathrm{pdf}(f(S_{I[\mathrm{a}]})) \neq \mathrm{pdf}(f(S_{I[\mathrm{b}]})) \neq \mathrm{pdf}(f(S_{I[\mathrm{c}]})) \tag{6.5}$$

Consequently, to obtain the probability intervals according to likelihoods in BG_{n+1}, Monte Carlo simulations need to be done. In this case, to achieve an accuracy of 1%, a minimum of 10,000 randomly selected S_{In+1} values must be utilised. While such a Monte Carlo simulation can provide the appropriate probability density in BG_{n+1}, it is too computationally expensive to generate useful and effective probability intervals quickly enough for clinical decision support.

6.3.2 Clinical Feasibility of Probability Intervals

An estimated computational comparison between calculating the equal-tailed and the probability intervals according to likelihoods is summarised in Table 6.3. The computational time frame for calculating the probability intervals according to likelihoods is clearly not currently feasible for this type of real-time clinical control. In conclusion, assuming equal-tailed probability intervals provides fast, clinically viable and slightly conservative estimates for the most likely ranges of BG_{n+1}. Therefore, it should not compromise patient safety when used to assist clinical decision making. As the example in Figure 6.6 shows, the 0.90 equal-tailed probability interval in BG_{n+1} ([1.9, 5.4]) covers most of the 0.90 most probable range ([1.8, 4.5] and [4.7, 4.9]), providing an effective and clinically useful estimate with far less effort.

Table 6.3 Comparison between probability interval computational cost for equal-tailed and Monte Carlo methods

0.90 probability interval computation	Equal-tailed	Comp. Time	Monte Carlo	Comp. Time
Steps	1. Calculate the 5^{th} and 95^{th} percentiles in S_{In+1}, $S_{In+1[5]}$ and $S_{In+1[95]}$	∼0 sec	1. Generate 10,000 S_{In+1} using the derived pdf from the stochastic model	2 sec
	2. Equal-tailed 0.90 probability interval in $BG_{n+1} = [f(S_{In+1[95]}), f(S_{In+1[5]})]$	1 sec	2. Calculate BG_{n+1} for each of the 10,000 S_{In+1} values	5,000 sec = 83 min
			3. Sort the 10,000 BG_{n+1} values and find the 5^{th} and 95^{th} percentiles	1 sec
Total Time		*∼1 sec*		*∼83 min*

6.4 Higher Dynamic Model Validation

Method

Again, the stochastic S_I model can be integrated into the glucose-insulin system model of Equations (2.9)–(2.13) for use in control. This step allows the blood glucose level probability intervals one hour following a known insulin and/or nutrition intervention to be found directly based on the defined probability density function of S_{In+1}. Cross validation was performed to test the generality of the SPRINT cohort and the method of creating the stochastic model. In addition, cross validation will ensure that the higher dynamic shown in the stochastic model is not only from a few outlying patients, but is a genuine behaviour of generic S_I variation in critical care.

For cross validation, the 165 SPRINT patients are divided into 5 random groups. Each group has comparable medical conditions, sex, age, and APACHE scores. Five stochastic S_I models are then built, each one using fitted S_I data from 4 out of 5 groups, leaving one group out each time. Each stochastic model is then evaluated against the group that is not used for creating the model.

Table 6.4 shows the general information on the 5 patient groups used in cross validation. An example of how a stochastic model created from Groups 1, 2, 3 and 4 is evaluated against a patient in Group 5 is shown in the following steps:

1. At hour 0, the patient's identified S_I is S_{I0}. The stochastic model then produces the 5^{th}, 25^{th}, 75^{th} and 95^{th} percentiles for probable S_I at hour 1, denoted $S_{I1[5]}$, $S_{I1[25]}$, $S_{I1[75]}$ and $S_{I1[95]}$.

2. Examine if the identified S_{I1} is within the inter-quartile probability interval between $S_{I1[25]}$ and $S_{I1[75]}$, and the equal-tailed 0.90 probability interval between $S_{I1[5]}$ and $S_{I1[95]}$.

3. Do the same procedure for hour 1, and repeat the process until the end of the patient trial data.

All possible combinations of 4 out of 5 groups are tested.

Results

The percentage of fitted S_I within the equal-tailed 0.90 and inter-quartile probability intervals for the group not used in creating the cross validation model is summarised in Table 6.5. Each group produced similar results, which were also comparable to the overall result. Thus, there is no significant difference between the 5 stochastic models created and the SPRINT cohort can be considered a generic representation of this ICU population.

More specifically, the mean of per patient average of identified S_I values within the equal-tailed probability intervals is 86.6%, and 54.0% for the inter-quartile probability intervals. The use of equal tailed 0.90 probability intervals slightly underestimates the identified S_I range, because when S_{In} is close to its fitting constraints, the S_{In+1} probability density function tends to peak near the boundary value. This behaviour causes some regions outside of the equal-tailed 0.90 probability intervals to have higher probability density than some regions within the interval, as shown in Figures 6.3 and 6.6. Thus, the compromise of using equal-tailed probability intervals has negligible impact compared to the computational gain over calculating the blood glucose ranges of the highest 0.90 probability density.

Table 6.4 Sub-cohorts of 165 SPRINT patients for cross validation

Group	no. of patients	age (yr)	gender (% male)	average blood glucose level (mmol/L)	length of trial (hr)
1	33	57.4 (19.4)	69.7%	6.2 (1.9)	144.6 (189.1)
2	33	66.5 (13.8)	63.6%	5.9 (0.7)	141.1 (167.7)
3	33	61.0 (15.6)	63.6%	6.0 (0.9)	138.6 (169.4)
4	33	63.7 (15.9)	60.6%	6.0 (0.7)	142.7 (143.2)
5	33	56.5 (18.1)	72.7%	5.9 (0.8)	139.8 (169.0)
overall	165	61.0 (16.6)	66.1%	6.0 (1.0)	141.4 (167.7)

Group	time in 4–6.1 mmol/L band (%)	average insulin usage (U/hr)	average absolute goal feed(ml/hr)	average % goal feed	mortality (%)	APACHE II
1	58.1 (24.5)	2.6 (1.1)	75.3 (10.6)	48.3 (38.7)	72.7%	20.5 (8.8)
2	59.0 (17.3)	2.6 (1.2)	73.0 (10.3)	52.0 (36.0)	81.8%	17.7 (7.1)
3	59.8 (22.1)	2.6 (0.7)	74.7 (10.7)	52.5 (42.3)	84.8%	20.9 (8.8)
4	58.2 (16.1)	2.7 (1.0)	70.9 (10.3)	54.0 (32.7)	87.9%	21.3 (6.4)
5	59.1 (21.0)	2.5 (0.7)	77.3 (10.4)	52.7 (32.5)	82.4%	20.5 (7.3)
overall	58.9 (20.2)	2.6 (0.9)	74.2 (10.5)	51.9 (36.4)	81.9%	20.2 (7.7)

*data displayed as [mean (std)] where appropriate

Table 6.5 Stochastic insulin sensitivity model cross validation results

Group	Groups used in creating stochastic model	Average percentage of fitted S_I within equal-tailed 0.90 probability interval	Average percentage of fitted S_I within inter-quartile probability interval
1	[-,2,3,4,5]	85.7%	54.2%
2	[1,-,3,4,5]	83.2%	52.3%
3	[1,2,-,4,5]	87.4%	54.7%
4	[1,2,3,-,5]	88.7%	54.1%
5	[1,2,3,4,-]	87.9%	54.8%
overall	[1,2,3,4,5]	86.6%	54.0%

The inter-quartile probability intervals include slightly over 50% of fitted S_I, suggesting that most of the time the higher probability density is concentrated about the median of the probability density functions, as also seen in Figures 6.3 and 6.6. Similarly, the 0.90 probability interval has slightly less than 90% of all measurements, suggesting that there are slightly more outliers than represented in the model. Both results suggest that the assumptions used are slightly inaccurate, but within typical variations in fitted S_I that might be seen as a result of the 7–12% measurement error [Arkray, 2001; Lotz et al., 2006a].

The higher dynamic stochastic model is also verified against clinical data, reflecting observed clinical variations. The more dynamic behaviour seen in this second stochastic model exists across the entire cohort, and cannot be simply eliminated by data smoothing. The higher dynamic is thus genuine and generic. Intelligent and careful use of this higher dynamic model will therefore lead to a more accurate probability prediction assisted glycemic control.

6.5 Comparison to the Initial Model

The stochastic models presented in Chapters 5 and 6 capture the S_I variation dynamics in the critically ill on two levels. The initial model captures fundamental dynamics, while the higher dynamic model in this chapter uses greater data and data density to capture additional subtle and higher order dynamics as well. Both models would be implemented the same way in a clinical setting, despite the more rigorous effort in the validation of the higher dynamic model. A comparison of the two models is presented in Table 6.6. The raw data plots are shown in Figure 6.7.

A pictorial comparison of the 3-dimensional kernel probability density function is presented in Figure 6.8.

Table 6.6 Stochastic model comparison

Patient cohort used to create model

	no. of patients	cohort APACHE II med. [range]	hours of fitted data	data frequency (hr)
Initial Model	18	22 [8–36]	1,278	3–4
Higher Dynamic Model	165	19 [1–43]	23,324	mostly 1, occasionally 2

Prediction performance on SPRINT data

	$\%S_I$ within 0.90 probability interval	$\%S_I$ within inter-quartile interval
Initial Model	87.3	53.7
Higher Dynamic Model*	86.6	54.0

*result from cross validation

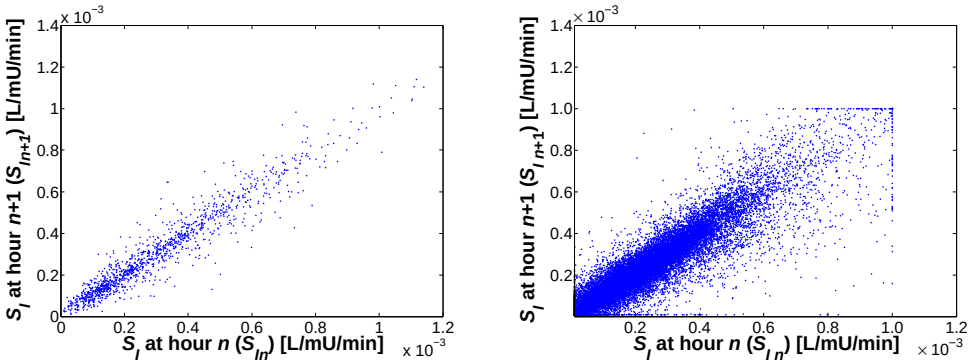

(a) 18-patient S_I data

(b) 165-patient S_I data

Figure 6.7 Fitted S_I comparison

A tighter fitting constraint was placed on fitting S_I for the 165 patients, when creating the second model, as is evident in the shaded areas in Figure 6.8(f). The same constraint value that was used in the initial model was also used in a first

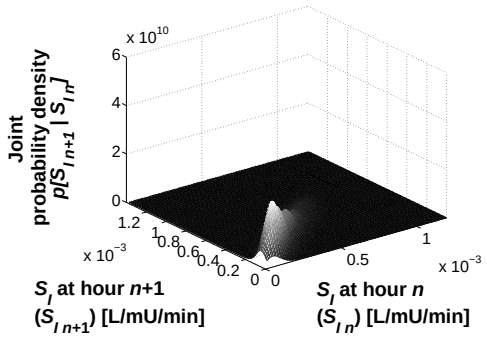

(a) Initial stochastic model joint probability density. (The area under the entire surface sums to 1.)

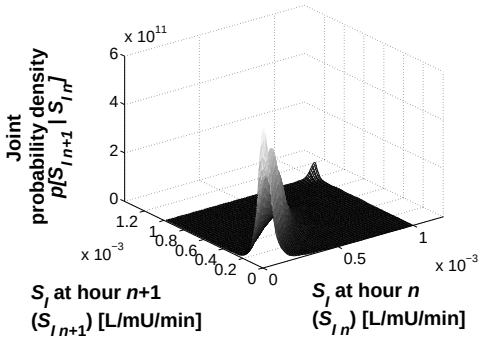

(b) Higher dynamic stochastic model joint probability density. (The area under the entire surface sums to 1.)

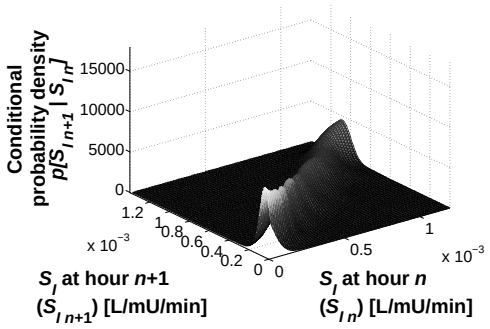

(c) Initial stochastic model conditional probability density. (The surface slices along the S_{In+1} axis has area under the curve summing to 1.)

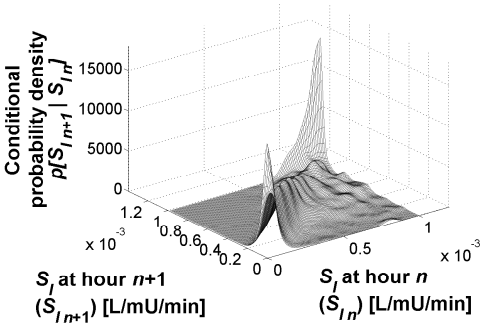

(d) Higher dynamic stochastic model conditional probability density. (The surface slices along the S_{In+1} axis has area under the curve summing to 1.)

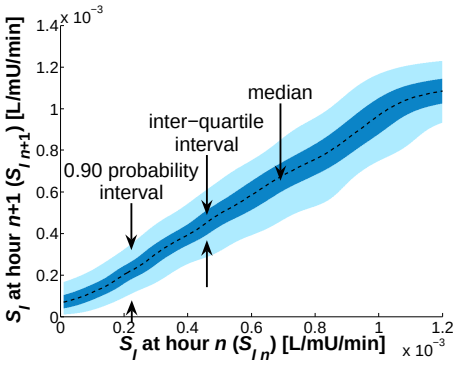

(e) Initial model probability interval

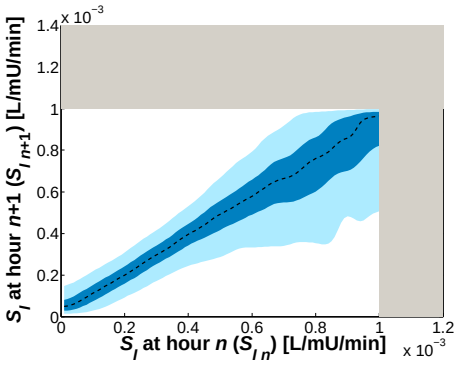

(f) Higher dynamic model probability interval

Figure 6.8 Stochastic model comparison

attempt. However, data outside of this region is very sparse in the SPRINT cohort, and the conditional probability density function in this region became extremely skewed from normalising to very low joint probability density. The effect of normalisation across the entire S_I range can be seen going from Figure 6.8(a) to 6.8(c) and from Figure 6.8(b) to 6.8(d).

Therefore, a slightly tighter constraint was used, and the resulting quality of the fit was near identical. In fact, the median probability curve in Figure 6.8(f) is near linear for $S_{In} \leq 0.001$, and flattens out afterwards. Therefore, any fitted $S_I \geq 0.001$ may be caused by abnormal, acute or sudden medical events, for example atrial fibrillation [Wong et al., 2006b]. These events are obviously reflected in the modelled S_I, but do not represent insulin sensitivity variation literally in this model context. This tighter constraint is further supported by the very similar probability interval prediction performance on SPRINT between the initial model and the higher dynamic model in this chapter. Finally, it is evident from the similarities, that a slightly smaller modelling region does not exclude clinically observable insulin sensitivity variations, including acute cases.

However, the fact that a higher dynamic model does not noticeably improve prediction performance was not originally expected. The reason for this discrepancy may be that the higher dynamic model uses equal-tailed probability intervals that also include regions of outlying lower probability, as explained in Section 6.2. Note that the percentage values listed in Table 6.6 for the higher dynamic model are from cross validation testing. A model built using the entire cohort would increase these percentage values slightly.

For prediction assisted glycemic control application, the wider probability interval in the higher dynamic model can provide a more conservative, therefore safer, prediction based intervention advice than the initial model. In the end, the higher dynamic model was created using a larger, more representative glycemic controlled ICU cohort, with 3–4 times higher data density. The validity of the model was also able to be more optimally tested using cross validation, as well as against the previous stochastic model. Both comparisons showed good, predictable and fully generalisable performance. Finally, in practice, both are represented as similar sized look-up tables. Therefore, the higher dynamic model represents a better choice going forward.

6.6 Stochastic Models Summary

The S_I stochastic model can define the probability density functions of blood glucose levels one hour following a known glycemic control intervention, and thus enable more knowledgeable and accurate prediction for glycemic control. The 2-dimensional kernel density estimation method employed allows the Markovian S_I stochastic model capture the essence of clinically observed variation. The stochastic model acts as a tool to assist clinical intervention decisions, maximise the probability of achieving desired glycemic regulation, while maintaining patient safety. The impact of control inputs on probabilistic blood glucose results can be assessed, giving confidence in the effectiveness of the control protocol against evolving patient dynamics, particularly with respect to avoiding hypoglycemia.

The initial model created from 18 retrospective study patients was evaluated on 8 insulin-nutrition control trials and 165 SPRINT trials. Both results agreed with the model probability intervals. The second finer stochastic model was created using clinical data from 165 SPRINT trials, resulting in a model with more complex dynamics. The more dynamic model used data that are 3–4 times denser than that used for the initial model, and the total duration of data was also 18 times greater. Both models gave similar probability interval prediction when tested on data from 165 SPRINT trials. The probability interval prediction from both models are slightly conservative, but accurately capture the cohort. For prediction assisted glycemic control, the wider probability interval in the higher dynamic model provides a more conservative, therefore safer, prediction based intervention advice than the initial model.

The quality of blood glucose control is closely linked with patient condition, in particular with respect to insulin sensitivity [Chase et al., 2006b]. Higher identified S_I levels give tighter blood glucose probability intervals, making tighter and safer control possible with subtle control efforts. Blood glucose probability intervals widen at lower S_I levels, limiting the accuracy of tight glycemic regulations. Caution against sudden reductions in glycemic levels is needed at typically low levels of S_I, where significant doses of insulin are typically administered [Wong et al., 2006b; Chase et al., 2005c, 2006b], while the range of possible change in blood glucose levels is broad.

Finally, it should be noted that the methods presented and their clinical use can be readily generalised to similar cohorts, such as hyperglycemic patients in other hospital wards needing glycemic control. Models could also be built, given enough data, for different patient types/diagnoses and/or APACHE scores or similar. This approach would provide even greater ability to mimic specific clinical trials or cohorts in testing or validating models and/or drug delivery protocols. In addition, the method and approach can be applied to other pharmacodynamic/drug delivery problems. As many pharmacodynamic systems and models share great similarity, particularly in turns of drug/stimulus sensitivity, critical sensitivity parameters can be identified and modelled stochastically to gain greater knowledge of its metabolic variation and aid the control approach. An example of this is the agitation-sedation problem [Shaw et al., 2003], which share very similar pharmacodynamics to the glucose-insulin system. Currently, there exists no crisp picture of the received effect of stimulus and sedative in patients. Inter- and intra-patient variability is poorly addressed in this clinical control problem. A stochastic model of these effects can aid understanding of the problem and further assist controlling it. Therefore, while the models presented in Chapters 5 and 6 represent the stochastic modelling applications in critical care glycemic control, the ability to generalise these modelling methods holds significant additional promise.

Chapter 7

Virtual Patients and Protocol Simulations

The stochastic model developed has been shown to closely reflect the metabolic dynamics of hyperglycemic ICU patients. Being able to reflect a typical critical care patient's S_I variation means that it can also act as a patient simulator for developing glycemic control protocols. This chapter presents the development of "virtual patients" for protocol development and virtual trials, as well as a computerised glycemic control protocol that utilises the stochastic model's probability interval prediction ability. Hence, it independently uses the model to simulate patients and to assist control by predicting clinical outcomes. As a further form of validation, both applications are compared to clinical data and results to clearly identify its clinical potential.

7.1 Creating Virtual Patient Cohort

Incorporating the stochastic model developed into the glucose-insulin system model presented in Equations (2.9)–(2.13), typical critical care patient dynamics can be reproduced numerically. The primary requirement is initial conditions in G, Q and I, along with starting dextrose and insulin inputs. To create a virtual patient, a starting S_I value is also required to initiate the stochastic model.

A cohort of "virtual patients" was generated to be similar to the 165 SPRINT patients. It can thus serve to test the model's ability to represent a clinical patient cohort. Initial conditions to Equations (2.9)–(2.13) are generated to approximate the statistical distribution of these parameters, as they were recorded from the SPRINT cohort. Initial S_I values are randomly selected from the initial values

fitted from the SPRINT S_I data. Trial lengths were also randomly generated to create a similar statistical distribution of trial lengths to those in the SPRINT trial.

Profiles of S_I that are representative of ICU patient condition evolution are then generated according to the stochastic model. Using these profiles with Equations (2.9)–(2.13), "virtual patients" are created that (statistically) approximate the SPRINT cohort from which the model was created. This "virtual patient" cohort then provides a platform for clinical trial simulation and development of control algorithms, as well as a potential further source of validation in comparison of these protocols' clinical results to clinical results from SPRINT.

7.2 Probability Interval Assisted Targeted Control Protocol

For this study, the (virtual) control trial (simulation) protocol consists of hourly cycles of the following glycemic control steps:

1. **Virtual Patient:** Generate an hourly S_{In+1} value from the stochastic model defined probability density function of the previous hourly S_I value S_{In}.
2. **Virtual Patient:** Generate the end-of-hour virtual blood glucose level using the generated S_{In+1} and the specified control (insulin and nutrition) interventions at hour $n+1$ in Equations (2.9)–(2.13). Standard Glucocard^{TM} blood glucose measurement error [Arkray, 2001] is numerically added to the generated blood glucose level, matching the clinical conditions in Christchurch Hospital ICU [Wong et al., 2006b].
3. **Glycemic Controller:** A new S_I, denoted $S_I{}'$, is fit to the blood glucose levels including random noise that are "measured" during hour $n+1$. Integral-based parameter identification is used to identify $S_I{}'$ [Hann et al., 2005; Wong et al., 2006b]. Not that $S_I{}' \neq S_I$ will likely occur due to the glucose measurement noise added.
4. **Glycemic Controller:** The median and equal-tailed 0.90 and inter-quartile probability interval of potential physiological S_I are generated from the

identified $S_I{}'$ obtained from step 3, using the identified value of $S_I{}'$ in the stochastic model. This step essentially looks up the probability density function of $p[S_{In+1}|S_{In}]$ at $S_{In} = S_I{}'$ as described in Figure 6.4.

5. **Glycemic Controller:** Control interventions are determined that position the median glycemic value and the probability intervals in blood glucose level one hour later. The actual one hour later position is determined using criterion defined by the control algorithm.

6. **Virtual Patient:** Return to step 1 with the stochastic model generated S_{In+1} being the new S_{In}.

Essentially, a virtual patient's physiological S_I evolution follows the joint probability density contour in Figure 6.1, making its way to the highest probability density regions. Each S_{In+1} is dependent on the previous state, S_{In}, where the probability density function of of S_{In+1} is defined in Equations (5.9)–(5.10). Hence, in step 1 above, S_I takes a walk to a point, say y, along the probability density function curve $p(S_{In+1} = y|S_{In} = x)$ as shown in Figure 6.4. Step 6 then "walk" the S_I across (along S_{In+1} axis) to where $S_{In} = y$, and the process repeats.

As a result, a physiological stochastic S_I profile that is representative of observed clinical dynamics is generated to define the virtual patient dynamics. These profiles result in similarly dynamic glycemic profiles. The controller, in these virtual trials, uses glucose measurements with added noise to identify and estimate the stochastic model generated S_I to determine the control input.

7.2.1 Virtual Trial Control Algorithm

The specific control algorithm designed here is a target-shooting algorithm that minimises the risk of hypoglycemia in a probabilistic sense. Control interventions include insulin bolus injections, insulin infusions, and dextrose infusions. The algorithm obeys the following rules, or criterion, in a prioritised order. Thus, satisfying each rule does not violate the preceding rules.

Control and Safety:

1. The lower bound of the equal-tailed 0.90 probability intervals in blood glucose levels resulted from control interventions must never be lower than 4 mmol/L.

2. The controller specified dextrose feeding rate must be greater than or equal to a clinical specified patient specific minimum [Krishnan et al., 2003; Rubinson et al., 2004; Wong et al., 2006b; Lonergan et al., 2006b].

3. The total hourly insulin input must not exceed 6 U [Chase et al., 2004, 2005c].

4. The model-based controller estimated saturation in Q in Equation (2.9) must not exceed 300 mU/L at any time [Chase et al., 2005c]:

$$Q - \frac{Q}{1 - \alpha_G Q} \leq 300 \text{ mU/L} \tag{7.1}$$

Intervention Priority:

5. The target blood glucose level (median of the predicted, one hour later blood glucose probability density function) is 85% or more of the blood glucose level at the time of intervention, to a minimum of 4.5 mmol/L.

6. To lower blood glucose levels, the control algorithm seeks to lower the dextrose feeding rate before adding insulin in bolus (injection) form. Dextrose feeding rates are not lowered below the clinically specified minimum (Rule 2). Insulin infusions may be used to lower blood glucose levels without resulting in excess interstitial insulin saturation (Rule 4) or oversize hourly doses (Rule 3).

7. To increase low blood glucose levels, the control algorithm reduces insulin inputs first, and then increases dextrose rates.

The first 4 rules are designed for patient safety. If the target blood glucose level cannot be achieved without violating any of these first 4 rules, the target blood glucose level is "bounded" so it can be achieved within these limitations. The final 3 rules define how the algorithm prioritises achieving the target blood glucose level using the available control interventions. Rule 5 can fit in either

category, as setting a maximum rate of fall of 15% per hour is both a safety and control priority.

Note that the insulin saturation limit in Q in Rule 4 is significantly higher than the 30 mU/L limit set for the controller in the insulin only glycemic control protocol presented in Section 4.1. This is because the insulin only protocol used a model insulin distribution space of $V_I = 12$ L, and a glucose distribution space of $V_G = 12$ L. The revised insulin and glucose distribution volumes used here are 3.15 and 13.3 L. Therefore, the saturation limit is raised accordingly. Insulin injections producing modelled saturation of $Q - \bar{Q} \cong 300$ mU/L when $V_I = 3.15$ L and $V_G = 13.3$ L roughly produces modelled saturation of $Q - \bar{Q} \cong 30$ mU/L when $V_I = V_G = 12$ L.

7.3 Results and Discussion

A virtual cohort of 200 patients was created to match the SPRINT clinical cohort and tested in simulated trials. Blood glucose probability intervals were produced for each control intervention using the stochastic model and identified hourly S_I values ($S_I{}'$). Hourly blood glucose measurements, including normally distributed random measurement noise, were analysed against the probability intervals to test the predictive ability of the model.

An example of a virtual trial is shown in Figure 7.1. The top panel shows the blood glucose excursion through time. The bold crosses are the virtually generated blood glucose levels at one hour intervals, with thick bars indicating the standard 7% Glucocard$^{\text{TM}}$ measurement error [Arkray, 2001]. Hourly constant insulin sensitivity parameter values, $S_I{}'$, are fitted every hour and shown in the bottom panel. Across 200 virtual trials, the controller fitted hourly $S_I{}'$ profiles closely follow the stochastic model generated virtual S_I profiles. The average percentage difference between the fitted $S_I{}'$ and the virtual S_I is +4%. The 5^{th}–95^{th} percentile range for the ratio between $S_I{}'$ and S_I is [0.83, 1.18]. The difference between $S_I{}'$ and S_I is a result of the measurement noise added to the virtually generated blood glucose data, which ranges 7–12%.

The stochastic model is used to derive the median, equal-tailed 0.90 and inter-quartile probability intervals in S_I every hour using the value fitted for the

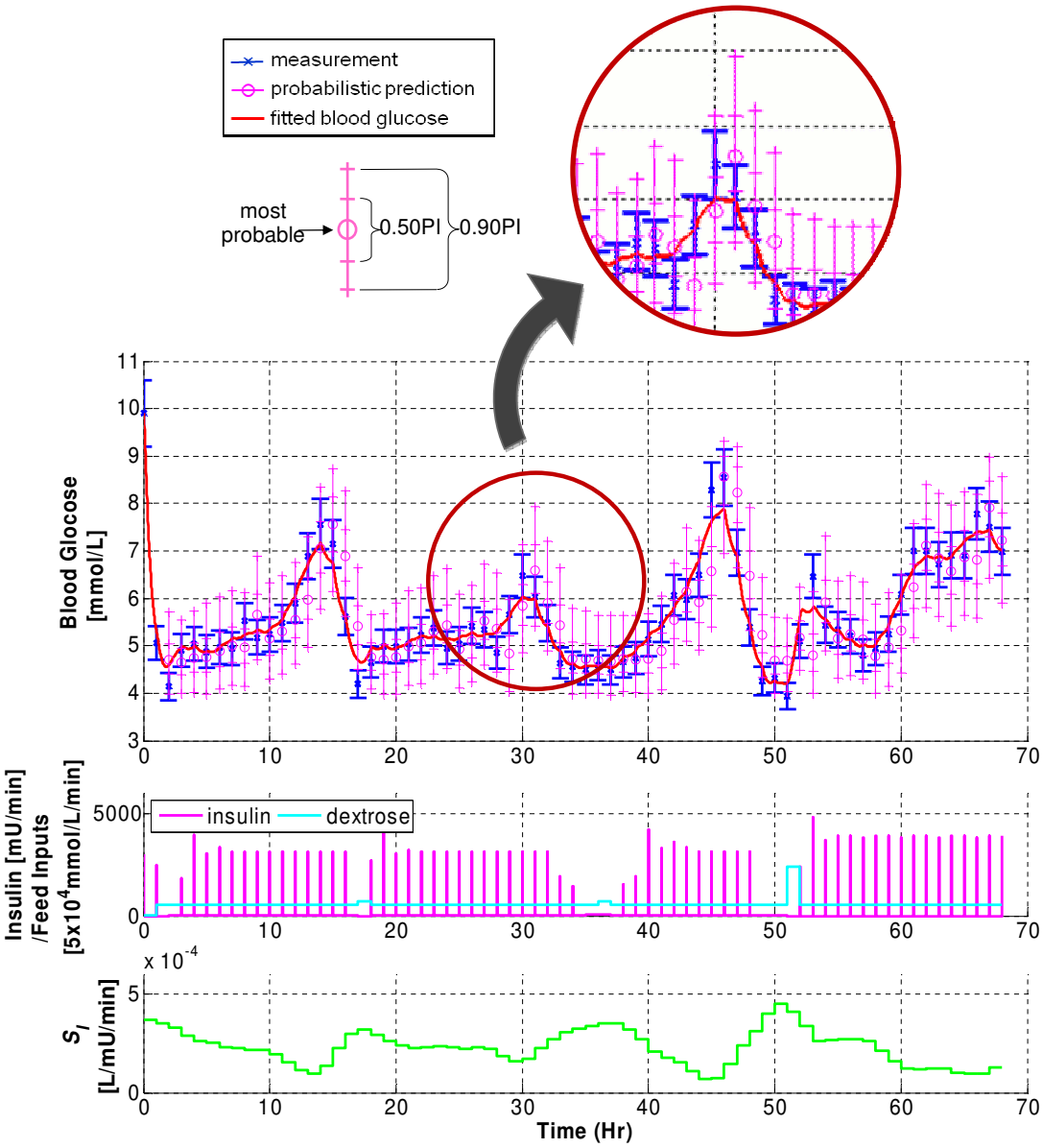

Figure 7.1 Example of a virtual trial. The top panel displays the blood glucose evolution, where bold crosses are virtually generated blood glucose levels at one hour intervals, with thick bars indicating measurement error. The controller predicted blood glucose levels are shown in circles, with thin bars indicating their probability intervals. The middle panel shows the control intervention during the trial. The bottom panel is the controller fitted insulin sensitivity, $S_I{}'$, which closely follows the virtual S_I profile (not shown) generated from the stochastic model.

prior hour. Control interventions are determined hourly and shown in the middle panel, producing probability median values and intervals in blood glucose levels shown as circles with bars in the top panel. In this virtual trial example, the probabilistic predictions accurately capture the evolution of blood glucose levels, as shown by the measurements falling well within the probability intervals in almost all cases.

The average fractions of virtual trial blood glucose levels within the equal-tailed 0.90 and inter-quartile probability intervals for each patient are shown in Figure 7.2 and approximately follow the logistic distribution. The logistic mean of percentage blood glucose levels within the equal-tailed 0.90 and inter-quartile probability interval are 87.0% and 45.7% respectively. These results are in good general agreement with the stochastic model cross validation results in Table 6.5 in Section 6.4. These per patient results also show the overall validity in total, as well as over all virtual patients, with very few outlying virtual patients.

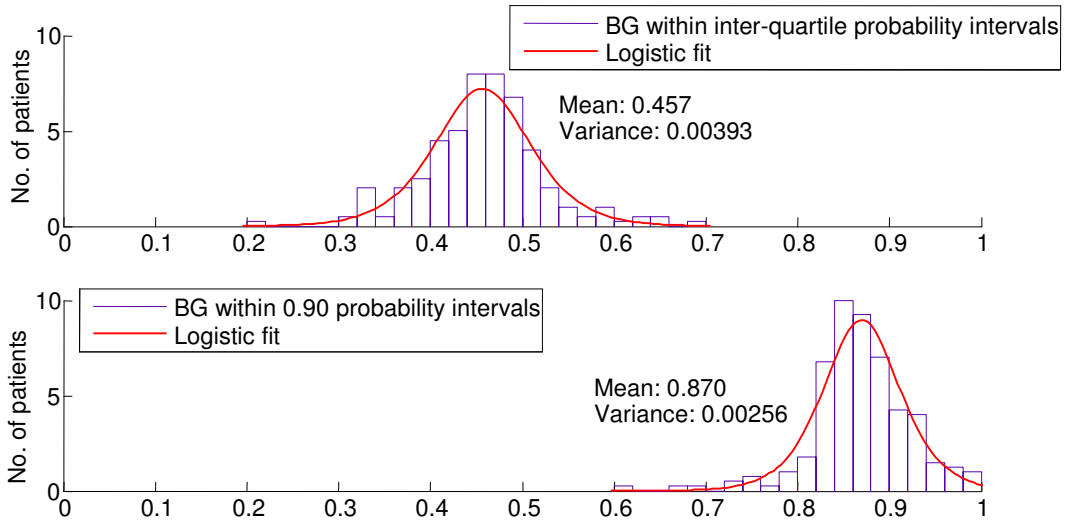

Figure 7.2 Virtual trial probability interval analysis per patient (N=200) for the IQR and 0.90 intervals. The ideal theoretical result is having one spike at 0.5 on the top panel and one spike at 0.9 on the bottom panel.

A few trials in Figure 7.2 have comparatively lower percentage of blood glucose levels within the corresponding probability intervals. These trials are all significantly shorter in length. Consequently, a small number of blood glucose levels outside of the probability intervals are reported as higher percentages of the total for that trial, leading to the outliers seen in Figure 7.2.

Figure 7.3 illustrates how shorter trials can produce outliers, where most variability has disappeared after 50–75 hours. This behaviour might indicate an increasing stabilised patient condition, or at least glycemia, under long term, tight glycemic control with little variability in glycemic level. It also shows how, as the length of the trial increases, the 0.90 and inter-quartile probability intervals are both slightly conservative estimates by 2–4%. This latter result is also evident in the median values of Figure 7.2, as well as the cross validation results in Section 6.4.

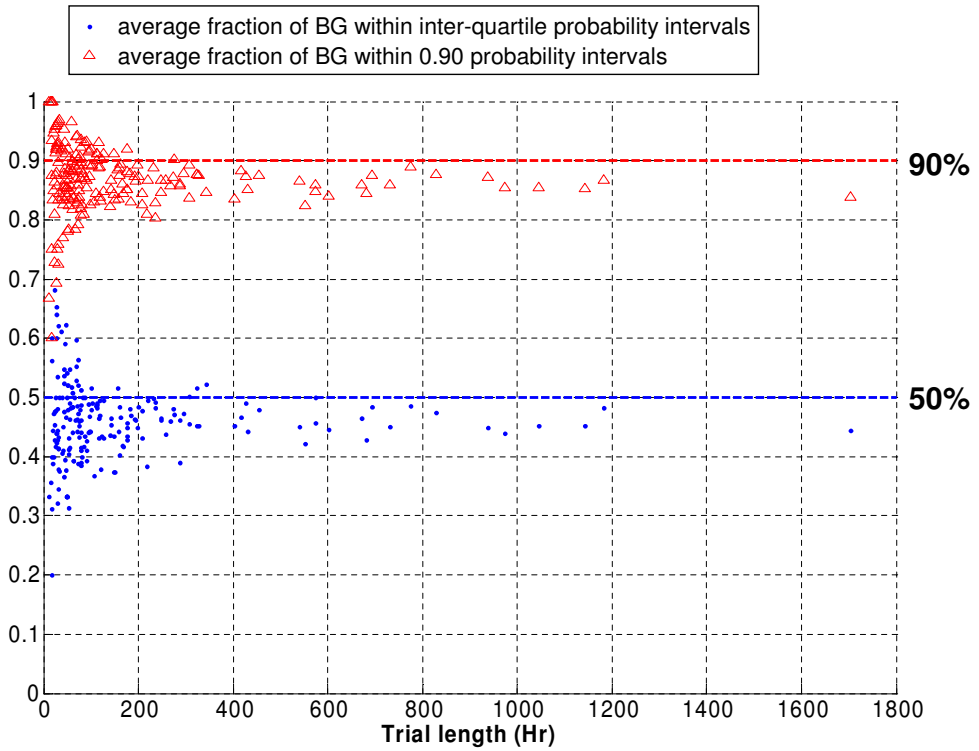

Figure 7.3 Virtual trial length versus probability interval accuracy (N=200). Each data point represents the average fraction of blood glucose levels within either the IQR or the 0.90 interval for a virtual trial.

The control algorithm used to run these virtual trials targets the blood glucose probability density medians at the desired controlled levels. The controller specified interventions should therefore theoretically result in the probabilistic median blood glucose level being at the chosen level one hour after implementation. The distribution of virtual trial blood glucose measurement deviations (percentage value) from the probability density medians is shown in Figure 7.4. The mean per patient average deviation is 8.84%, which compares well to the normally distributed random measurement error of 7–12% [Arkray, 2001]. The outliers in Figure 7.4 are again associated with shorter trial length.

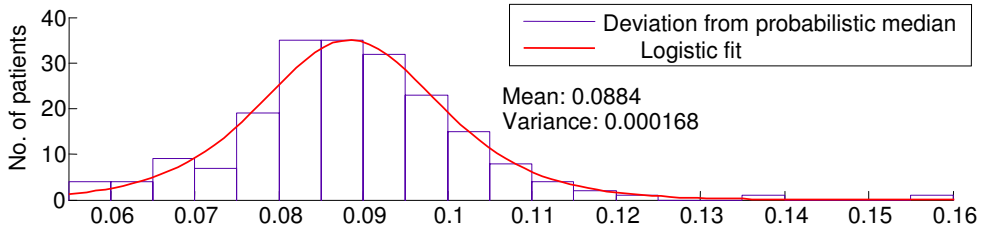

Figure 7.4 Percentage deviation of virtual trial blood glucose levels from probabilistic medians

Examining the signed blood glucose deviations from probabilistic medians, 58% are negative. This result suggests that a slightly higher density may be concentrated at higher S_I in the probability density functions. For future work, this blood glucose deviation can perhaps be "corrected" for in the control algorithm by targeting a percentile higher than the 50^{th}, for example the 58^{th} percentile, until the deviation is minimised. Such an approach might further improve the targeting accuracy of this controller. Similar manipulation might also be carried out to "correct" or optimise the accuracy of the probability intervals.

7.4 Validation of Virtual Trial Results Against Clinical SPRINT Results

The virtual trials presented used the stochastic model to aid glycemic control. This stochastic model-based glycemic controller is compared to the actual clinical SPRINT trial results [Chase et al., 2006a; Lonergan et al., 2006a] to assess the stochastic model-based controller performance. Simulated SPRINT trials were also performed on the same virtual cohort as a validation of the model's ability to create a virtual trial. The results are summarised in Table 7.1. A similar comparison of blood glucose measurements can be seen in the cumulative distributions in Figure 7.5.

The simulated SPRINT results compares well with the clinical results. This result is expected as the stochastic model used to generate the virtual cohort was created using clinical SPRINT data. Under the stochastic model-based glycemic controller, the virtual patients' blood glucose levels are shown to be more tightly controlled, with a lower mean controlled blood glucose level (5.5 v.s 5.9 and

Table 7.1 Virtual trial results compared to SPRINT (Data are expressed as median [5^{th}–95^{th} percentile range] as appropriate)

	Clinical SPRINT	Simulated SPRINT	Virtual Trials	
Overall data				
Number of patients	165	200	200	
Hours of control	23,324	33,889	33,889	hours
Total *BG* measurements	15,874	26,721	34,089	
BG mean*	5.9 [4.1–8.3]	5.7 [4.2–7.9]	5.5 [3.6–7.8]	mmol/L
BG standard deviation*	1.3	1.2	1.3	mmol/L
Percentage between 4–6.1 mmol/L	61%	57%	72%	
Percentage between 4–7.0 mmol/L	82%	81%	82%	
Percentage between 4–7.75 mmol/L	89%	92%	87%	
Percentage < 4 mmol/L	3.3%	3.1%	4.5%	
Percentage < 2.5 mmol/L	0.1%	0.2%	0.02%	
Per-patient data				
Hours of control	95 [12–447]	79 [20–688]	79 [20–688]	hours
Number of measurements	68 [10–271]	66 [17–530]	80 [21–689]	
BG mean*	5.9 [5.0–7.4]	5.8 [5.3–6.3]	5.3 [4.6–7.5]	mmol/L
BG standard deviation*	1.1 [0.7–2.3]	1.2 [0.7–1.6]	1.0 [0.5–2.1]	mmol/L
Median hourly insulin	2.5 [1.3–4.1]	2.6 [1.8–3.2]	3.2 [1.3–4.4]	U
Median nutrition† rate	37.5 [0–80.3]	39.6 [18.6–62.0]	28.2 [18.1–42.9]	ml/hr
(assuming 1.06 cal/ml [Novartis, 2005])	954 [0–2043]	1006 [474–1577]	717 [4610–1093]	cal/day
Median percentage of goal feed	52.7% [29.7–70.3%]	63.6% [39.1–78.5%]	38.4% [29.3–67.6%]	

*Lognormal distribution
†RESOURCE® Diabetic

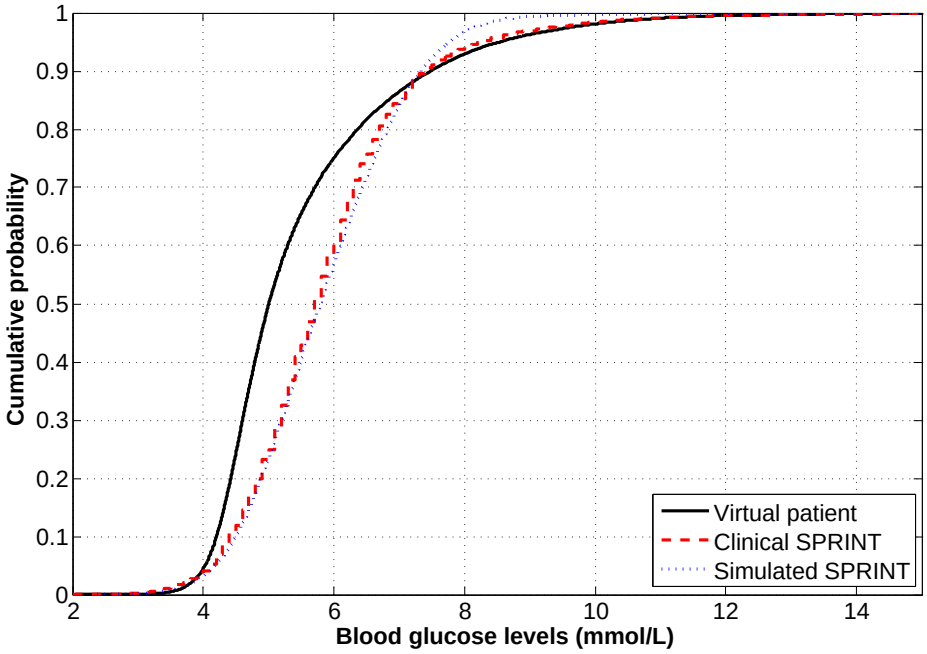

Figure 7.5 All blood glucose measurement distribution comparison between virtual trials under the stochastic model assisted controller presented and the clinical and simulated SPRINT results

5.7 mmol/L). More precisely, the percentage of blood glucose levels within the 4–6 mmol/L range increases from 61% for the clinical SPRINT result, or 57% for the simulated SPRINT result, to 72% in Table 7.1. This result shows that the stochastic targeting controller can more specifically maintain the glycemic levels. This is a very significant difference as tighter control has been shown to imply a better mortality outcome [Chase et al., 2007].

Again, the control quality in terms of controlled mean blood glucose levels and variance for each patient is associated with trial length. Shorter trial length tends to give a sparser distribution of controlled blood glucose levels and thus greater variance. This result was also seen clinically in SPRINT where the cohort with length of stay <3 days had greater glycemic variability.

In Figure 7.5 and Table 7.1, the percentage of blood glucose levels below 4 mmol/L is slightly increased from 3.3% or 3.1% to 4.5%. However, the percentage below 2.5 mmol/L decreased to effectively zero from 0.1% or 0.2%. The percentage of blood glucose values lower than 4 mmol/L that still exists can easily be reduced in the controller by setting a higher limit on the percentile in Rule 1 of

the control protocol, and/or by increasing the minimum target from 4.5 mmol/L to 4.8–5.0 mmol/L (Rule 5).

7.5 Summary

"Virtual patients" created from the stochastic model reflect clinical observed ICU patient dynamics, and present a platform to experiment different clinical control protocols with a probabilistic knowledge based on clinically observed evolving dynamics. Simulated control inputs can be evaluated on realistic virtual patient dynamics driven by the S_I profiles.

The virtual trials performed in this chapter show that a computerised stochastically targeted control can outperform a simplified version of the same basic insulin and nutrition control protocol, demonstrating further benefits of stochastic modelling and/or computer control in general. Future control protocol development enabled with virtual patient simulations has great potential in bringing better glycemic control with minimal labour input in critical care settings. In addition, applying the developed stochastic modelling to other patient groups can eventually extend glycemic control benefits outside ICU, down the control environment pyramid of 1.2 in Chapter 1.

Chapter 8

Conclusions

The work in this thesis presents a complete system for stochastic, model-based tight glycemic management in the critical care environment. The system includes four important components:

1. A valid control-applicable physiological system model
2. A novel, low-computation integral-based convex parameter identification method
3. A stochastic model of insulin sensitivity variation in the critically ill to aid prediction and control
4. An insulin and nutrition based glycemic control protocol utilising all 3 elements above to optimise glycemic control

This work is initiated to reduce the risk and harm of hyperglycemia, and to reduce the health care burden of hyperglycemia management in intensive care units. The prevalence of hyperglycemia in critical care has a significant impact on patient mortality and outcome, as well as health care cost and clinical effort. Recent studies have shown that a 17–45% reduction in mortality can be gained if tight glucose regulation is achieved to average levels from 6.1–7.75 mmol/L [Van den Berghe et al., 2001, 2003; Krinsley, 2003b, 2004]. Significantly reductions in other negative clinical outcomes can also be reaped. However, it often comes at a cost of significant clinical effort for an often mixed return. The secondary goal of this research was to enable reliable and consistent tight control with minimum clinical effort and (probabilistically) guaranteed results. Finally,

with the growing concern of the global diabetes epidemic, effective glycemic management solutions may eventually be extended to the wider diabetic population.

Traditional ad-hoc protocols often result in vicious cycles of hyper- and/or hypoglycemia. The highly dynamic characteristics of critically ill patients present a particularly difficult challenge. Given the range of sensor technology available, model-based predictive glycemic control has gotten more attention in recent years. Model-based glycemic control offers significant advantages over traditional ad-hoc protocols, which includes:

- It is accurate and adaptable to different patients
- It is adaptable to evolving critical illness
- It provides systematic glycemic reduction or regulation
- It will perform to specifically designed performance criteria
- It can deliver predictions of intervention outcomes
- It ensures better patient safety, particularly against hypoglycemia

These advantages, particularly the last two, promise more intelligent and reliable glycemic control solutions over other methods.

The physiological model presented in this thesis is robust, adaptable to patient specific condition, and most importantly, clinically validated and applicable. The model features an interstitial compartment for insulin storage to account for the delay between insulin secretion, or infusion, and utilization. Saturation dynamics reflect plasma insulin pooling and saturable interstitial insulin effect, addressing several shortcomings seen in the Minimal Model for clinical control applications.

This model was verified using critical care patient data, is robust to different clinical interventions, and accurately captures clinical observations. Overall, it represents a balanced tradeoff of complexity and non-linearity versus simplicity with respect to other models, which span a range of these tradeoffs.

The integral-based parameter identification method presented in this thesis enables fast and accurate identification of patient parameters. The integral fitting method is ∼1,000+ times faster than traditional non-linear and non-convex fitting methods. This difference in convexity and computational effort is important given the typically non-linear, non-convex dynamic systems of glucose-insulin regulatory system models. In particular, it does not require extensive iterations, nor multiple starting points to ensure accurate, optimal solutions. The most critical patient specific parameter for glycemic control was identified as the insulin sensitivity parameter, S_I, with the endogenous glucose removal parameter, p_G, being the second most critical patient specific parameter but also effectively constant. Sensitivity studies on other parameters indicate the adequacy of adapting generic population values.

Insulin sensitivity is seen to exhibit significant variation over time, reflecting the highly dynamic critical care patients. Some of this variability is due to the highly variable condition of critical care patients, characterised by large variations in the level of counter-regulatory hormones present and hence in effective insulin sensitivity. In addition, drug therapies such as beta-blockers or vaso-active drugs can also have a significant impact on effective insulin sensitivity. Overall, insulin sensitivity is shown to be a highly variable parameter in this population that drives the glycemia of the critically ill patient.

The physiological model and the integral-based parameter identification method were validated clinically in glycemic control trials in the ICU [Chase et al., 2005b,c; Wong et al., 2006a,b]. These trials followed model predictive control protocols, where the controller determined insulin and/or nutrition interventions based on prediction into the future glycemia. The model and the fitting method were verified to be clinically effective and accurate for glycemic control applications. It was also concluded that utilising both insulin and nutrition delivers the best glycemic management. Nutritional adjustment provides a means to regulate glycemic levels even in the presence of insulin resistant and/or insulin effect saturation.

While these methods achieved good clinical predictive accuracy, there were also occasions where significant changes in insulin sensitivity were encountered. Therefore, further understanding of the stochastic behaviour of patient specific parameters, particularly S_I, was investigated to further aid controller predictive

performance. A stochastic model of S_I behavior for ICU was thus developed as the major focus and contribution of this thesis.

The S_I stochastic model can define the probability density functions of blood glucose levels one hour following a known glycemic control intervention. It thus enables likelihood-based clinical intervention decision support. Clinicians can have more confidence in implementing interventions, and avoid hypoglycemia in particular. In addition, the stochastic model ascribes the difference between the targeted blood glucose level and the actual resulting patient blood glucose level in terms of the expected and the wider ranges of patient variation. Thus, this approach effectively differentiates the hour to hour changes in patient condition from model or measurement errors. Essentially, the stochastic model can better delineate model error and patient variability in assessing control efficacy.

The stochastic model was created with a 2-dimensional kernel density estimation method. This method allows the Markovian S_I stochastic model capturing the essence of clinically observed variation. Therefore, this model developed using ICU data specifically reflects critically ill patients' insulin sensitivity dynamics.

Two stochastic insulin sensitivity models were created using two different critically ill cohorts. The initial model was created from 18 retrospective study patients, whose data was collected 3–4 hourly, totalling 1,277 hours of data. The second model was created using 165 SPRINT trial patients, whose data was collected primarily hourly, and occasionally 2 hourly, totalling 23,324 control hours. The second model has more complex dynamics, possibly because of the much denser data available in its creation. However, both models gave largely similar and similarly accurate probability interval prediction when tested on clinical SPRINT trial data. The probability interval prediction from both models are slightly conservative, but accurately capture the cohort. For assisting model-based predictive glycemic control, the wider probability interval in the higher dynamic model provides a more conservative, therefore safer, prediction based intervention advice than the initial model.

It is also shown that "Virtual patients" created using the stochastic model can reflect clinically observed ICU patient dynamics. They thus create a platform to experiment with different clinical control protocols using a probabilistic knowledge based on clinically observed evolving dynamics. Simulated control inputs

can then be evaluated on realistic, validated virtual patient dynamics driven by the S_I profiles.

The virtual trial results reported in Chapter 7 show that a computerised stochastically targeted control can outperform a simplified version of the same basic insulin and nutrition control protocol. This result further demonstrates the benefits of stochastic modelling to aid control decision making, as well as computer control of hyperglycemia in general. Future control protocol development enabled with virtual patient simulations has great potential in bringing better glycemic control with minimal labour input in critical care settings. In addition, applying the developed stochastic modelling to other patient groups can eventually extend glycemic control benefits outside the ICU, extending these solutions to wider populations suffering from diabetes.

In summary, the glycemic control system presented in this thesis has a strong focus on clinical control feasibility and patient safety. The system has been tested through 4 stages of clinical trials in the ICU. The stochastic insulin sensitivity variation model has yet to be implemented in clinical trials. However, it has been validated against a wealth of clinical data to ensure its ability to capture patient variation. This stochastic model can thus help deliver more intelligible glycemic control, and promise better patient safety. The overall work presents a novel, knowledgeable contribution to solving the critical care glycemic control problem. Furthermore, its methods and approach may be readily generalised.

Chapter 9

Future Avenues

The work in this thesis presents a glycemic control system for critical care environments. The system is effective and novel, with a pronounced focus on clinical control feasibility and patient safety. This work thus addresses the main requirements for glycemic control in the ICU. However, it is also readily generalised in method, mathematics and approach to wider situations and similar problems, It thus opens many doors to other areas of applications that may have significant potential.

9.1 Further Glycemic Control Protocol Experimentation using Virtual Patients

Chapter 7 demonstrates the power of virtual patients in permitting fast and safe development of control protocols for glycemic control and broader drug delivery problems. Virtual patients can create realistic virtual cohorts that are statistically indifferent to real clinical cohorts. The control algorithm presented in Chapter 7 is only an example of one possible algorithm. Many other control algorithms are yet to be tested and compared for this glycemic control problem.

Currently, it is difficult to assess the performance between protocols from different research studies. First of all, the patient cohort is variable. Second, different groups measure controller performance with different metrics. With "virtual patients", this difficulty in objectively assessing protocol performance can be resolved. With decades of research in the broader glycemic control field, comparisons and experiments can be performed amongst the vast range of con-

trol theories. For example, the long studied proportional-derivative (PD) and proportional-integral-derivative (PID) controllers [e.g. Chee et al., 2003b; Steil et al., 2004] can be experimented with different gains, and objectively compared without the variability in small clinical studies over different cohorts. The options are almost literally endless.

As a further example, the SPRINT study results show that a very simplified, easy to use look-up table protocol can deliver very similar performance to the computerised predecessor it mimics. Therefore, it is not impossible to further fine tune the protocol to have it achieving closer performance to the computerised version by using virtual patients. Overall, the concept of developing a desired protocol and then systematically reducing it to a simpler form followed by further fine tuning, can be done with ease at each step using virtual patients.

In summary, protocol experimentations on virtual patients can lead to improvements in the likelihood of a particular trial producing positive results. In addition, this benefit can also be generalised to other hospitals or areas of medical treatment.

9.2 Investigation of Stochastic Behaviours in Different Critical Care Patient Groups

The stochastic models presented in this thesis are created using general ICU patient data. This data may be readily broken down into different patient groups by factors such as age, gender, APACHE II score, septic or non-septic diagnosis, trauma or non-trauma. Given enough patients to define each group well, this breakdown will perhaps isolate some particular characteristics of a specific patient group in the resulting stochastic model. Otherwise, it can help by confirming that insulin sensitivity variation, as modelled, is generic across critically ill patients.

If this study results in different stochastic models for different patient cohorts, it can further help developing different protocols for different patient groups. Glycemic management could then become even more patient specific. The overall result would be more certainty and better tailored control.

9.3 Computerised Protocol and Graphical User Interface

The clinical results from SPRINT show that the ease of use of the SPRINT look-up wheels significantly contribute to its large-scale adoption by clinical staff and effective implementation. The nursing staff at the Christchurch Hospital ICU favour SPRINT over other protocols for its ready adaptability to the ICU environment. However, deviations from protocols can not be accounted for. Thus, any deviation presents an interruption to SPRINT. These deviations include clinician prescribed change in infusion, surgeries, medical examinations, all of which are common practice in the ICU.

As computer power advances, hospitals are growingly adopting computerised systems at various levels in their practice. These computerised systems can synchronise and manage patient data, as well as being increasingly used for various clinical decision support systems. One major advantage of such a computerised system is that it can be patient specific and account for different aspects concerning their treatment. Specifically speaking of the glycemic management problem, deviations from any designed protocol can be managed. Thus, the consequent recovery to the designed protocol and control goals can be faster utilising the computational power.

Therefore, a computerised protocol, implemented through an easily used graphical user interface, could be designed to fit into the busy ICU environment. The graphical user interface should definitely satisfy the following requirements to ensure ready adoption and uptake:

- Clear in its purpose — blood glucose control
- Clearly display the current patient blood glucose level
- Accept deviations from the protocol at any time
- Advise on data collection times and requirements
- Advise on control interventions and estimated trajectories
- Provide for audit of glycemic control and compliance

The design process of the graphical user interface layout should also include consultation to promote clarity and user-friendliness without hindering efficacy.

9.4 Optimising Glucose Sensor Usage and Frequency

The work presented in this thesis used pin-stick bedside test kits to measure blood glucose levels. These test kits are currently the standard sensors in most, if not all, ICUs, as well as for most ambulatory diabetic individuals. They offer rapid results and comparatively well accepted accuracy. However, measuring with these sensors requires pricking extremities, or the presence of an arterial canula for drawing blood. Thus, the feasible measuring frequency is not higher than once every 1–2 hours, as any higher frequency starts to interfere with ICU labour requirements.

The insulin sensitivity stochastic models reveal that the majority of the S_I variation tends to be mild, and can be accounted for with great certainty (the lower left corners of Figures 5.5 and 6.2. Therefore, the allowable or optimal measuring intervals can be explored using virtual patient simulation. SPRINT has already applied the concept that stable patients require less monitoring of their blood glucose levels. Further simulation studies can lead to more knowledgable determination of measuring frequency and control quality, including the potential for customised and variable sampling based on the evolution of patient condition.

Finally, emerging continuous glucose sensors have long been the hoped-for ideal for control applications. However, these sensors do not provide satisfactory accuracy to be directly applied into control systems. Thus, advanced signal processing is certainly an area worthy of research, to better utilise the current technology until better accuracy can be delivered by these sensors. The stochastic model developed here can be integrated with these studies to optimise the integration of sensor and control protocol with no loss of control performance.

9.5 Clinical Trials and Data Audit

All simulation work eventually should lead to clinical testing to realistically justify the performance of the developed protocol. Clinical testing will also help strengthen the protocols. It is this systematic and calculated trial and errors process that will eventually perfect any such control solution.

The first set of clinical testing should be the implementation of the stochastic models developed in this thesis. This will help verifying the control applicability of the yet to be fully clinically validated work in this thesis. From the results, any shortcoming can be identified and improved as required.

9.6 Extension to Other Glycemic Control Problems

The work in this thesis presents initial successful glycemic management in the ICUs. Sharing similar glucose-insulin dynamics with the ICU glycemic control problem, the work presented here can act as a starting point for other environments with glycemic control problems.

Critical care units present a highly controlled environment where the control system's inputs and outputs are more easily accounted for. Extending the glycemic control system from this research to other glycemic control problems will require re-evaluation of the physiological model used in this thesis. Variables that account for uncertainties outside ICUs will need to be added. Some patient dynamics such as endogenous insulin and/or glucose production will also need to be reassessed.

To start, hospital wards, such as cardiac ICUs and neonatal ICUs that share similarities to the general ICU, can probably more readily adapt the control system developed in this thesis. Eventually, the research in this thesis can work its way down the control environment pyramid of Figure 1.2 in Chapter 1 to ambulatory diabetic individuals.

9.7 Extension to Other Pharmacokinetic Drug Delivery Problems

Many human pharmacodynamic systems share similar characteristics with the glucose-insulin regulatory system. Therefore, it is possible that the same control system development presented in this thesis can apply to other pharmacodynamic control problems. In particular, the application of stochastic models can help gaining insights into critical system parameters. This will lead to an overall better understanding and appreciation to the problem presented. Whether the probability interval assisted decision support concept will be applicable or not, the stochastic model will provide better knowledge into the pharmacodynamic system's behaviour. At least, the stochastic model will act as a patient simulator, enabling faster and safer protocol developments.

Appendix A

Local S_I Data Variance

In the 2-dimensional kernel estimation method used for building the glucose-insulin model (Equations (2.9)–(2.13)) parameter stochastic models, the form of the kernel chosen is the Gaussian kernel, ρ, as defined in Equation (5.4). The variance of the kernel depends on the local data density such that the shape of the kernel is optimised to produce smooth approximation of the true data behaviour. To define the local data density, standard orthonormalisation is performed. Let $x = S_{In}$ and $y = S_{In+1}$, $n = 1, 2, \ldots, k$, totalling a data set of k samples. Both x and y are column vectors. The orthonormalisation steps are as follows.

1. Solve for the covariance of $[x, y]$.

$$C = \mathbf{cov}\left([x, y]\right) \tag{A.1}$$

where

$$C(1,1) = \sum_{i}^{k} \frac{(x_i - \bar{x})^2}{k} \tag{A.2}$$

$$C(2,2) = \sum_{i}^{k} \frac{(y_i - \bar{y})^2}{k} \tag{A.3}$$

$$C(1,2) = C(2,1) = \sum_{i}^{k} \frac{(x_i - \bar{x})(y_i - \bar{y})}{k} \tag{A.4}$$

2. Perform a Cholesky factorisation on C.

$$C = RR^T \tag{A.5}$$

3. Calculate the transformation matrix A.

$$A = (R^T)^{-1} \tag{A.6}$$

4. Centre the samples and perform a space transformation with A.

$$\hat{x} = x - \bar{x} \tag{A.7}$$

$$\hat{y} = y - \bar{y} \tag{A.8}$$

$$[\tilde{x}\ \tilde{y}] = A \cdot [\hat{x}\ \hat{y}] \tag{A.9}$$

The 18-patient cohort data samples before and after orthonormalisation are shown in Figure A.1.

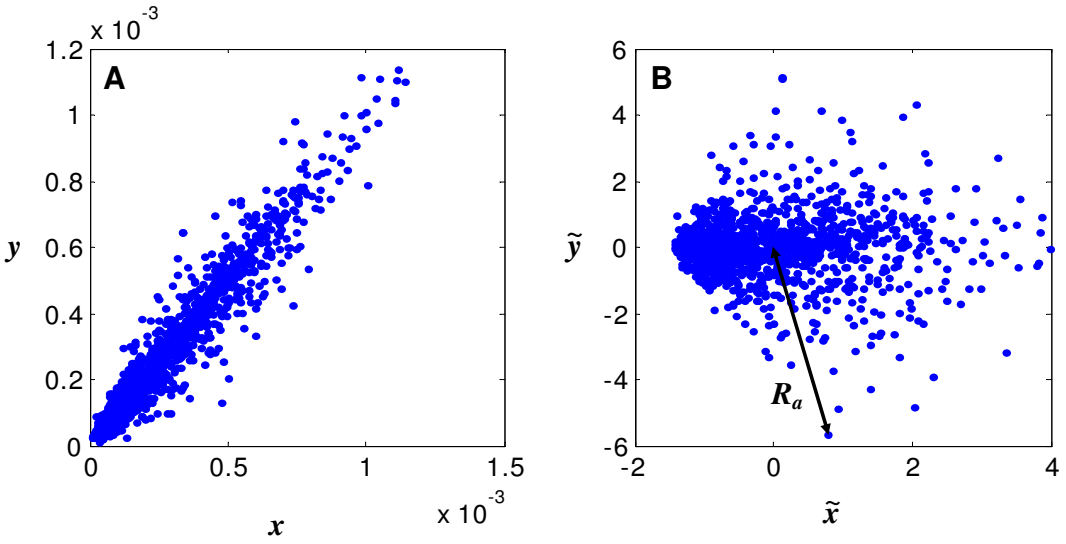

Figure A.1 18-patient cohort data sample space orthonormalisation. Panel A is the original space and panel B is the orthonormalised space.

5. Define the spread of the samples in the transformed space by calculating the maximum distance between the furthest sample and the origin. (Also see Figure A.1, panel B).

$$R_a = \max\left(\sqrt{\tilde{x}^2 + \tilde{y}^2}\right) \tag{A.10}$$

6. Calculate the variance σ_x and σ_y.

$$S_x = \min\left(\text{std}(x), \frac{\text{IQR}(x)}{1.348}\right) \tag{A.11}$$

$$S_y = \min\left(\text{std}(y), \frac{\text{IQR}(y)}{1.348}\right) \tag{A.12}$$

$$\sigma_x = S_x \left(m R_a^2 k^{1/3}\right)^{-1/6} \tag{A.13}$$

$$\sigma_y = S_y \left(m R_a^2 k^{1/3}\right)^{-1/6} \tag{A.14}$$

where $m =$ the number of samples within a radius of $k^{-1/6}$ from corresponding entries of $[\tilde{x}, \tilde{y}]$.

References

Abumrad, N. N., Cherrington, A. D., Williams, P. E., Lacy, W. W., and Rabin, D. (1982). Absorption and disposition of a glucose-load in the conscious dog. *American Journal of Physiology*, 242(6):E398–E406.

Ackerman, E., Gatewood, L. C., Rosevear, J. W., and Molnar, G. D. (1965). Model studies of blood-glucose regulation. *Bull. Math. Biophys.*, 27(Suppl.):21–37.

ADA (American Diabetes Association) (1998). Economic consequences of diabetes mellitus in the U.S. in 1997. *Diabetes Care*, 21(2):296–309.

ADA (American Diabetes Association) (2002). The prevention or delay of type 2 diabetes. *Diabetes Care*, 25(4):742–9.

Ahrens, C. L., Barletta, J. F., Kanji, S., Tyburski, J. G., Wilson, R. F., Janisse, J. J., and Devlin, J. W. (2005). Effect of low-calorie parenteral nutrition on the incidence and severity of hyperglycemia in surgical patients: a randomized, controlled trial. *Crit Care Med*, 33(11):2507–12.

Alberti, K. G. and Zimmet, P. Z. (1998). Definition, diagnosis and classification of diabetes mellitus and its complications. Part 1: diagnosis and classification of diabetes mellitus provisional report of a WHO consultation. *Diabet Med*, 15(7):539–53.

Albisser, A. M., Leibel, B. S., Ewart, T. G., Davidovac, Z., Botz, C. K., Zingg, W., Schipper, H., and Gander, R. (1974). Clinical control of diabetes by the artificial pancreas. *Diabetes*, 23(5):397–404.

Amiel, S. A., Tamborlane, W. V., Simonson, D. C., and Sherwin, R. S. (1987). Defective glucose counterregulation after strict glycemic control of insulin-dependent diabetes mellitus. *N Engl J Med*, 316(22):1376–1383.

Angus, D. C. and Abraham, E. (2005). Intensive insulin therapy in critical illness — when is evidence enough? *Am J Respir Crit Care Med*, 172(11):1358–9.

Arasaradnam, M. P., Morgan, L., Wright, J., and Gama, R. (2002). Diurnal variation in lipoprotein lipase activity. *Ann Clin Biochem*, 39(Pt 2):136–139.

Araujo-Vilar, D., Rega-Liste, C. A., Garcia-Estevez, D. A., Sarmiento-Escalona, F., Mosquera-Tallon, V., and Cabezas-Cerrato, J. (1998). Minimal model of glucose metabolism: modified equations and its application in the study of insulin sensitivity in obese subjects. *Diabetes Res Clin Pract*, 39(2):129–41.

Arkray (2001). Glucocard^{TM} test strip 2 data sheet.

Avogaro, A., Bristow, J. D., Bier, D. M., Cobelli, C., and Toffolo, G. (1989). Stable-label intravenous glucose tolerance test minimal model. *Diabetes*, 38(8):1048–1055.

Barrett-Connor, E. and Khaw, K. T. (1988). Diabetes mellitus: an independent risk factor for stroke? *Am J Epidemiol*, 128(1):116–123.

Basi, S., Pupim, L. B., Simmons, E. M., Sezer, M. T., Shyr, Y., Freedman, S., Chertow, G. M., Mehta, R. L., Paganini, E., Himmelfarb, J., and Ikizler, T. A. (2005). Insulin resistance in critically ill patients with acute renal failure. *American Journal of Physiology-Renal Physiology*, 289(2):F259–F264.

Basu, A., Basu, R., Shah, P., Vella, A., Johnson, C. M., Jensen, M., Nair, K. S., Schwenk, W. F., and Rizza, R. A. (2001). Type 2 diabetes impairs splanchnic uptake of glucose but does not alter intestinal glucose absorption during enteral glucose feeding — additional evidence for a defect in hepatic glucokinase activity. *Diabetes*, 50(6):1351–1362.

Basu, R., Basu, A., Johnson, C. M., Schwenk, W. F., and Rizza, R. A. (2004). Insulin dose-response curves for stimulation of splanchnic glucose uptake and suppression of endogenous glucose production differ in nondiabetic humans and are abnormal in people with type 2 diabetes. *Diabetes*, 53(8):2042–2050.

Beard, J. C., Bergman, R. N., Ward, W. K., and Porte, D. J. (1986). The insulin sensitivity index in nondiabetic man. correlation between clamp-derived and IVGTT-derived values. *Diabetes*, 35:362–9.

Bellomo, R. and Egi, M. (2005). Glycemic control in the intensive care unit: why we should wait for nice-sugar. *Mayo Clin Proc*, 80(12):1546–8.

Ben-Mahmud, B. M., Chan, W. H., Abdulahad, R. M., Datti, A., Orlacchio, A., Kohner, E. M., and Chibber, R. (2006). Clinical validation of a link between TNF-alpha and the glycosylation enzyme core 2 GlcNAc-T and the relationship of this link to diabetic retinopathy. 49(9):2185–2191.

Beneteau-Burnat, B., Bocque, M. C., Lorin, A., Martin, C., and Vaubourdolle, M. (2004). Evaluation of the blood gas analyzer gem premier 3000. *Clin Chem Lab Med*, 42(1):96–101.

Bergman, R. N., Finegood, D. T., and Ader, M. (1985). Assessment of insulin sensitivity in vivo. *Endocr Rev*, 6(1):45–86.

Bergman, R. N., Ider, Y. Z., Bowden, C. R., and Cobelli, C. (1979). Quantitative estimation of insulin sensitivity. *Am J Physiol*, 236(6):E667–77.

Bergman, R. N., Phillips, L. S., and Cobelli, C. (1981). Physiologic evaluation of factors controlling glucose tolerance in man: measurement of insulin sensitivity and beta-cell glucose sensitivity from the response to intravenous glucose. *J Clin Invest*, 68(6):1456–1467.

Bergman, R. N., Prager, R., Volund, A., and Olefsky, J. M. (1987). Equivalence of the insulin sensitivity index in man derived by the minimal model method and the euglycemic glucose clamp. *J Clin Invest*, 79(3):790–800.

Bettini, F., Caumo, A., and Cobelli, C. (1995). Minimal models in meal-like protocols: Simulation studies to assess precision and physiological plausibility of parameter estimates. In *17th Annual International Conference of the IEEE-EMBS*, volume 2, pages 1361–1362.

Bistrian, B. R. (2001). Hyperglycemia and infection: Which is the chicken and which is the egg? *J Parenter Enteral Nutr*, 25(4):180–181.

Bland, D. K., Fankhanel, Y., Langford, E., Lee, M., Lee, S. W., Maloney, C., Rogers, M., and Zimmerman, G. (2005). Intensive versus modified conventional control of blood glucose level in medical intensive care patients: a pilot study. *Am J Crit Care*, 14(5):370–6.

Bloomgarden, Z. T. (2003). Inflammation and insulin resistance. *Diabetes Care*, 26(6):1922–1926.

Bolli, G. B., Dimitriadis, G. D., Pehling, G. B., Baker, B. A., Haymond, M. W., Cryer, P. E., and Gerich, J. E. (1984). Abnormal glucose counterregulation

after subcutaneous insulin in insulin-dependent diabetes mellitus. *N Engl J Med*, 310(26):1706–1711.

Boyne, M. S., Silver, D. M., Kaplan, J., and Saudek, C. D. (2003). Timing of changes in interstitial and venous blood glucose measured with a continuous subcutaneous glucose sensor. *Diabetes*, 52(11):2790–4.

Branco, R. G., Garcia, P. C., Piva, J. P., Casartelli, C. H., Seibel, V., and Tasker, R. C. (2005). Glucose level and risk of mortality in pediatric septic shock. *Pediatr Crit Care Med*, 6(4):470–2.

Buhling, K. J., Henrich, W., Kjos, S. L., Siebert, G., Starr, E., Dreweck, C., Stein, U., and Dudenhausen, J. W. (2003). Comparison of point-of-care-testing glucose meters with standard laboratory measurement of the 50g-glucose-challenge test (GCT) during pregnancy. *Clin Biochem*, 36(5):333–7.

Butler, S. O., Btaiche, I. F., and Alaniz, C. (2005). Relationship between hyperglycemia and infection in critically ill patients. *Pharmacotherapy*, 25(7):963–76.

Callegari, T., Caumo, A., and Cobelli, C. (2002). Generalization of map estimation in SAAM II: Validation against ADAPT II in a glucose model case study. *Annals of Biomedical Engineering*, 30:961–968.

Capes, S. E., Hunt, D., Malmberg, K., and Gerstein, H. C. (2000). Stress hyperglycaemia and increased risk of death after myocardial infarction in patients with and without diabetes: a systematic overview. *Lancet*, 355(9206):773–778.

Carroll, K. F. and Nestel, P. J. (1973). Diurnal-variation in glucose-tolerance and in insulin-secretion in man. *Diabetes*, 22(5):333–348.

Carson, E. R. and Cobelli, C. (2001). *Modelling methodology for physiology and medicine*. Academic Press Series in Biomedical Engineering. Academic Press, San Diego.

Casella, G. and Berger, R. L. (2002). *Distributions of Functions of a Random Variable*. Duxbury, 2nd edition.

Caumo, A., Vicini, P., Zachwieja, J. J., Avogaro, A., Yarasheski, K., Bier, D. M., and Cobelli, C. (1999). Undermodeling affects minimal model indexes: insights from a two-compartment model. *Am J Physiol*, 276(6 Pt 1):E1171–1193.

CDC (Centers for Disease Control and Prevention) (2005). National diabetes fact sheet: general information and national estimates on diabetes in the United States, 2005. Technical report, U.S. Department of Health and Human Services, Centers for Disease Control and Prevention.

CDC (Centers for Disease Control and Prevention) (2006). Diabetes: Disabling, deadly, and on the rise — at a glance 2006. Technical report, U.S. Department of Health and Human Services, Centers for Disease Control and Prevention.

Chase, J., Shaw, G., Le Compte, A., Lee, D., Lonergan, T., Willacy, M., Wong, X., Lin, J., Lotz, T., and Hann, C. (2006a). Tight glycaemic control in critical care using insulin and nutrition — the SPRINT protocol. In Klonoff, D., editor, *6th Annual Diabetes Technology Meeting*, Atlanta, GA. Diabetes Technology Society.

Chase, J., Shaw, G. M., Wong, X. W., Lotz, T., Lin, J., and Hann, C. E. (2006b). Model-based glycaemic control in critical care — a review of the state of the possible. *Biomedical Signal Processing & Control*, 1(1):3–21.

Chase, J. G., Hann, C. E., Shaw, G. M., Wong, X. W., Lin, J., Lotz, T., Le Compte, A. J., and Lonergan, T. (2007). An overview of glycemic control in critical care — relating performance and clinical results. *Diabetes Society and Technology*, 1(1):82–91.

Chase, J. G., Lonergan, T., Le Compte, A., Willacy, M., Shaw, G. M., Wong, X. W., Lin, J., Lotz, T., and Hann, C. E. (2005a). Tight glucose control in critically ill patients using a specialized insulin-nutrition table. In *Proc. of the 12th International Conf on Biomedical Engineering (ICBME 2005)*, Singapore.

Chase, J. G., Shaw, G. M., Doran, C. V., Hudson, N. H., and Moorhead, K. T. (2003). Derivative weighted active insulin control algorithms and trials. In *IFAC Symposium*, pages 83–89, Melbourne, Australia.

Chase, J. G., Shaw, G. M., Lin, J., Doran, C. V., Bloomfield, M., Wake, G. C., Broughton, B., Hann, C., and Lotz, T. (2004). Impact of insulin-stimulated glucose removal saturation on dynamic modelling and control of hyperglycaemia. *International Journal of Intelligent Systems Technologies and Applications (IJISTA)*, 1(1/2):79–94.

Chase, J. G., Shaw, G. M., Lin, J., Doran, C. V., Hann, C., Lotz, T., Wake, G. C., and Broughton, B. (2005b). Targeted glycemic reduction in critical care using closed-loop control. *Diabetes Technol Ther*, 7(2):274–82.

Chase, J. G., Shaw, G. M., Lin, J., Doran, C. V., Hann, C., Robertson, M. B., Browne, P. M., Lotz, T., Wake, G. C., and Broughton, B. (2005c). Adaptive bolus-based targeted glucose regulation of hyperglycaemia in critical care. *Med Eng Phys*, 27(1):1–11.

Chee, F., Fernando, T., and van Heerden, P. V. (2003a). Closed-loop glucose control in critically ill patients using continuous glucose monitoring system (CGMS) in real time. *IEEE Trans Inf Technol Biomed*, 7(1):43–53.

Chee, F., Fernando, T. L., Savkin, A. V., and van Heeden, V. (2003b). Expert PID control system for blood glucose control in critically ill patients. *IEEE Trans Inf Technol Biomed*, 7(4):419–25.

Chen, E. T., Nichols, J. H., Duh, S. H., and Hortin, G. (2003). Performance evaluation of blood glucose monitoring devices. *Diabetes Technol Ther*, 5(5):749–68.

Christensen, D. (2001). Critical care: Sugar limit saves lives. *Science News*, 159(26):159.

Christiansen, C., Toft, P., Jorgensen, H. S., Andersen, S. K., and Tonnesen, E. (2004). Hyperglycaemia and mortality in critically ill patients — a prospective study. *Intensive Care Medicine*, 30(8):1685–1688.

Clarke, W. L. (2005). The original Clarke error grid analysis (EGA). *Diabetes Technol Ther*, 7(5):776–9.

Cobelli, C., Caumo, A., and Omenetto, M. (1999). Minimal model S_G overestimation and S_I underestimation: improved accuracy by a bayesian two-compartment model. *Am J Physiol*, 277(3 Pt 1):E481–488.

Cobelli, C., Toffolo, G., and Foster, D. M. (1992). Tracer-to-tracee ratio for analysis of stable isotope tracer data: link with radioactive kinetic formalism. *Am J Physiol*, 262(6 Pt 1):E968–75.

Consoli, A. (1992). Role of liver in pathophysiology of NIDDM. *Diabetes Care*, 15(3):430–441.

Coursin, D. B. and Murray, M. J. (2003). How sweet is euglycemia in critically ill patients? *Mayo Clin Proc*, 78(12):1460–2.

Cummins, A. J. (1952). Absorption of glucose and methionine from the human intestine. Influence of the glucose concentration in the blood and the intestinal lumen. *J. Clin. Invest.*, 31:928–937.

Dandona, P., Chaudhuri, A., Ghanim, H., and Mohanty, P. (2006). Anti-inflammatory effects of insulin and pro-inflammatory effects of glucose: relevance to the management of acute myocardial infarction and other acute coronary syndromes. *Rev Cardiovasc Med*, 7(Suppl 2):S25–34.

Das, U. N. (2003). Insulin in sepsis and septic shock. *J Assoc Physicians India*, 51:695–700.

DeFronzo, R. A., Tobin, J. D., and Andres, R. (1979). Glucose clamp technique: a method for quantifying insulin secretion and resistance. *Am J Physiol*, 237(3):E214–23.

Demers, J., Kane, M. P., Bakst, G., Busch, R. S., and Hamilton, R. A. (2003). Accuracy of home blood glucose monitors using forearm blood samples: Freestyle versus one touch ultra. *Am J Health Syst Pharm*, 60(11):1130–5.

Di Nardo, M. M., Korytkowski, M. T., and Siminerio, L. S. (2004). The importance of normoglycemia in critically ill patients. *Crit Care Nurs Q*, 27(2):126–34.

Dickerson, R. N. (2005). Hypocaloric feeding of obese patients in the intensive care unit. *Curr Opin Clin Nutr Metab Care*, 8(2):189–96.

Dickerson, R. N., Boschert, K. J., Kudsk, K. A., and Brown, R. O. (2002). Hypocaloric enteral tube feeding in critically ill obese patients. *Nutrition*, 18(3):241–6.

DirectNet, The Diabetes Research in Children Network Study Group (2004). Accuracy of the GlucoWatch G2 biographer and the continuous glucose monitoring system during hypoglycemia. *Diabetes Care*, 27(3):722–726.

DirectNet, The Diabetes Research in Children Network Study Group (2005). Accuracy of newer-generation home blood glucose meters in a Diabetes Research in Children Network (DirecNet) inpatient exercise study. *Diabetes Technol Ther*, 7(5):675–680.

Diringer, M. N. (2005). Improved outcome with aggressive treatment of hyperglycemia — hype or hope? *Neurology*, 64(8):1330–1331.

Doran, C. V. (2004). *Modelling and Control of Hyperglycemia in Critical Care Patients*. Masters of Engineering (ME) Thesis, University of Canterbury.

Doran, C. V., Chase, J. G., Shaw, G. M., Moorhead, K. T., and Hudson, N. H. (2004a). Automated insulin infusion trials in the intensive care unit. *Diabetes Technol Ther*, 6(2):155–65.

Doran, C. V., Hudson, N. H., Moorhead, K. T., Chase, J. G., Shaw, G. M., and Hann, C. E. (2004b). Derivative weighted active insulin control modelling and clinical trials for ICU patients. *Med Eng Phys*, 26(10):855–66.

Duckworth, W. C. and Kitabchi, A. E. (1981). Insulin metabolism and degradation. *Endocr Rev*, 2(2):210–33.

Duncan, G. E., Perri, M. G., Theriaque, D. W., Hutson, A. D., Eckel, R. H., and Stacpoole, P. W. (2003). Exercise training, without weight loss, increases insulin sensitivity and postheparin plasma lipase activity in previously sedentary adults. *Diabetes Care*, 26(3):557–562.

Dunn, T. C., Eastman, R. C., and Tamada, J. A. (2004). Rates of glucose change measured by blood glucose meter and the glucowatch biographer during day, night, and around mealtimes. *Diabetes Care*, 27(9):2161–5.

Elia, M., Ceriello, A., Laube, H., Sinclair, A. J., Engfer, M., and Stratton, R. J. (2005). Enteral nutritional support and use of diabetes-specific formulas for patients with diabetes: A systematic review and meta-analysis. *Diabetes Care*, 28(9):2267–79.

Ellemann, K., Thorsteinsson, B., Fugleberg, S., Feldt-Rasmussen, B., Andersen, O. O., Gronbaek, P., and Binder, C. (1987). Kinetics of insulin disappearance from plasma in cortisone-treated normal subjects. *Clin Endocrinol (Oxf)*, 26(5):623–628.

Esposito, K., Marfella, R., and Giugliano, D. (2003). Stress hyperglycemia, inflammation, and cardiovascular events. *Diabetes Care*, 26(5):1650–1651.

Ferrannini, E. and Cobelli, C. (1987a). The kinetics of insulin in man. I. General aspects. *Diabetes Metab Rev*, 3(2):335–63.

Ferrannini, E. and Cobelli, C. (1987b). The kinetics of insulin in man. II. Role of the liver. *Diabetes Metab Rev*, 3(2):365–97.

Ferrannini, E., Gastaldelli, A., Miyazaki, Y., Matsuda, M., Mari, A., and DeFronzo, R. A. (2005). Beta-cell function in subjects spanning the range from normal glucose tolerance to overt diabetes: a new analysis. *J Clin Endocrinol Metab*, 90(1):493–500.

Ferrannini, E. and Mari, A. (2004). Beta cell function and its relation to insulin action in humans: a critical appraisal. *Diabetologia*, 47(5):943–56.

Ferrannini, E., Simonson, D. C., Katz, L. D., Reichard, G., Bevilacqua, S., Barrett, E. J., Olsson, M., and Defronzo, R. A. (1988). The disposal of an oral glucose-load in patients with non-insulin-dependent diabetes. *Metabolism-Clinical and Experimental*, 37(1):79–85.

Finney, S. J., Zekveld, C., Elia, A., and Evans, T. W. (2003). Glucose control and mortality in critically ill patients. *J. American Medical Association*, 290(15):2041–2047.

Firth, R., Bell, P., Marsh, H., Hansel, I., and Rizza, R. (1985). Post-prandial hyperglycemia in patients with non-insulin dependent diabetes mellitus: role of hepatic and extrahepatic tissues. *J. Clin. Invest.*, 74:1525–1532.

Fischer, U., Salzsieder, E., Freyse, E. J., and Albrecht, G. (1990). Experimental validationof a glucose-insulin control model to simulate patterns in glucose turnover. *Comput. Methods Programs Biomed.*, 32:249–258.

Fischer, U., Schenk, W., Salzsieder, E., Albrecht, G., Abel, P., and Freyse, E. J. (1987). Does physiological blood glucose control require an adaptive strategy? *IEEE Trans Biomed Eng*, BME-34:575–82.

Frost, D. P., Srivastava, M. C., Jones, R. H., Nabarro, J. D., and Sonksen, P. H. (1973). The kinetics of insulin metabolism in diabetes mellitus. *Postgrad Med J*, 49:Suppl 7:949–54.

Furler, S. M., Kraegen, E. W., Smallwood, R. H., and Chisholm, D. J. (1985). Blood glucose control by intermittent loop closure in the basal mode: computer simulation studies with a diabetic model. *Diabetes Care*, 8(6):553–561.

Garg, S. K., Potts, R. O., Ackerman, N. R., Fermi, S. J., Tamada, J. A., and Chase, H. P. (1999). Correlation at fingerstick blood glucose measurements

with glucowatch biographer glucose results in young subjects with type 1 diabetes. *Diabetes Care*, 22(10):1708–1714.

Gilligan, B. C., Shults, M., Rhodes, R. K., Jacobs, P. G., Brauker, J. H., Pintar, T. J., and Updike, S. J. (2004). Feasibility of continuous long-term glucose monitoring from a subcutaneous glucose sensor in humans. *Diabetes Technol Ther*, 6(3):378–86.

Godje, O., Fuchs, A., Dewald, O., Fischlein, T., and Reichart, B. (1997). [on-site laboratory monitoring on the intensive care unit. Blood gas, electrolyte, glucose, hemoglobin and lactate determination with the CIBA Corning 865 Analysis System]. *Anasthesiol Intensivmed Notfallmed Schmerzther*, 32(9):549–56.

Goldberg, P. A., Siegel, M. D., Russell, R. R., Sherwin, R. S., Halickman, J. I., Cooper, D. A., Dziura, J. D., and Inzucchi, S. E. (2004a). Experience with the continuous glucose monitoring system in a medical intensive care unit. *Diabetes Technol Ther*, 6(3):339–47.

Goldberg, P. A., Siegel, M. D., Sherwin, R. S., Halickman, J. I., Lee, M., Bailey, V. A., Lee, S. L., Dziura, J. D., and Inzucchi, S. E. (2004b). Implementation of a safe and effective insulin infusion protocol in a medical intensive care unit. *Diabetes Care*, 27(2):461–7.

Gubern, C., Lopez-Bermejo, A., Biarnes, J., Vendrell, J., Ricart, W., and Fernandez-Real, J. M. (2006). Natural antibiotics and insulin sensitivity: the role of bactericidal/permeability-increasing protein. *Diabetes*, 55(1):216–24.

Guyton, A. C. and Hall, J. E. (1996). Insulin, glucagon, and diabetes mellitus. In *Textbook of Medical Physiology*, pages 971–983. W.B. Saunders Company, 9th edition.

Hann, C., Chase, J., and Shaw, G. (2006). Integral-based identification of patient specific parameters for a minimal cardiac model. *Computer Methods and Programs in Biomedicine*, 81(2):181–192.

Hann, C. E., Chase, J. G., Lin, J., Lotz, T., Doran, C. V., and Shaw, G. M. (2005). Integral-based parameter identification for long-term dynamic verification of a glucose-insulin system model. *Comput Methods Programs Biomed*, 77(3):259–70.

Hansen, T. K., Thiel, S., Wouters, P. J., Christiansen, J. S., and Van den Berghe, G. (2003). Intensive insulin therapy exerts antiinflammatory effects in critically ill patients and counteracts the adverse effect of low mannose-binding lectin levels. *The Journal of clinical endocrinology and metabolism*, 88(3):1082–8.

Hirsch, I. B. and Brownlee, M. (2005). Should minimal blood glucose variability become the gold standard of glycemic control? *J Diabetes Complications*, 19(3):178–81.

Holm, C., Horbrand, F., Mayr, M., von Donnersmarck, G. H., and Muhlbauer, W. (2004). Acute hyperglycaemia following thermal injury: friend or foe? *Resuscitation*, 60(1):71–7.

Hossain, P., Kawar, B., and El Nahas, M. (2007). Obesity and diabetes in the developing world — a growing challenge. *N Engl J Mmed*, 356:3.

Hovorka, R., Canonico, V., Chassin, L. J., Haueter, U., Massi-Benedetti, M., Federici, M. O., Pieber, T. R., Schaller, H. C., Schaupp, L., Vering, T., and Wilinska, M. E. (2004). Nonlinear model predictive control of glucose concentration in subjects with type 1 diabetes. *Physiological Measurement*, 25(4):905–920.

Hovorka, R., Chassin, L. J., and Wilinska, M. E. (2003). Virtual type 1 diabetic treated by CSII: Model description. In *WC2003*, Sydney, Australia.

Hovorka, R., Shojaee-Moradie, F., Carroll, P. V., Chassin, L. J., Gowrie, I. J., Jackson, N. C., Tudor, R. S., Umpleby, A. M., and Jones, R. H. (2002). Partitioning glucose distribution/transport, disposal, and endogenous production during IVGTT. *Am J Physiol Endocrinol Metab*, 282(5):E992–1007.

Hovorka, R. and Vicini, P. (2001). Parameter estimation. In Carson, E. and Cobelli, C., editors, *Modelling Methodology for Physiology and Medicine*, pages 107–151. Academic Press, London.

IDF (International Diabetes Federation) (2003). *Diabetes Atlas*. International Diabetes Federation,, Brussels, Belgium, 2nd edition.

Insel, P. A., Liljenquist, J. E., Tobin, J. D., Sherwin, R. S., Watkins, P., Andres, R., and Berman, M. (1975). Insulin control of glucose metabolism in man. *J Clin Invest*, 55(5):1057–66.

Iyer, P. U. (2002). Nutritional support in the critically ill child. *Indian J Pediatr*, 69(5):405–10.

Javid, P. J., Halwick, D. R., Betit, P., Thompson, J. E., Long, K., Zhang, Y., Jaksic, T., and Agus, M. S. (2005). The first use of live continuous glucose monitoring in patients on extracorporeal life support. *Diabetes Technol Ther*, 7(3):431–9.

Jeandidier, N. and Boullu-Sanchis, S. (2006). Hyperglycemia and acute illness. *Ann Endocrinol*, 67(3):224–32.

Jeremitsky, E., Omert, L. A., Dunham, C. M., Wilberger, J., and Rodriguez, A. (2005). The impact of hyperglycemia on patients with severe brain injury. *J Trauma*, 58(1):47–50.

Jeschke, M.G., D. K. and Herndon, D. (2004). Insulin treatment improves the systemic inflammatory reaction to severe trauma. *Annals of surgery*, 239(4):553–60.

Johnson, R. N. and Baker, J. R. (1998). Accuracy of devices used for self-monitoring of blood glucose. *Ann Clin Biochem*, 35(Pt1):68–74.

Johnson, R. N. and Baker, J. R. (1999). Analytical error of home glucose monitors: a comparison of 18 systems. *Ann Clin Biochem*, 36(Pt 1):72–9.

Katz, H., Butler, P., Homan, M., Zerman, A., Caumo, A., Cobelli, C., and Rizza, R. (1993). Hepatic and extrahepatic insulin action in humans: measurement in the absence of non-steady-state error. *Am J Physiol Endocrinol Metab.*, 264(27):E561–566.

Kim, H., Son, E., Kim, J., Choi, K., Kim, C., Shin, W., and Suh, O. (2003). Association of hyperglycemia and markers of hepatic dysfunction with dextrose infusion rates in Korean patients receiving total parenteral nutrition. *Am J Health Syst Pharm*, 60(17):1760–6.

King, H. (1999). Who and the international diabetes federation: regional partners. *Bull World Health Organ*, 77(12):954.

Kiwanuka, E., Barazzoni, R., and Tessari, P. (2001). Glucose kinetics and splanchnic uptake following mixed meal ingestion in cirrhotic-diabetic subjects. *Diabetes Nutrition & Metabolism*, 14(6):315–324.

Klonoff, D. C. (2002). European trends in diabetes technology — continuous glucose measurements and computerized information-processing tools. *Diabetes Technol Ther*, 4(6):763–4.

Klonoff, D. C. (2005a). Continuous glucose monitoring: Roadmap for 21st century diabetes therapy. *Diabetes Care*, 28(5):1231–9.

Klonoff, D. C. (2005b). A review of continuous glucose monitoring technology. *Diabetes Technol Ther*, 7(5):770–5.

Kobayashi, T., Sawano, S., Itoh, T., Kosaka, K., Hirayama, H., and Kasuya, Y. (1983). The pharmacokinetics of insulin after continuous subcutaneous infusion or bolus subcutaneous injection in diabetic patients. *Diabetes*, 32(4):331–6.

Koster, I., von Ferber, L., Ihle, P., Schubert, I., and Hauner, H. (2006). The cost burden of diabetes mellitus: the evidence from Germany-the CoDiM study. *Diabetologia*, 49(7):1498–504.

Kovatchev, B. P., Clarke, W. L., Breton, M., Brayman, K., and McCall, A. (2005). Quantifying temporal glucose variability in diabetes via continuous glucose monitoring: Mathematical methods and clinical application. *Diabetes Technol Ther*, 7(6):849–62.

Kovatchev, B. P., Gonder-Frederick, L. A., Cox, D. J., and Clarke, W. L. (2004). Evaluating the accuracy of continuous glucose-monitoring sensors: continuous glucose-error grid analysis illustrated by TheraSense Freestyle Navigator data. *Diabetes Care*, 27(8):1922–8.

Kraegen, E. W. and Chisholm, D. J. (1984). Insulin responses to varying profiles of subcutaneous insulin infusion: kinetic modelling studies. *Diabetologia*, 26(3):208–213.

Krajicek, B. J., Kudva, Y. C., and Hurley, H. A. (2005). Potentially important contribution of dextrose used as diluent to hyperglycemia in hospitalized patients. *Diabetes Care*, 28(4):981–2.

Krinsley, J. S. (2003a). Association between hyperglycemia and increased hospital mortality in a heterogeneous population of critically ill patients. *Mayo Clin Proc*, 78(12):1471–1478.

Krinsley, J. S. (2003b). Decreased mortality of critically ill patients with the use of an intensive glycemic management protocol. *Crit Care Med*, 31:A19.

Krinsley, J. S. (2004). Effect of an intensive glucose management protocol on the mortality of critically ill adult patients. *Mayo Clin Proc*, 79(8):992–1000.

Krishnan, J. A., Parce, P. B., Martinez, A., Diette, G. B., and Brower, R. G. (2003). Caloric intake in medical ICU patients: consistency of care with guidelines and relationship to clinical outcomes. *Chest*, 124(1):297–305.

Kuehn, L. and Blundell, T. (1980). Insulin and glucagons receptors. In Schulster, D. and Levitski, A., editors, *Cellular receptors for hormones and neurotransmitters*, pages 185–196. John Wiley and Sons, Chichester.

Laird, A. M., Miller, P. R., Kilgo, P. D., Meredith, J. W., and Chang, M. C. (2004). Relationship of early hyperglycemia to mortality in trauma patients. *J Trauma*, 56(5):1058–62.

Langouche, L., Vanhorebeek, I., Vlasselaers, D., Vander Perre, S., Wouters, P. J., Skogstrand, K., Hansen, T. K., and Van den Berghe, G. (2005). Intensive insulin therapy protects the endothelium of critically ill patients. *J Clin Invest*, 115(8):2277–86.

Larsen, M. O., Rolin, B., Wilken, M., Carr, R. D., and Svendsen, O. (2002). High-fat high-energy feeding impairs fasting glucose and increases fasting insulin levels in the Gottingen minipig — results from a pilot study. In *Lipids and Insulin Resistance: The Role of Fatty Acid Metabolism and Fuel Partitioning*, volume 967 of *Annals of the New York Academy of Sciences*, pages 414–423.

Laver, S., Preston, S., Turner, D., McKinstry, C., and Padkin, A. (2004). Implementing intensive insulin therapy: development and audit of the Bath insulin protocol. *Anaesth Intensive Care*, 32(3):311–6.

Lee, A., Ader, M., Bray, G. A., and Bergman, R. N. (1992). Diurnal-variation in glucose-tolerance — cyclic suppression of insulin action and insulin-secretion in normal-weight, but not obese, subjects. *Diabetes*, 41(6):750–759.

Lee, J. M., Okumura, M. J., Davis, M. M., Herman, W. H., and Gurney, J. G. (2006). Prevalence and determinants of insulin resistance among U.S. adolescents: A population study. *Diabetes Care*, 29(11):2427–32.

Lehmann, E. D. and Deutsch, T. (1992). A physiological model of glucose-insulin interaction in type 1 diabetes mellitus. *J Biomed Eng*, 14(3):235–42.

Lehmann, E. D. and Deutsch, T. (1996). Computer assisted diabetes care: a 6-year retrospective. *Comput Methods Programs Biomed*, 50(3):209–230.

Li, C., Ford, E. S., McGuire, L. C., Mokdad, A. H., Little, R. R., and Reaven, G. M. (2006). Trends in hyperinsulinemia among nondiabetic adults in the U.S. *Diabetes Care*, 29(11):2396–2402.

Lind, L. and Lithell, H. (1994). Impaired glucose and lipid metabolism seen in intensive care patients is related to severity of illness and survival. *Clin Intensive Care*, 5(3):100–5.

Livingstone, C. and Ferns, G. A. (2003). Insulin-like growth factor-related proteins and diabetic complications. *Br J Diabetes Vasc Dis*, 3(5):326–331.

Lonergan, T., Compte, A. L., Willacy, M., Chase, J. G., Shaw, G. M., Hann, C. E., Lotz, T., Lin, J., and Wong, X. W. (2006a). A pilot study of the SPRINT protocol for tight glycemic control in critically ill patients. *Diabetes Technol Ther*, 8(4):449–62.

Lonergan, T., Le Compte, A., Willacy, M., Chase, J. G., Shaw, G. M., Wong, X. W., Lotz, T., Lin, J., and Hann, C. E. (2006b). A simple insulin-nutrition protocol for tight glycemic control in critical illness: Development and protocol comparison. *Diabetes Technol Ther*, 8(2):191–206.

Lotz, T., Chase, J. G., McAuley, K., Shaw, G., Wong, X.-W., Lin, J., and Le Compte, A. (2006a). Highly correlated model-based testing of insulin sensitivity — initial results for a proposed low-intensity test. In *6th Annual Diabetes technology Meeting*, page A103, Atlanta, USA.

Lotz, T. F., Chase, J. G., McAuley, K. A., Lee, D. S., Lin, J., Hann, C. E., and Mann, J. I. (2006b). Transient and steady-state euglycemic clamp validation of a model for glycemic control and insulin sensitivity testing. *Diabetes Technol Ther*, 8(3):338–46.

Louie, R. F., Tang, Z., Sutton, Dv, Lee, J. H., and Kost, G. J. (2000). Point-of-care glucose testing: effects of critical care variables, influence of reference instruments, and a modular glucose meter design. *Arch Pathol Lab Med*, 124(2):257–66.

Ludvik, B., Nolan, J. J., Roberts, A., Baloga, J., Joyce, M., Bell, J. M., and Olefsky, J. M. (1995). A noninvasive method to measure splanchnic glucose-uptake after oral glucose-administration. *Journal of Clinical Investigation*, 95(5):2232–2238.

Ludvik, B., Nolan, J. J., Roberts, A., Baloga, J., Joyce, M., Bell, J. M., and Olefsky, J. M. (1997). Evidence for decreased splanchnic glucose uptake after oral glucose administration in non-insulin-dependent diabetes mellitus. *Journal of Clinical Investigation*, 100(9):2354–2361.

Mackenzie, I., Ingle, S., Zaidi, S., and Buczaski, S. (2005). Tight glycaemic control: a survey of intensive care practice in large English hospitals. *Intensive Care Med*, 31(8):1136.

Mainous, A. G., Baker, R., Koopman, R. J., Saxena, S., Diaz, V. A., Everett, C. J., and Majeed, A. (2006). Impact of the population at risk of diabetes on projections of diabetes burden in the United States: an epidemic on the way. *Diabetologia*, 99(9):463–9.

Mari, A. (1998). Assessment of insulin sensitivity and secretion with the labelled intravenous glucose tolerance test: improved modelling analysis. *Diabetologia*, 41(9):1029–39.

Mari, A., Pacini, G., Murphy, E., Ludvik, B., and Nolan, J. J. (2001). A model-based method for assessing insulin sensitivity from the oral glucose tolerance test. *Diabetes Care*, 24(3):539–548.

Mari, A., Stojanovska, L., Proietto, J., and Thorburn, A. W. (2003). A circulatory model for calculating non-steady-state glucose fluxes. Validation and comparison with compartmental models. *Computer Methods and Programs in Biomedicine*, 71(3):269–281.

Mari, A. and Valerio, A. (1997). A circulatory model for the estimation of insulin sensitivity. *Control Eng Practice*, 5(12):1747–1752.

Marik, P. E. and Raghavan, M. (2004). Stress-hyperglycemia, insulin and immunomodulation in sepsis. *Intensive Care Medicine*, 30(5):748–756.

McCowen, K. C., Malhotra, A., and Bistrian, B. R. (2001). Stress-induced hyperglycemia. *Crit Care Clin*, 17(1):107–24.

McDonald, C., Dunaif, A., and Finegood, D. T. (2000). Minimal-model estimates of insulin sensitivity are insensitive to errors in glucose effectiveness. *J Clin Endocrinol Metab*, 85(7):2504–2508.

McDonnell, C. M., Donath, S. M., Vidmar, S. I., Werther, G. A., and Cameron, F. J. (2005). A novel approach to continuous glucose analysis utilizing glycemic variation. *Diabetes Technol Ther*, 7(2):253–63.

McGuire, E. A., Tobin, J. D., Berman, M., and Andres, R. (1979). Kinetics of native insulin in diabetic, obese, and aged men. *Diabetes*, 28(2):110–20.

Mentula, P., Kylanpaa, M. L., Kemppainen, E., Jansson, S. E., Sarna, S., Puolakkainen, P., Haapiainen, R., and Repo, H. (2005). Early prediction of organ failure by combined markers in patients with acute pancreatitis. *British Journal of Surgery*, 92(1):68–75.

Mesotten, D., Swinnen, J. V., Vanderhoydonc, F., Wouters, P. J., and Van den Berghe, G. (2004). Contribution of circulating lipids to the improved outcome of critical illness by glycemic control with intensive insulin therapy. *J Clin Endocrinol Metab*, 89(1):219–26.

Milton, B., Holland, P., and Whitehead, M. (2006). The social and economic consequences of childhood-onset Type 1 diabetes mellitus across the lifecourse — a systematic review. *Diabetic Medicine*, 23:821–9.

Mizock, B. A. (2001). Alterations in fuel metabolism in critical illness: hyperglycaemia. *Best Pract Res Clin Endocrinol Metab*, 15(4):533–51.

Narayan, K. M. V., Boyle, J. P., Geiss, L. S., Saaddine, J. B., and Thompson, T. J. (2006). Impact of recent increase in incidence on future diabetes burden: U.S., 2005–2050. *Diabetes Care*, 29(9):2114–2116.

Narayan, K. M. V., Boyle, J. P., Thompson, T. J., Sorensen, S. W., and Williamson, D. F. (2003). Life time risk for diabetes mellitus in the United States. *J. American Medical Association*, 290(14):1884–90.

Natali, A., Gastaldelli, A., Camastra, S., Sironi, A. M., Toschi, E., Masoni, A., Ferrannini, E., and Mari, A. (2000). Dose-response characteristics of insulin action on glucose metabolism: a non-steady-state approach. *Am J Physiol Endocrinol Metab*, 278(5):E794–801.

Nestler, J. E., Clore, J. N., and Blackard, W. G. (1988). Reduced insulin clearance in normal subjects due to extreme hyperinsulinemia. *Am J Med Sci*, 295(1):15–22.

New Zealand Ministry of Health (2002). Diabetes in New Zealand: Models and forecasts 1996–2011.

Nielsen, M. F., Basu, R., Wise, S., Caumo, A., Cobelli, C., and Rizza, R. A. (1998). Normal glucose-induced suppression of glucose production but impaired stimulation of glucose disposal in type 2 diabetes: evidence for a concentration-dependent defect in uptake. *Diabetes*, 47(11):1735–47.

Novartis (2005). RESOURCE® Diabetic nutrition information. Novartis Medical Nutrition, Minneapolis, MN.

Nyomba, B. L. G., Berard, L., and Murphy, L. J. (2003). Facilitating access to glucometer reagents increases blood glucose self-monitoring frequency and improves glycaemic control: a prospective study in insulin-treated diabetic patients. *Diabetic Medicine*, 21:129135.

Oddo, M., Schaller, M. D., Calandra, T., and Liaudet, L. (2004). [new therapeutic strategies in severe sepsis and septic shock]. *Rev Med Suisse Romande*, 124(6):329–32.

Ollerton, R. L. (1989). Application of optimal control theory to diabetes mellitus. *Int. J. Control*, 50(6):2503–2522.

Ousman, Y. (2002). Hyperglycemia in the hospitalized patient. *Clinical Diabetes*, 20(3):147–148.

Pacini, G. and Bergman, R. N. (1986). MINMOD: a computer program to calculate insulin sensitivity and pancreatic responsivity from the frequently sampled intravenous glucose tolerance test. *Comput Methods Programs Biomed*, 23(2):113–22.

Papadea, C., Foster, J., Grant, S., Ballard, S. A., Cate, J. C. t., Southgate, W. M., and Purohit, D. M. (2002). Evaluation of the i-STAT Portable Clinical Analyzer for point-of-care blood testing in the intensive care units of a university children's hospital. *Ann Clin Lab Sci*, 32(3):231–43.

Parker, R. S. and Doyle, F. J., r. (2001). Control-relevant modeling in drug delivery. *Adv Drug Deliv Rev*, 48(2-3):211–228.

Parker, R. S., Doyle, F. J., r., and Peppas, N. A. (1999). A model-based algorithm for blood glucose control in type I diabetic patients. *IEEE Trans Biomed Eng*, 46(2):148–157.

Parker, R. S., Doyle, F. J., r., and Peppas, N. A. (2001). The intravenous route to blood glucose control — a review of control algorithms for noninvasive monitoring and regulation in Type I diabetic patients. *IEEE Eng Med Biol*, 20:65–73.

Patino, J. F., de Pimiento, S. E., Vergara, A., Savino, P., Rodriguez, M., and Escallon, J. (1999). Hypocaloric support in the critically ill. *World J Surg*, 23(6):553–9.

Peck, P. (2004). Intensive glucose management reduces in-hospital mortality. In *SCCM 33rd Annual Congress*, Orlando, Florida. Medscape Medical News.

Peet, A. C., Kennedy, D. M., Hocking, M. D., and Ewer, A. K. (2002). Near-patient testing of blood glucose using the Bayer Rapidlab 860 analyser in a regional neonatal unit. *Ann Clin Biochem*, 39(Pt 5):502–8.

Pehling, G., Tessari, P., Gerich, J. E., Haymond, M. W., Service, F. J., and Rizza, R. A. (1984). Abnormal meal carbohydrate disposition in insulin-dependent diabetes — relative contributions of endogenous glucose-production and initial splanchnic uptake and effect of intensive insulin therapy. *Journal of Clinical Investigation*, 74(3):985–991.

Pillonetto, G., Sparacino, G., Magni, P., Bellazzi, R., and Cobelli, C. (2002). Minimal model $S_I = 0$ problem in NIDDM subjects: nonzero Bayesian estimates with credible confidence intervals. *Am J Physiol Endocrinol Metab*, 282(3):E564–573.

Pitzer, K. R., Desai, S., Dunn, T., Edelman, S., Jayalakshmi, Y., Kennedy, J., Tamada, J. A., and Potts, R. O. (2001). Detection of hypoglycemia with the GlucoWatch biographer. *Diabetes Care*, 24(5):881–885.

Plank, J., Blaha, J., Cordingley, J., Wilinska, M. E., Chassin, L. J., Morgan, C., Squire, S., Haluzik, M., Kremen, J., Svacina, S., Toller, W., Plasnik, A., Ellmerer, M., Hovorka, R., and Pieber, T. R. (2006). Multicentric, randomized, controlled trial to evaluate blood glucose control by the model predictive control algorithm versus routine glucose management protocols in intensive care unit patients. *Diabetes Care*, 29(2):271–6.

Prigeon, R. L., Roder, M. E., Porte, D., J., and Kahn, S. E. (1996). The effect of insulin dose on the measurement of insulin sensitivity by the minimal model technique. evidence for saturable insulin transport in humans. *J Clin Invest*, 97(2):501–7.

PWC (PriceWaterhouseCoopers) (2001). Type 2 diabetes, managing for better health outcomes. Technical report, Diabetes New Zealand Inc.

Radziuk, J., McDonald, T. J., Rubenstein, D., and Dupre, J. (1978). Initial splanchnic extraction of ingested glucose in normal man. *Metabolism-Clinical and Experimental*, 27(6):657–669.

Radziuk, J. and Pye, S. (2006). Diurnal rhythm in endogenous glucose production is a major contributor to fasting hyperglycaemia in type 2 diabetes. suprachiasmatic deficit or limit cycle behaviour? *Diabetologia*.

Raskin, P. (1984). The somogyi phenomenon. sacred cow or bull? *Arch Intern Med.*, 144(4):781–787.

Rebrin, K., Steil, G. M., Van Antwerp, W. P., and Mastrototaro, J. J. (1999). Subcutaneous glucose predicts plasma glucose independent of insulin: implications for continuous monitoring. *American Journal of Physiology-Endocrinology and Metabolism*, 277(3):E561–E571.

Rizza, R. A., Mandarino, L. J., and Gerich, J. E. (1981). Dose-response characteristics for effects of insulin on production and utilization of glucose in man. *Am J Physiol*, 240(6):E630–639.

Rubinson, L., Diette, G. B., Song, X., Brower, R. G., and Krishnan, J. A. (2004). Low caloric intake is associated with nosocomial bloodstream infections in patients in the medical intensive care unit. *Crit Care Med*, 32(2):350–7.

Saad, M. F., Anderson, R. L., Laws, A., Watanabe, R. M., Kades, W. W., Y.-D., I. C., Sands, R. E., Pei, D., Savage, P. J., and Bergman, R. N. (1994). A comparison between the minimal model and the glucose clamp in the assessment of insulin sensitivity across the spectrum of glucose tolerance. *Diabetes*, 43:1114–21.

Salzsieder, E., Albrecht, G., Fischer, U., and E.-J., F. (1985). Kinetic modeling of the glucoregulatory system to improve insulin therapy. *IEEE Trans Biomed Eng*, 32:846–55.

Salzsieder, E., Albrecht, G., Fischer, U., Rutscher, A., and Thierbach, U. (1990a). Computer-aided systems in the management of type I diabetes: the application of a model-based strategy. *Computer Methods and Programs in Biomedicine*, 32:215–224.

Salzsieder, E., Fischer, U., Stoewhas, H., Thierbach, U., Rutscher, A., Menzel, R., and Albrecht, G. (1990b). A model-based system for the individual prediction of metabolic responses to improve therapy in type I diabetes. *Horm Metab Res Suppl*, 24:10–9.

Scholtz, H. E., Pretorius, S. G., Wessels, D. H., and Becker, R. H. A. (2005). Pharmacokinetic and glucodynamic variability: assessment of insulin glargine, NPH insulin and insulin ultralente in healthy volunteers using a euglycaemic clamp technique. *Diabetologia*, 48(10):1988–1995.

Scott, D. W. (1992). *Multivariate density estimation: theory, practice, and visualization*. Wiley series in probability and mathematical statistics. John Wiley & sons, Inc., New York.

Shaw, G. M., Chase, J. G., Lee, D. S., Bloomfield, M., Doran, C. V., and Lin, J. (2004). How high ARE blood glucose levels in intensive care? In *ANZICS ASM*, Wellington, New Zealand.

Shaw, G. M., Chase, J. G., Lee, D. S., Bloomfield, M., Doran, C. V., Lin, J., and Lotz, T. (2005). Peak and range of blood glucose are also associated with ICU mortality,. *Critical Care Medicine*, 32(12):A125.

Shaw, G. M., Chase, J. G., Rudge, A. D., Starfinger, C., Lam, Z., Lee, D., Wake, G. C., Greenfield, K., and Dove, R. (2003). Rethinking sedation and agitation management in critical illness. *Critical Care and Resuscitation*, 5:198–206.

Shaw, G. M., Chase, J. G., Wong, J., Lin, J., Lotz, T., Le Compte, A. J., Lonergan, T. R., Willacy, M. B., and Hann, C. E. (2006). Rethinking glycaemic control in critical illness — from concept to clinical practice change. *Crit Care Resusc*, 8(2):90–9.

Sherwin, R. S., Kramer, K. J., Tobin, J. D., Insel, P. A., Liljenquist, J. E., Berman, M., and Andres, R. (1974). A model of the kinetics of insulin in man. *J Clin Invest*, 53(5):1481–92.

Simonoff, J. S. (1996). *Smoothing methods in statistics*. Springer series in statistics. springer-Verlag New York, Inc., New York.

Solnica, B., Naskalski, J. W., and Sieradzki, J. (2001). The evaluation of analytical performance of the Precision G point-of-care glucometer. *Clin Chem Lab Med*, 39(12):1283–6.

Solnica, B., Naskalski, J. W., and Sieradzki, J. (2003). Analytical performance of glucometers used for routine glucose self-monitoring of diabetic patients. *Clin Chim Acta*, 331(1-2):29–35.

Sonksen, P. H., Tompkins, C. V., Srivastava, M. C., and Nabarro, J. D. (1973). A comparative study on the metabolism of human insulin and porcine proinsulin in man. *Clin Sci Mol Med*, 45(5):633–54.

Soop, M., Duxbury, H., Agwunobi, A., Gibson, J., Hopkins, S., Childs, C., Cooper, R., Maycock, P., Little, R., and Carlson, G. (2002). Euglycemic hyperinsulinemia augments the cytokine and endocrine responses to endotoxin in humans. *Am J Physiol Endocrinol Metab*, 282(6):E1276–85.

Steil, G. M., Panteleon, A. E., and Rebrin, K. (2004). Closed-loop insulin delivery-the path to physiological glucose control. *Adv Drug Deliv Rev*, 56(2):125–44.

Stokes, C. L. (2000). Biological systems modeling: powerful discipline for biomedical *e*-R&D. *AIChE J.*, 46:430–33.

Thomson, S., Beaven, D., Jamieson, M., Snively, S., Howl, A., and Christophersen, A. (2001). Type 2 diabetes: Managing for better health outcomes. Price-waterhouse-coopers report, Diabetes New Zealand Inc.

Thorburn, A., Litchfield, A., Fabris, S., and Proietto, J. (1995). Abnormal transient rise in hepatic glucose-production after oral glucose in non-insulin-dependent diabetic subjects. *Diabetes Research and Clinical Practice*, 28(2):127–135.

Thorell, A., Rooyackers, O., Myrenfors, P., Soop, M., Nygren, J., and Ljungqvist, O. H. (2004). Intensive insulin treatment in critically ill trauma patients normalizes glucose by reducing endogenous glucose production. *J Clin Endocrinol Metab*, 89(11):5382–6.

Thorsteinsson, B. (1990). Kinetic models for insulin disappearance from plasma in man. *Dan Med Bull*, 37(2):143–53.

Tierney, M. J., Tamada, J. A., Potts, R. O., Eastman, R. C., Pitzer, K., Ackerman, N. R., and Fermi, S. J. (2000). The Glucowatch® biographer: a frequent, automatic and noninvasive glucose monitor. *Annals of Medicine*, 32(9):632–641.

Tierney, M. J., Tamada, J. A., Potts, R. O., Jovanovic, L., and Garg, S. (2001). Clinical evaluation of the GlucoWatch® biographer: a continual, non-invasive glucose monitor for patients with diabetes. *Biosensors & Bioelectronics*, 16(9-12):621–629.

Toffolo, G., Campioni, M., Basu, R., Rizza, R. A., and Cobelli, C. (2006). A minimal model of insulin secretion and kinetics to assess hepatic insulin extraction. *Am J Physiol Endocrinol Metab*, 290(1):E169–E176.

Toffolo, G., Cefalu, W. T., and Cobelli, C. (1999). Beta-cell function during insulin-modified intravenous glucose tolerance test successfully assessed by the C-peptide minimal model. *Metabolism*, 48(9):1162–6.

Transberg, K., Hagander, P., and Thorell, J. (1981). Disappearance of insulin in man: variation with the plasma insulin level. *Acta Endocrinol (Copenh)*, 97:391–397.

Tsalikian, E., Beck, R. W., Tamborlane, W. V., Chase, P., Buckingham, B. A., Weinzimer, S. A., Mauras, N., Ruedy, K. J., Kollman, C., Xing, D. Y., Fiallo-Scharer, R., Fisher, J. H., Tansey, M. J., Larson, L. F., Wysocki, T., Gagnon, K. M., Todd, P., Wilson, D. M., Block, J. M., Kunselman, E. L., Doyle, E. A., Moke, P. S., Labastie, L. M., Becker, D. M., Cox, C., Ryan, C. M., White, N. H., White, P. C., Steffes, M. W., Bucksa, J. M., Nowicki, M. L., Grave, G. D., Linder, B., and Winer, K. K. (2004). Accuracy of the GlucoWatch G2 Biographer and the continuous glucose monitoring system during hypoglycemia — experience of the diabetes research in children network. *Diabetes Care*, 27(3):722–726.

Turina, M., Fry, D. E., and Polk, H. C. (2005). Acute hyperglycemia and the innate immune system: clinical, cellular, and molecular aspects. *Crit Care Med*, 33(7):1624–33.

Turnheim, K. and Waldhausl, W. K. (1988). Essentials of insulin pharmacokinetics. *Wien Klin Wochenschr*, 100(3):65–72.

Umpierrez, G. E., Isaacs, S. D., Bazargan, N., You, X., Thaler, L. M., and Kitabchi, A. E. (2002). Hyperglycemia: an independent marker of in-hospital mortality in patients with undiagnosed diabetes. *J Clin Endocrinol Metab*, 87(3):978–982.

Van Cauter, E., Mestrez, F., Sturis, J., and Polonsky, K. S. (1992). Estimation of insulin secretion rates from C-peptide levels. comparison of individual and standard kinetic parameters for C-peptide clearance. *Diabetes*, 41(3):368–77.

Van den Berghe, G. (2004a). How does blood glucose control with insulin save lives in intensive care? *J Clin Invest*, 114(9):1187–95.

Van den Berghe, G. (2004b). How to compare adequacy of algorithms to control blood glucose in the intensive care unit? *Crit Care*, 8(3):151–2.

Van den Berghe, G., Schoonheydt, K., Becx, P., Bruyninckx, F., and Wouters, P. J. (2005). Insulin therapy protects the central and peripheral nervous system of intensive care patients. *Neurology*, pages 1348–1353.

Van den Berghe, G., Wilmer, A., Hermans, G., Meersseman, W., Wouters, P. J., Milants, I., Van Wijngaerden, E., Bobbaers, H., and Bouillon, R. (2006). Intensive insulin therapy in the medical ICU. *N Engl J Med*, 354(5):449–61.

Van den Berghe, G., Wouters, P., Weekers, F., Verwaest, C., Bruyninckx, F., Schetz, M., Vlasselaers, D., Ferdinande, P., Lauwers, P., and Bouillon, R. (2001). Intensive insulin therapy in the critically ill patients. *N Engl J Med*, 345(19):1359–1367.

Van den Berghe, G., Wouters, P. J., Bouillon, R., Weekers, F., Verwaest, C., Schetz, M., Vlasselaers, D., Ferdinande, P., and Lauwers, P. (2003). Outcome benefit of intensive insulin therapy in the critically ill: Insulin dose versus glycemic control. *Crit Care Med*, 31(2):359–366.

Verrillo, A., Deteresa, A., Martino, C., Dichiara, G., Pinto, M., Verrillo, L., Torello, F., and Gattoni, A. (1989). Differential roles of splanchnic and peripheral-tissues in determining diurnal fluctuation of glucose-tolerance. *American Journal of Physiology*, 257(4):E459–E465.

Vicini, P., Caumo, A., and Cobelli, C. (1997). The hot IVGTT two-compartment minimal model: indexes of glucose effectiveness and insulin sensitivity. *Am J Physiol*, 273(5 Pt 1):E1024–1032.

Vicini, P., Caumo, A., and Cobelli, C. (1999). Glucose effectiveness and insulin sensitivity from the minimal models: consequences of undermodeling assessed by Monte Carlo simulation. *IEEE Trans Biomed Eng*, 46(2):130–137.

Vogelzang, M., Horst, I. C. v. d., and Nijsten, M. W. (2004). Hyperglycaemic index as a tool to assess glucose control: A retrospective study. *Crit Care*, 8(3):R122–7.

Waeschle, R. M., Moerer, O., Wahaha, D., Neumann, P., and Quintel, M. (2005). Intensive insulin therapy on ICU: Comparison of two algorithms to control the blood glucose level. *Intensive Care Med*, 31(S1):S203.

Weekers, F., Giulietti, A. P., Michalaki, M., Coopmans, W., Van Herck, E., Mathieu, C., and Van den Berghe, G. (2003). Metabolic, endocrine, and immune effects of stress hyperglycemia in a rabbit model of prolonged critical illness. *Endocrinology*, 144(12):5329–38.

Weinzimer, S. A., DeLucia, M. C., Boland, E. A., Steffen, A., and Tamborlane, W. V. (2003). Analysis of continuous glucose monitoring data from nondiabetic and diabetic children: a tale of two algorithms. *Diabetes Technol Ther*, 5(3):375–80.

Weissman, C. (1999). Nutrition in the intensive care unit. *Crit Care*, 3(5):R67–75.

Weitgasser, R., Gappmayer, B., and Pichler, M. (1999). Newer portable glucose meters — Analytical improvement compared with previous generation devices? *Clinical Chemistry*, 45(10):1821–1825.

Wild, S., Roglic, G., Green, A., Sicree, R., and King, H. (2004). Global prevalence of diabetes: estimates for the year 2000 and projections for 2030. *Diabetes Care*, 27(5):1047–53.

Wilinska, M. E., Bodenlenz, M., Chassin, L. J., Schaller, H. C., Schaupp, L. A., Pieber, T. R., and Hovorka, R. (2004). Interstitial glucose kinetics in subjects with type 1 diabetes under physiologic conditions. *Metabolism*, 53(11):1484–91.

Williams, R. (2005). Medical and economic case for prevention of type 2 diabetes and cardiovascular disease. *European Heart Journal Supplements*, 7(Supplement D):D14–17.

Wong, X. W., Chase, J. G., Shaw, G. M., Hann, C. E., Lin, J., and Lotz, T. (2005). Comparison of adaptive and sliding-scale glycaemic control in critical care and the impact of nutritional inputs. In *Proc. of the 12th International Conf on Biomedical Engineering (ICBME 2005)*, pages 4–pages, Singapore.

Wong, X. W., Chase, J. G., Shaw, G. M., Hann, C. E., Lotz, T., Lin, J., Singh-Levett, I., Hollingsworth, L. J., Wong, O. S., and Andreassen, S. (2006a). Model predictive glycaemic regulation in critical illness using insulin and nutrition input: a pilot study. *Med Eng Phys*, 28(7):665–81.

Wong, X. W., Singh-Levett, I., Hollingsworth, L. J., Shaw, G. M., Hann, C. E., Lotz, T., Lin, J., Wong, O. S., and Chase, J. G. (2006b). A novel, model-based insulin and nutrition delivery controller for glycemic regulation in critically ill patients. *Diabetes Technol Ther*, 8(2):174–90.

Woolfson, A. M. (1980). Control of blood glucose during nutritional support in ill patients. *Intensive Care Med*, 7(1):11–14.

Yang, Y. J., Youn, J. H., and Bergman, R. N. (1987). Modified protocols improve insulin sensitivity estimation using the minimal model. *Am J Physiol*, 253(6 Pt 1):E595–602.